False Biosignatures on Mars: Anticipating Ambiguity

JGS
Journal of the Geological Society

Review article

Published Online First

https://doi.org/10.1144/jgs2021-050

False biosignatures on Mars: anticipating ambiguity

Sean McMahon[1,2*] and Julie Cosmidis[3]

[1] UK Centre for Astrobiology, School of Physics and Astronomy, University of Edinburgh, James Clerk Maxwell Building, Peter Guthrie Tait Road, Edinburgh EH9 3FD, UK
[2] School of GeoSciences, University of Edinburgh, Grant Institute, James Hutton Road, Edinburgh EH9 3FE, UK
[3] Department of Earth Sciences, University of Oxford, South Parks Road, Oxford OX1 3AN, UK
SM, 0000-0001-8589-2041; JC, 0000-0003-3428-8447
* Correspondence: sean.mcmahon@ed.ac.uk

Abstract: It is often acknowledged that the search for life on Mars might produce false positive results, particularly via the detection of objects, patterns or substances that resemble the products of life in some way but are not biogenic. The success of major current and forthcoming rover missions now calls for significant efforts to mitigate this risk. Here, we review known processes that could have generated false biosignatures on early Mars. These examples are known largely from serendipitous discoveries rather than systematic research and remain poorly understood; they probably represent only a small subset of relevant phenomena. These phenomena tend to be driven by kinetic processes far from thermodynamic equilibrium, often in the presence of liquid water and organic matter, conditions similar to those that can actually give rise to, and support, life. We propose that strategies for assessing candidate biosignatures on Mars could be improved by new knowledge on the physics and chemistry of abiotic self-organization in geological systems. We conclude by calling for new interdisciplinary research to determine how false biosignatures may arise, focusing on geological materials, conditions and spatiotemporal scales relevant to the detection of life on Mars, as well as the early Earth and other planetary bodies.

Thematic collection: This article is part of the Astrobiology: Perspectives from the Geology of Earth and the Solar System collection available at: https://www.lyellcollection.org/cc/astrobiology-perspectives-from-geology-of-earth-and-solar-system

Received 3 May 2021; **revised** 30 September 2021; **accepted** 7 October 2021

These are exciting times for astrobiology. The search for evidence of past life on Mars is the central scientific objective of two contemporary rover missions: NASA's Mars 2020 Mission (Perseverance rover, touchdown February 2021) and the ESA-RosCosmos ExoMars Mission (Rosalind Franklin rover, scheduled for launch in 2022). Both rovers will seek geological biosignatures in clay-rich, subaqueously deposited sedimentary rocks of Noachian age (*c.* 4 Ga), probably representing habitable palaeoenvironments (Horgan *et al.* 2020; Quantin-Nataf *et al.* 2021). Both rovers are equipped with sophisticated multispectral cameras and instruments for the analysis of these rocks and any organic matter they may contain.

The two missions differ slightly in their technical abilities. For example, the Rosalind Franklin rover carries a drill capable of extracting samples from 2 m below the surface, where the overlying rock may have protected organic molecules from oxidation or radiation damage. The Perseverance rover can detect organic matter, but not extract it from such depths nor characterize it in as much detail. However, Perseverance is equipped with a sample-caching system that will enable it to extract astrobiologically promising geological samples and seal them for subsequent collection and return to Earth, probably in a joint ESA–NASA operation (Muirhead *et al.* 2020). These will be the first samples brought back from Mars and will serve as a rich source of data for the investigation of martian geology and astrobiology. In theory, it will become possible to analyse rocks from Mars using almost the full range of techniques used to detect ancient biosignatures on Earth.

Studies of the Earth's biosphere and geological record have illuminated an enormous variety of biosignatures that astrobiologists might detect either *in situ* on Mars or in returned samples. For instance, samples may contain: morphological fossils as small as individual microbial cells, colonies or biofilms, or as large as stromatolites; organic materials with a compositional profile, complexity, modular molecular construction and/or stereoisomerism that suggest biosynthetic origins; or isotopic, geochemical or mineralogical anomalies that would normally be interpreted as evidence of life (Westall *et al.* 2015; Hays *et al.* 2017; Vago *et al.* 2017, 2019; McMahon *et al.* 2018).

Astrobiologists have amassed innumerable examples of these and other kinds of microbial biosignatures from ancient and modern Mars-analogue environments, providing an immensely rich set of reference data or 'search images'. We might reasonably argue, therefore, that the risk of false negative results in the search for life is low, or at least lower for the forthcoming rover missions than it was for the Viking landers of the 1970s: if evidence of life is really present in the materials that either the Rosalind Franklin or Perseverance rover brings to light, there is now a good chance that we will find and recognize it. What concerns us here is the risk of false positive errors in the detection of life, specifically those arising from the misinterpretation of abiotic geological and chemical features that are misleadingly life-like (rather than analytical false positives or spacecraft contamination).

One reason for concern is that such errors have been frequent in the history of palaeobiology and astrobiology down to the present day. In the nineteenth century, intricate layered and tubular structures found in serpentine-rich metacarbonate rocks from the Canadian shield were interpreted as the fossilized tests of ancient forams, designated *Eozoon canadense*, the 'dawn animal of Canada'; it took much heated debate, and some decades of careful work, to show that these were abiotic textures (Adelman 2007). Palaeontologists in the twentieth century repeatedly made similar misdiagnoses; examples listed by Cloud (1973) include spurious 'worm tracks' (drag marks), 'medusae' (pyrite rosettes), 'arthropods' (mud curls around desiccation cracks) and numerous

Proterozoic 'microfossils' (crystallites, contaminating spores and preparation artefacts).

The difficulty of correctly determining the biogenicity of life-like geological substances and structures has continued to plague palaeontology, and the new field of astrobiology, often despite laudable efforts to practice the 'care, patience, and critical attitude' recommended by Cloud. For example, McKay *et al.* (1996) reported multiple lines of evidence in the martian meteorite ALH84001 that were suggestive of past life on Mars, making news bulletins around the world. These included carbonate globules and magnetite crystals resembling bacteriogenic precipitates, polyaromatic hydrocarbon compounds and worm-like microstructures interpreted as morphological fossils. The origins of these features are still unclear today, but abiotic explanations have been offered for all of them, and the overall case for life in ALH84001 no longer seems compelling (Martel *et al.* 2012). This example warns us that it is not enough to have 'multiple lines of evidence' for biogenicity (an oft-repeated mantra) if each line of evidence is ambiguous.

Other ongoing debates concern the oldest fossil and geochemical evidence of life on Earth. Schopf (1993) presented fossil 'cyanobacteria' from the 3.5-Gyr-old Apex Chert of Western Australia, which were later reinterpreted as abiotic carbon organized around spherulitic quartz growth and/or worm-like delaminated clay booklets (Brasier *et al.* 2002, 2005; Wacey *et al.* 2016*a*). Recent work highlights the possibility that organic matter in such cherts might be biogenic even if it has been abiotically redistributed (Duda *et al.* 2018), while Schopf *et al.* (2018) have claimed that morphology-specific carbon isotope values confirm the biogenicity of the Apex microstructures and reveal them to include methane-cycling archaea; this controversy continues (e.g. Alleon and Summons 2019). Nutman *et al.* (2016) described triangular features exposed on 3.7-Gyr-old metasedimentary rocks from the Isua supracrustal belt in Greenland and interpreted them as fossil stromatolites; these have been reinterpreted by some researchers as abiotic deformation features on the basis of 3D imaging and geochemical analysis (Allwood *et al.* 2018; Zawaski *et al.* 2020), although Nutman and co-workers stand by their original view (Nutman *et al.* 2021). Dodd *et al.* (2017) described hematite tubules in a *c.* 4-Gyr-old hydrothermal chert from the Nuvvuagittuq Greenstone Belt in Canada as the mineralized sheaths of ancient Fe-oxidizing bacteria; these have been queried as possible chemical gardens (McMahon 2019), but further analyses are needed.

These examples show that the return of samples from Mars will not necessarily solve once and for all the problem of the existence of (ancient) life on that planet. Although we must hope for definitive results, candidate biosignatures are likely to be at least somewhat ambiguous (García-Ruiz *et al.* 2002) and may spark debates that cannot be quickly resolved. To give an extreme example from Earth, the biogenicity of the filamentous mineral networks found in 'moss agates' has been unclear for more than 200 years (e.g. Daubenton 1782; MacCulloch 1814; Bowerbank 1842; Göppert 1848; Liesegang 1914; Brown 1957; Hopkinson *et al.* 1998; Hofmann and Farmer 2000; McMahon 2019; Götze *et al.* 2020). As in all the debates cited here, the key evidence will come from the investigation of abiotic physicochemical systems and their capacity to mimic the forms and properties of life. Yet this area of enquiry has received rather scant and unsystematic attention from astrobiologists, who have tended to focus their published work on expanding our knowledge of life's signatures rather than its abiotic mimics. This problem was lamented by Cady *et al.* (2003), who predicted that:

> … images and spectroscopic data indicative of life will continue to accumulate in the peer-reviewed literature. At the same time, millions of images and spectra from dubiofossils (of unknown origin) and pseudofossils (abiotic mimics) will also continue to accumulate, yet they will rarely appear in publication.

With this motivation, we here attempt to summarize the physicochemical processes so far known to generate life-like morphologies, minerals, molecules and other phenomena, and consider how and where they may have taken place on early Mars, with a particular focus on the materials that the Rosalind Franklin and Perseverance rovers may encounter and sample at Oxia Planum and Jezero Crater, respectively. We note that, by definition, a biosignature is more than simply a phenomenon produced by life: it is a phenomenon that specifically requires a biological agent – that is, it could not have been produced naturally by non-living systems (e.g. Des Marais *et al.* 2008). The reliability of any detected biosignatures on Mars therefore depends crucially on our understanding of the abiotic processes that might mimic them (Brasier and Wacey 2012; Chan *et al.* 2019).

This paper is not intended to criticize or undermine the search for geological evidence of life on Mars (or the early Earth), but to facilitate the formulation and testing of abiotic 'null hypotheses' for the evaluation of candidate biosignatures if and when they are discovered. It is intended to complement the many existing reviews on the possible biosignatures that may be found on Mars (e.g. Westall *et al.* 2015; Hays *et al.* 2017; Vago *et al.* 2017; McMahon *et al.* 2018). For the most part, however, we do not attempt to provide 'biogenicity criteria' for evaluating the credibility of candidate biosignatures. Rather, we emphasize that such criteria will become more reliable as the formation of false biosignatures becomes better understood. Significant progress in this field will require the numerical, experimental and analytical skills and specialist knowledge of chemists, physicists, geologists, mineralogists and materials scientists, among others.

Abiotic organic matter: molecular pseudofossils

The search for ancient organic matter is a central element of the life-detection strategy for ExoMars, Mars 2020 and the anticipated joint ESA–NASA sample return mission. Indigenous martian organic matter with a chemical fingerprint sufficiently similar to (degraded) biomass would be an exciting potential biosignature in its own right and could significantly strengthen the credibility of any associated morphological, isotopic or mineralogical potential biosignatures (Summons *et al.* 2011). Despite the pervasively oxidizing and ionizing conditions at the martian surface, the Sample Analysis at Mars (SAM) instrument aboard the Curiosity rover has confirmed that ancient organic matter has survived where shielded and protected by minerals, particularly clays. This instrument measured trace amounts of aliphatic and aromatic molecular fragments in drill powder extracted from a Noachian–Hesperian mudstone, which had been exposed relatively recently by scarp retreat (Glavin *et al.* 2013; Farley *et al.* 2014; Ming *et al.* 2014; Freissinet *et al.* 2015; Eigenbrode *et al.* 2018). This organic matter has been altered diagenetically (e.g. sulfurized) and may have originally derived partly from carbonaceous meteorites and partly from indigenous sources on Mars (Eigenbrode *et al.* 2018; Franz *et al.* 2020). Interaction with perchlorates during sample pyrolysis chlorinated some hydrocarbons, further obscuring their original composition (Szopa *et al.* 2020). Ancient, probably indigenous, organic matter is also found in some basaltic martian meteorites, probably from abiotic sources (e.g. Steele *et al.* 2012).

Jezero Crater and Oxia Planum both host clay-rich Noachian sedimentary rocks with good potential to contain preserved organic matter, which both the Perseverance and Rosalind Franklin rovers would be capable of detecting and, to some extent, characterizing. Rosalind Franklin's Mars Organic Molecular Analyzer (MOMA) instrument can fingerprint organic molecules in drill powders with

Table 1. *Descriptions of analytical and imaging instruments aboard the Perseverance and Rosalind Franklin rovers, with their respective spatial resolutions*

Instrument name	Description	Relevant spatial resolution
Perseverance rover		
Mastcam-Z	Long-range (2–100 m) multispectral, stereoscopic imager; wavelength selection using narrowband filters provides some mineralogical information	150 μm per pixel to 7.4 mm per pixel depending on distance
WATSON	Camera for fine-scale imaging of textures and structures on the martian surface	15.9 μm per pixel
SHERLOC	Deep UV Raman and fluorescence spectrometer for the detection and mapping of organic molecules and minerals; combined with a high-resolution camera (context imager)	*c.* 50 μm per pixel (spectroscopy) 10.1 μm per pixel (context imager)
SuperCam	Laser-induced breakdown spectroscopy, Raman and time-resolved luminescence spectroscopy, and visible and infrared reflectance spectroscopy for remote (up to *c.* 12 m) mineralogy and elemental and molecular chemical characterization (including organic molecules); combined with a remote micro-imager	0.5–5 mm per spot depending on technique and distance (spectroscopy) *c.* 30 μm per pixel at 1.5 m (imager)
PIXL	X-ray fluorescence spectrometer to map the distribution and abundance variations of chemical elements at the sub-millimetre scale	58 μm per pixel
Rosalind Franklin rover		
Panoramic camera (PanCAM)	Two wide-angle stereo cameras, one high-resolution camera	*c.* 170 μm per pixel at 2 m distance
CLose UP Imager (CLUPI)	Close-range (50 cm) 'hand lens' imager for imaging rocks and drill powders	7.8 μm per pixel
Infrared Spectrometer for ExoMars (ISEM)	Infrared spectrometer for remote mineralogical characterization and identification of rock targets	3–10 cm per spot depending on distance
Mars Multispectral Imager for Subsurface Studies (Ma_MISS)	Visible and near-infrared spectroscopy to characterize the mineralogy of the walls of drilled boreholes	120 μm spatial resolution
MicrOmega	Near-infrared and visible light spectromicroscopy for spatially resolved characterization of minerals and organic molecules in drill powders	20 μm per pixel
Raman laser spectrometer (RLS)	Raman spectrometry to identify mineralogy and organic matter in drill powders	Spot size *c.* 50 μm
Mars Organic Molecule Analyzer (MOMA)	UV laser desorption and pyrolysis (with or without derivatization agent), gas chromatography–mass spectrometry to identify and characterize organic molecules (alkanes, lipids, carboxylic acids, fatty acids, amino acids, nucleobases, amines, alcohols; chirality)	N/A

Data from Beegle *et al.* (2015), Bibring *et al.* (2017), Coates *et al.* (2017), De Sanctis *et al.* (2017), Goesmann *et al.* (2017), Josset *et al.* (2017), Korablev *et al.* (2017), Rull *et al.* (2017), Allwood *et al.* (2020), Wiens *et al.* (2020), Bell *et al.* (2021), Maurice *et al.* (2021).

very high sensitivity and specificity, even allowing enantiomeric excesses to be measured in some compounds (Goesmann *et al.* 2017) (Table 1). Unfortunately, determining the biogenicity of any organic matter detected may not be straightforward. Noachian Mars, like the early Earth, was presumably supplied with a rich complement of organic matter derived from meteorites and from a variety of endogenous abiotic processes (Chyba and Sagan 1992). Among the latter, the most frequently discussed involve either the reduction of inorganic carbon catalysed on mineral surfaces under hydrothermal conditions (e.g. Fischer–Tropsch type synthesis, organosulfur pathways and electrochemical pathways), high-temperature carbonate decomposition or (mineral-catalysed) photochemical carbon fixation and cycling (e.g. McCollom 2013; Milesi *et al.* 2015; Dalai *et al.* 2016; Steele *et al.* 2018; Franz *et al.* 2020). Taken together, these various sources would have provided, *inter alia*, polyaromatic hydrocarbons, alkanes, amines, fatty acids/lipids, carboxylic acids, amino acids, nucleobases, aldehydes, ketones and carbohydrates, all of which are present – along with marked enantiomeric excesses – in carbonaceous chondrites (Botta and Bada 2002; Simoneit 2004; Myrgorodska *et al.* 2015; Dalai *et al.* 2016; Furukawa *et al.* 2019; Lai *et al.* 2019).

On Earth, hydrothermal cherts as old as 3.5 Ga contain abundant kerogen-like carbonaceous matter suggested (although not conclusively demonstrated) to derive from Fischer–Tropsch type synthesis (Lindsay *et al.* 2005; Alleon *et al.* 2019) and it has been argued that 'the abiotic organic output from [such] hydrothermal systems may overwhelm any early biospheric geochemical signal' (Lindsay *et al.* 2005). On Mars, the structurally simple products of abiotic carbon fixation may be easier to interpret given the lack of metamorphic overprint compared with the Earth (assuming minimal degradation by diagenesis, oxidation and ionizing radiation).

Difficulty arises, however, from the fact that the relatively simple building blocks produced by abiotic carbon fixation can give rise to much more complex products, especially where thermodynamic disequilibrium is available to drive chemical self-organization; this much is evident from the existence of life on Earth. In other words, abiotic organic matter on Mars may have undergone transformations that are on the road to life (e.g. enantiomeric selection, metabolism-like reaction networks and autocatalytic cycles, the formation of complex polymers with repeating subunits, unexpected molecular weight distributions), but without reaching this destination. We lack a good understanding of these processes or of the diversity of molecular (or multimolecular) pseudofossils they might produce, although computational studies of prebiotic systems chemistry potentially offer some important clues (e.g. Wołos *et al.* 2020). If current models for the origin of life on Earth are any guide, then homochirality, polypeptides/proteins, RNA and DNA may all have emerged in prebiotic chemical reaction systems prior to the onset of Darwinian life (e.g. Orgel 2004; Brack 2007; Dalai *et al.* 2016; Erastova *et al.* 2017; Teichert *et al.* 2019; Xu *et al.* 2020), so even these are not necessarily unambiguous biosignatures by themselves.

None of this is to deny that anomalies or patterns in the overall molecular profile of martian organic matter could still be strongly suggestive of biosynthesis (despite pitfalls; even meteoritic carbon can apparently show a preference for odd-over-even carbon numbers; Westall *et al.* 2018). Some molecules – which, once life is established, it produces continuously – are too complex to assemble in large numbers without biologically evolved machinery (see Marshall *et al.* 2017 for a discussion of where the abiotic/biotic 'threshold' might be). If we are lucky, it may be possible to recognize such anomalies even if martian life is built from a significantly different core chemistry from life on Earth (Goesmann *et al.* 2017; Marshall *et al.* 2017). But timing is everything: sedimentary rocks at Jezero Crater and Oxia Planum were probably deposited within only a few hundred million years of the origin of life on Earth; even if they post-date an origin of life on Mars, it may

be impossible to detect any biotic signal amid the complex products of a still largely 'prebiotic' carbon cycle (Lindsay *et al.* 2005).

Assessment of the biogenicity of organic matter (or any other candidate biosignature) will require close study of the geological context by the Rosalind Franklin or Perseverance rovers. An association between complex organic matter and evidence for local serpentinization, hydrothermal conditions favourable for Fischer–Tropsch type synthesis, or perhaps ferrocyanide salts (Sasselov *et al.* 2020), could be especially suggestive of abiotic/prebiotic chemistry rather than biotic chemistry. From this point of view, the lack of clear mineralogical evidence (so far) for local hydrothermal activity at the Oxia Planum landing site is reassuring. However, the large fluvial catchment area in this region may have concentrated organic matter of remote and diverse provenance and carbonate minerals in Jezero Crater could be related to serpentinization (Quantin-Nataf *et al.* 2021; Zastrow and Glotch 2021).

Conversely, any association between organic matter and other potential biosignatures (e.g. morphologies) could strengthen the case that life has been found. However, caution is needed again here. We lack a good understanding of how abiotic organic matter would have interacted with minerals and fluids on Noachian Mars and several forms of inorganic 'pseudobiosignature' might have adsorbed or passively entrained abiotic organic matter in some settings. In addition, organic matter itself can self-organize into life-like morphologies under some conditions (see following section on organic biomorphs).

Pseudomicrobialites

Microbialites are microbially influenced organo-sedimentary structures that result from the trapping and binding of sediment and the authigenic precipitation of calcium carbonate and other minerals in benthic microbial communities (Burne and Moore 1987). The interplay between these biotically driven processes and extrinsic hydrodynamic, sedimentary and physicochemical conditions generates a wide variety of microbialite morphologies and textures, many of which have a fossil record on Earth reaching back to the Archean (Noffke *et al.* 2006; Baumgartner *et al.* 2019). The most abundant fossil microbialites are stromatolites and microbially induced sedimentary structures (MISS). Stromatolites are laminated growth structures that project upwards as cones, domes, ridges and columns, whereas MISS are less vertically extended and can be restricted to single bedding planes (Noffke *et al.* 2001). MISS include fossil microbial mats, under-mat textures and wrinkle structures formed in microbially biostabilized clastic sediments; these macroscopic forms are commonly accompanied by micro-textural features such as oriented grains and crinkly organic-rich laminae (Noffke *et al.* 2001).

Microbialites have excellent preservation potential in carbonate, chert and siliciclastic facies and might easily be large enough to image at good spatial resolution using the Mars rover cameras and close-up imagers. Structures that resemble microbialites have been highlighted as attractive targets for sampling and return (Westall *et al.* 2015; Hays *et al.* 2017; Vago *et al.* 2017; McMahon *et al.* 2018). However, it is generally accepted that gross morphology alone is an unreliable indicator of the biogenicity of sedimentary structures and that (micro)textural and geochemical data will be necessary to confirm any tentative identification of microbialites on Mars (Noffke 2018). Relevant observations would include filamentous microfossils, crinkly carbon-rich laminae, fenestrae (fossilized gas bubbles, which can contain mineral grains indicative of local photosynthetic oxidation), oriented grains and grains 'floating' in an organic matrix (Noffke *et al.* 2001; Noffke 2018; Wilmeth *et al.* 2019). All of these features might (just) be large and distinct enough to resolve *in situ* using rover cameras (Table 1) if they are found in fresh drillcore (Noffke *et al.* 2001; Noffke 2018). Abiotic processes are also unlikely to mimic the conical form and regular spacing of some ancient stromatolites, features that are now understood to result from phototactic growth and competition for nutrients and light (e.g. Batchelor *et al.* 2004; Petroff *et al.* 2010). Microbialites that lack any of these features (or in which they cannot be detected by rover instruments) may be difficult to distinguish from pseudofossils. Indeed, there are several indications that pseudomicrobialites could have formed both on Earth and on early Mars.

The biogenicity of some stromatolite-like structures in very ancient (meta)sediments on Earth has often been contested (e.g. Grotzinger and Rothman 1996; Allwood *et al.* 2018; Zawaski *et al.* 2020). The presence of (pseudo)laminations can result from abiotic factors, including a variable energy/sediment supply during deposition and self-organization during crystallization, diagenesis, metamorphism and chemical weathering (Ortoleva 1994; Brasier *et al.* 2017, 2019; Allwood *et al.* 2018; Zawaski *et al.* 2020) (Fig. 1a). Domes and ridges can form via soft sediment or tectonic deformation (Antcliffe and McLoughlin 2008; Allwood *et al.* 2018). Grotzinger and Rothman (1996) showed that the laminations seen in some purported Precambrian stromatolites conform to the Kardar–Parisi–Zhang equation, which describes the growth of self-affine interfaces in terms of particle supply, surface-normal growth, random accretion and relaxation/diffusion. Because the Kardar–Parisi–Zhang equation captures the growth of a variety of interfaces, both biotic and abiotic, this result implies that organisms were not necessarily involved in shaping these laminations.

McLoughlin *et al.* (2008) showed experimentally that aerosolized colloidal paint sprayed onto a flat surface generates laminated deposits with remarkably stromatolite-like domes and columns, albeit on a small scale (column width <1 cm) (Fig. 1b, c). Many similar examples have been collected from factory floors where spray paint is applied to cars. The ballistic deposition of colloids (which can also be modelled using the Kardar–Parisi–Zhang equation) thus seems to be a plausible abiotic mechanism for the origin of stromatolite-like morphologies in the calcareous and

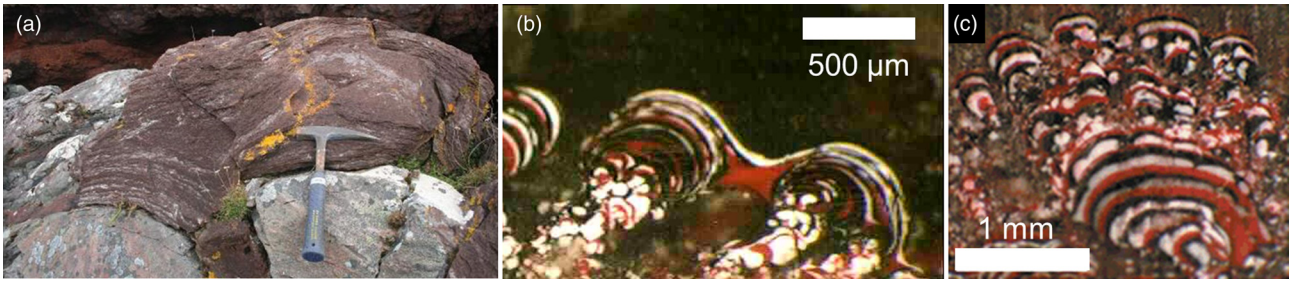

Fig. 1. Pseudomicrobialites. (**a**) Laminated red siltstones draping the surface of gneiss boulders (Brasier *et al.* 2017). (**b**, **c**) Stromatolite-like laminated domes and branching columns formed by aerosolized colloidal paint sprayed onto flat surfaces (McLoughlin *et al.* 2008). Images reproduced with permissions.

siliceous deposits found in hot spring 'splash zones' on Earth. Such deposits commonly contain fossil bacteria, but this does not necessarily mean that bacteria were instrumental in producing the macroscopic stromatolite-like growth pattern (McLoughlin *et al.* 2008). Small-scale, dendritic stromatolite- (and thrombolite-) like forms can also result from diffusion-limited aggregation at high surface tension (Duarte-Neto *et al.* 2014).

Less is known about how pseudo-MISS might form, but Davies *et al.* (2016) emphasized that particle-sticking, loading, fluid escape, impression, shear and shrinkage can generate complex, 'MISS-like' sedimentary surface textures in sufficiently cohesive and plastic sediments. They provide examples from modern and ancient settings where abiotic factors have imbued sediments with high viscosity and cohesivity, mimicking some of the patterns and textures associated with biostabilization (Davies *et al.* 2016).

We speculate that two general attributes of depositional environments on early Mars may have been especially conducive to the formation of pseudomicrobialites. First, fine-grained clay-rich sediments that were presumably not bioturbated by animals would have been naturally cohesive and thus able to form and retain a variety of sedimentary structures that might be mistaken for fossil MISS (Davies *et al.* 2016). Direct evidence for a high degree of sediment cohesion on early Mars has been discovered at Gale Crater in the form of fossil subaqueous shrinkage cracks, a sedimentary structure sometimes associated with microbial biostabilization on Earth (Siebach *et al.* 2014; McMahon *et al.* 2017).

Second, aqueous fluids interacting with early martian sediments may commonly have been rich in silica, salts and other dissolved minerals liable to precipitate as cements and crusts near the sediment–water(–atmosphere) interface, further enhancing sediment cohesion and potentially generating intrastratal cracks, polygons, tepee structures and related macroscopic effects that may superficially mimic MISS (McLennan *et al.* 2005). Pseudomicrobialites might also have adsorbed and absorbed a certain amount of abiotic organic matter from the environment as carbon-rich laminae (e.g. from 'primordial oil slicks'; Nilson 2002).

The effects of post-depositional processes may also confound the detection of true microbialites on Mars. Many martian outcrops are sculpted by wind abrasion and are unlikely to display well-preserved textures on bedding planes unless they have been very recently exposed. Irregular textures and forms that seem to resemble microbialites can result merely from the vagaries of erosion. Thus the MISS-like features identified by Noffke (2015) in Curiosity rover imagery from Gale Crater appear not to be primary sedimentary structures (Davies *et al.* 2016; McMahon *et al.* 2018).

Sinter-like hot spring silica deposits are unlikely to be encountered by the Perseverance or Rosalind Franklin rovers, but were previously observed by the Spirit rover in Gusev Crater (Ruff and Farmer 2016). This opaline deposit consists of porous, nodular material with millimetre- to centimetre-scale finger-like extensions, resembling fossil-microbe-bearing silica structures from hot springs on Earth described as 'microbially mediated microstromatolites' (Ruff and Farmer 2016; Ruff *et al.* 2020). A potential abiotic explanation for this morphology is that the silica precipitated evaporatively from sprayed or splashed droplets or accumulated from the ballistic deposition of suspended particles (McLoughlin *et al.* 2008). Experimental work to refine and test this hypothesis would be worthwhile.

Inorganic biomorphs

Mars rovers are not designed or equipped to detect microfossils of bacterial cell size *in situ* (Table 1). On Earth, some Archean cellular fossils are >100 µm across, but these are carbonaceous compressions and cannot be visualized clearly until they have been macerated out of the host rock with hydrofluoric acid (Javaux *et al.* 2010). Many Proterozoic and younger cherts on Earth contain morphologically diverse filamentous and spheroidal microorganisms preserved by carbonaceous material, which can also be hundreds of micrometres in maximum dimension (e.g. Barghoorn and Tyler 1965; Schopf 1968; Garwood *et al.* 2020). However, these cannot be visualized clearly except in finely polished rock slabs or petrographic thin sections, which will not be produced by the rovers *in situ*. Nevertheless, pseudofossils on the scale of micrometres to centimetres may confound the search for life on Mars for two reasons. First, objects at the upper end of this size range will be visible to rover cameras and may be associated with other apparent lines of evidence for biogenicity (e.g. organic matter). Second, objects at the lower end may be detected by microscopy in samples cached by the Perseverance rover if and when they are eventually returned to Earth, or in future studies of martian meteorites.

The term 'biomorph' is particularly associated with carbonate–silica precipitates, but is used here in a wider sense to describe all small abiotic structures that bear a morphological resemblance to living or fossil microbes (including, for example, mineralized extracellular sheaths). Biomorphs have been discovered in numerous reaction–diffusion–precipitation systems, both in nature and in the laboratory, some of which are more familiar to palaeontologists than others. Chemical gardens were discovered in the seventeenth century and their potential to misleadingly resemble fossils has long been recognized (Liesegang 1914; Hawley 1926), but bears repeating (McMahon 2019). For reasons not altogether clear, candidate fossils are often compared with carbonate–silicate biomorphs, even when other known classes of biomorph are more similar (e.g. Dodd *et al.* 2017; Gan *et al.* 2021).

Classical chemical gardens

First described at the dawn of modern chemistry (Glauber 1646), chemical gardens are plant-like structures formed by reactions between transition metal salts and aqueous anionic solutions of, for example, silicate (Barge *et al.* 2015) (Fig. 2a–d). In the classic chemical garden experiment, a salt seed crystal begins to dissolve in a sodium silicate solution (*c.* pH 12), releasing acid that reacts spontaneously with the alkaline medium to produce a semipermeable membrane of gelatinous silica around the crystal (within seconds to minutes). Osmotic inflow increases the pressure inside the membrane until it ruptures, expelling a jet of acidic fluid that tends to rise buoyantly. New silica membrane ensheaths the expelled fluid, forming a thin tube that connects to the rupture point and is contiguous with the original membrane envelope. The tube may remain open at the tip and continue to grow for some time; it may also produce branches of equal or lesser thickness. Multiple tubes may develop from a single seed crystal (Fig. 2a). Growth of the chemical garden continues until the seed crystal has fully dissolved.

Although initially soft and flexible, chemical garden tubes harden and become brittle as metal (oxyhydr)oxides precipitate on their interior walls (McMahon 2019; Kotopoulou *et al.* 2021) (Fig. 2d). The tubes are typically highly circular in cross-section and can show a variety of interesting biomimetic morphologies formed during growth, including helical twisting, coiling (Fig. 2c), pinching, swelling, tapering, sinuously curving growth trajectories, serial bifurcation (branching) (Fig. 2b) and occasional anastomosis – that is, the reconnection of independent branches (Leduc 1911; McMahon 2019). Tube diameters range from micrometres to several millimetres depending on the experimental conditions, with a wall thickness controlled by the extent of metal oxyhydroxide and silica precipitation, which can largely occlude the internal space (resulting in a porous, but 'filled', filament rather than an open tube; McMahon 2019).

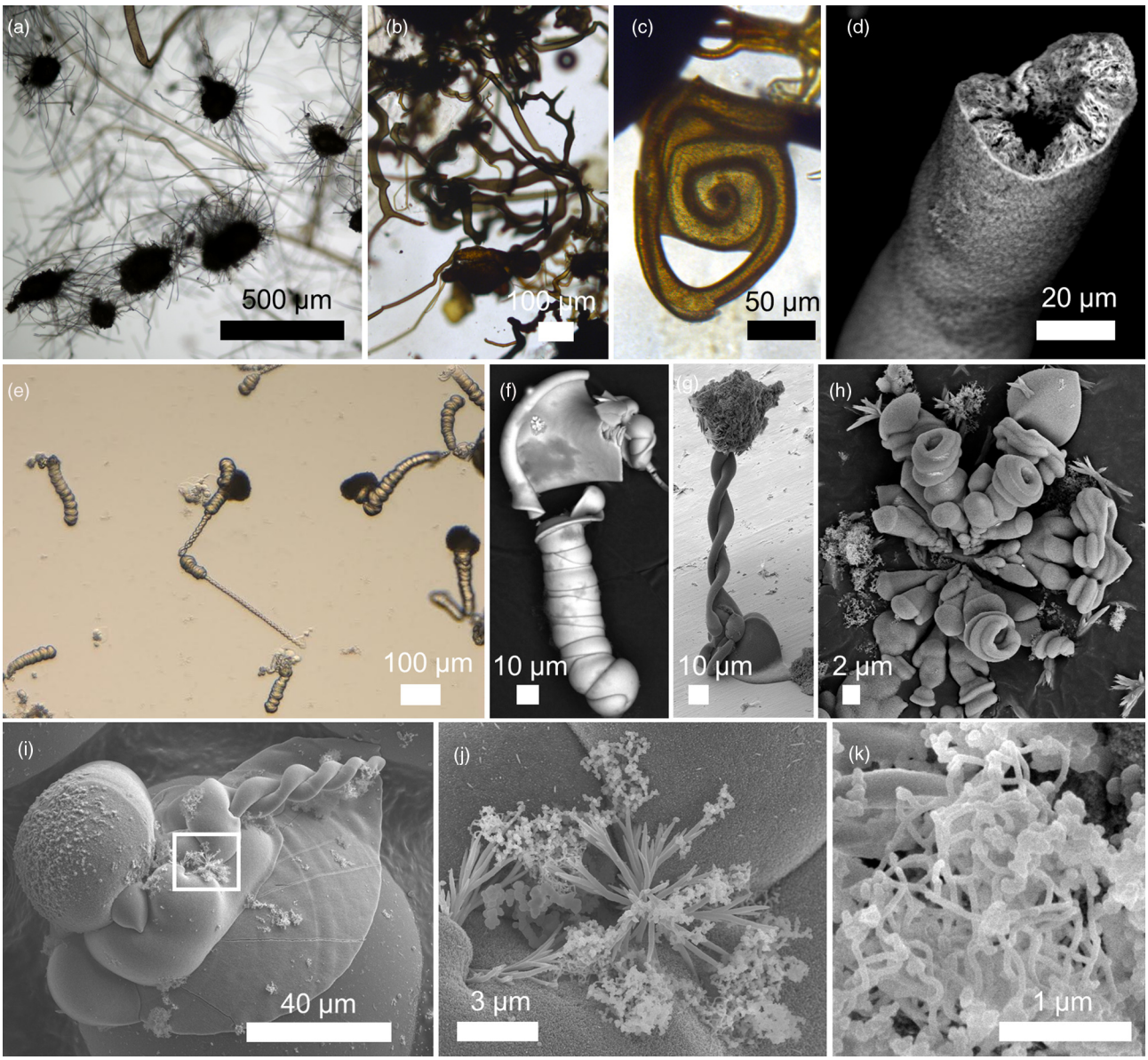

Fig. 2. (**a–d**) Chemical gardens and (**e–k**) carbonate–silica biomorphs. (**a**) Rosettes of tubes emerging from seed crystals. (**b**) Serially branching, irregularly curved tubes. (**c**) Snail-like coiled tube. (**d**) Siliceous tube with rough Fe (oxyhydr)oxide-coated interior and hollow central cavity. (**e**, **f**) Worm-like braid, (**g**) helicoidal and (**h**) mushroom-like biomorphs. (**i**) Composite of globular, sheet-like and helicoidal morphologies. (**j**) Close-up of the area depicted by the white rectangle in part (i) showing dendrites produced by fractal growth. (**k**) Close-up of thin sinuous filaments and globular amorphous silica. Chemical garden images SM (parts a–c) or reproduced from McMahon (2019) under creative commons license (creativecommons.org/licenses/by/4.0/) (part d). Images of carbonate–silica biomorphs courtesy of J. Rouillard and S. Borenstazjn (Institut de Physique du Globe de Paris) (parts e–h) and P. Knoll and O. Steinbock (Florida State University) (parts i–k).

Many variations on this theme have been explored, including chemical gardens formed on the injection of acidic solutions rather than the dissolution of salts, 'inverse' chemical gardens formed on the injection of the alkaline solution into the acid and quasi-2D chemical gardens confined in a narrow space between two flat plates (see Barge *et al.* 2015 for review). It is clear that chemical gardens can produce tubules from naturally occurring alkaline solutions and minerals, so they should not be dismissed as 'exotic' to natural environments (García-Ruiz 2000; García-Ruiz *et al.* 2017; McMahon 2019; McMahon *et al.* 2021).

As their name implies, chemical gardens are misleadingly life-like. Once solidified, they resemble fossil microorganisms, particularly Fe-mineralized fossil bacteria and fungi, in size, shape and composition. They may be relevant to the remarkable profusion of filaments composed of metal oxides, oxyhydroxides and (alumino)silicates found in siliceous and calcareous mineral deposits of all ages on Earth, including cavity fills in many volcanic and metavolcanic rocks (McMahon 2019; McMahon and Ivarsson 2019; McMahon *et al.* 2021). Many of these are probably fossils – indeed, fossils from a deep biosphere hosted in igneous rocks, with special relevance to some scenarios for life on Mars – but some are probably not and may result from chemical-garden-like processes and/or other types of self-organization that lead to filamentous crystals and aggregates (e.g. Hopkinson *et al.* 1998; Oaki and Imai 2003; Toramaru *et al.* 2003; Bonev *et al.* 2005).

The biotic interpretation receives support from the observed mineralizing behaviour of some modern organisms. Filamentous Fe-oxidizing bacteria, such as those in the *Sphaerotilus–Leptothrix* group, produce Fe-oxyhydroxide sheaths that conform to the filament surface, producing tubes that can bifurcate where cells divide, and are commonly vacated by cells leaving little or no organic residue (Emerson and Moyer 2002; Chan *et al.* 2016). The sheath exteriors can accumulate a flocculent Fe-oxyhydroxide coating up to several tens of micrometres thick (Schmidt *et al.*

2014). These microstructures are easily preserved in a silica matrix (chert) or in calcium carbonate and have a putative fossil record reaching back over million- to billion-year timescales (Dodd *et al.* 2017; Georgieva *et al.* 2021), although some of these purported fossils may be abiotic (Hopkinson *et al.* 1998; McMahon 2019; Johannessen *et al.* 2020; McMahon *et al.* 2021). Other Fe-oxidizing bacteria (e.g. *Gallionella*, *Mariprofundus*) secrete twisted, ribbon-like 'stalks' composed largely of Fe-oxhydroxides, which likewise can bifurcate during cell division (Chan *et al.* 2016). Again, however, there is a distinct potential for chemical gardens and other processes of crystallization and polycrystalline aggregate formation to generate twisted ribbons and other helical forms (Leduc 1911; García-Ruiz 2000; Oaki and Imai 2003; Jordan 2008).

Natural chemical gardens could plausibly have formed as a consequence of chemical weathering on Mars (García-Ruiz 2000; García-Ruiz *et al.* 2020; Sainz-Díaz *et al.* 2021). Soluble Fe and Mg sulfate salts have been identified at various martian localities (Johnson *et al.* 2007; Bishop *et al.* 2009; Ojha *et al.* 2015). Many of these likely formed in part through the dissolution and leaching of basaltic silicate minerals by sulfur-rich, acidic, oxidizing fumarolic fluids and vapours, which can be efficient even at very low temperatures (Tosca *et al.* 2004; Niles *et al.* 2017; Ruff *et al.* 2020); others probably formed by the aqueous oxidation of sulfide minerals (e.g. Dehouck *et al.* 2012). These sulfates would produce chemical gardens if introduced (as solids or in solution) to sufficiently silica-rich, alkaline fluids (e.g. in the subsurface).

Such fluids would have been supplied in some localities by serpentinization (i.e. the reaction of water with mafic and ultramafic minerals) and by the alteration of serpentinites, which, on Earth, can generate natural waters in which chemical gardens grow readily (García-Ruiz *et al.* 2017). Mineral assemblages suggestive of local serpentinization and serpentine alteration occur at several localities on Mars, including Jezero Crater (Ehlmann *et al.* 2010; Michalski *et al.* 2018; Brown *et al.* 2020; Zastrow and Glotch 2021). More generally, the copious production of silica-rich fluids on early Mars is attested by the widespread occurrence of hydrated silica deposits in fluviolacustrine and groundwater-influenced settings (Pan *et al.* 2021). It has been shown experimentally that chemical gardens can form even at temperatures and pressures characteristic of Amazonian and present-day Mars, close to the H_2O triple point (Sainz-Díaz *et al.* 2021).

Carbonate–silica biomorphs

Carbonate–silica biomorphs are strikingly biomorphic inorganic objects composed of amorphous silica and crystalline carbonates of the alkaline earth metals (Ba, Sr or, more rarely, Ca) (Fig. 2e–k). First described by Juan Manuel García-Ruiz in the early 1980s (García-Ruiz and Amorós 1981*a*, *b*), they are formed in the laboratory through the slow crystallization of a carbonate phase under moderately alkaline conditions (*c.* pH 8.5–11) in the presence of silica, originally present as a silica gel or, in more recent work, in solution. They display dimensions ranging from a few micrometres to a few hundred micrometres and can adopt a wide diversity of life-like morphologies, most of which can be classified into three categories: (1) helicoidal filaments (Fig. 2g, i); (2) worm-like braids (Fig. 2e, f); and (3) leaf-like flat sheets (Fig. 2i) (Kellermeier *et al.* 2012*c*). Under some conditions, more atypical morphologies – such as flower-like forms, 'trumpets', 'corals', 'moths', 'snails' or 'mushrooms' (Fig. 2h) – can also be found (Opel *et al.* 2018; Rouillard *et al.* 2018).

In addition to their curved or sinuous overall shapes, in appearance more akin to the living than to the mineral world, carbonate–silica biomorphs also display complex internal structures and textures that are reminiscent of biological objects. They frequently possess a core–shell structure, with an enveloping 'skin' of amorphous silica and an internal core composed of aggregated carbonate nanocrystals. The following section on mineralogical signatures shows that the polycrystalline core of the carbonate–silica biomorphs can be described as a quasi-mesocrystal, a characteristic of minerals formed by living organisms.

The complex morphologies of the carbonate–silica biomorphs emerge from purely inorganic mineral growth mechanisms. In an initial fractal growth stage, dendrites (Fig. 2j), dumbbells, framboids and spheroids are formed. Fractal growth here is due to silica poisoning of the surface of the carbonate crystallites, causing them to repeatedly split at non-crystallographic angles. In a second stage called 'curvilinear growth', polycrystalline mineral sheets grow radially in two dimensions, forming flat structures such as discs and leaves. Curling at the margins of these sheets introduces curvature and leads to the development of twisted shapes, such as helicoidal filaments and braids (García-Ruiz *et al.* 2009; Kellermeier *et al.* 2012*a*; Rouillard *et al.* 2018). The growth of these curling sheets is fed by an autocatalytic process in which carbonate precipitation locally decreases the pH, triggering the polymerization of amorphous silica, coating and cementing the carbonate crystallites and preventing further growth. In turn, silica polymerization locally increases the pH, allowing the precipitation of new carbonate building blocks (Kellermeier *et al.* 2012*b*).

Although purely inorganic, the curved and sinuous shapes of the biomorphs evoke biological objects, such as helical and segmented filamentous microbes, protists and even plants and animals. Interestingly, the hydrophobic surfaces of carbonate–silica biomorphs readily incorporate or adsorb organic molecules (García-Ruiz *et al.* 2002; Opel *et al.* 2016), which, as already discussed here, may have an abiotic origin on Mars. Although they have (so far) not been observed to form spontaneously in the environment, carbonate–silica biomorphs were obtained experimentally from natural alkaline silica-rich spring waters derived from serpentinization environments (García-Ruiz *et al.* 2017) and they may have formed in some hydrothermal environments of the early Earth (García-Ruiz 1994; García-Ruiz *et al.* 2020). Similar geochemical conditions, also conducive to the formation of chemical gardens, may have prevailed in alkaline, silica-rich fluids associated with serpentinization on early Mars.

Fibrous crystals, trichites and other crystallites

Strong or irregular curvature induced during the growth or deformation of fibrous or acicular crystals can generate shapes reminiscent of filamentous microorganisms. Muscente *et al.* (2018) described curving Mn oxide (MnO) crystals of probable metasomatic origin preserved in Neoarchean chert from the Pilbara Craton of Australia and noted that their simple morphology could be compared with some purported filamentous microfossils. In addition to Mn oxides, many clay and serpentine group minerals known or predicted to exist on Mars also show a fibrous habit, including sepiolite–palygorskite, celadonite and serpentine (Bishop *et al.* 2008; Ehlmann *et al.* 2010; Bristow and Milliken 2011). In addition, spectacularly complex and varied thread-like crystallites ('trichites') of pyroxene and other igneous minerals are found in volcanic and impact-related glasses, formed by the quenching of molten rock. Glass fragments are expected to be widespread in wind-blown sediments on Mars, albeit in a chemically weathered condition (Horgan and Bell 2012).

On Earth, trichites in natural glass are readily visible in thin section, where their resemblance to fossil microorganisms was first noted by Cloud (1976). They can be tightly coiled, looped, branched and irregularly curving (worm-like); they are sometimes found in spider-like starburst arrangements (Ross 1962; Engelhardt *et al.* 1995) (see Fig. 4a). They are commonly subdivided into smaller aligned crystallites, giving them a segmented appearance. Trichites commonly nucleate on the walls of vesicles formed by

trapped volatiles. Glass vesicles themselves can also resemble microfossils, as noted with respect to some scoria fragments found in the 3.4-Gyr-old Strelley Pool Formation of Western Australia, where vesicles are coated with kerogen-like carbonaceous material (Wacey *et al.* 2018).

It is unlikely that fibrous crystals, trichites and other crystallites would be large and distinct enough to resolve with Mars rover cameras (Table 1) and yet at the same time small enough to resemble microorganisms. They may be discovered in returned samples, but if they are well preserved, then it would then be straightforward to exclude them from consideration as microbial fossils because they can be recognized by their composition, crystallographic parameters and angular, faceted cross-sections. Diagnosis may be more difficult, however, where mineral particles have decomposed or altered to produce substances and morphologies more similar to mineralized microfossils, with softened/rounded cross-sections and hollow interiors. Thus, we tentatively suggest that solid and hollow filaments observed in impact glass by Sapers *et al.* (2014) could be modified trichites of some kind (*cf.* Pickersgill *et al.* 2021).

McMahon *et al.* (2021) described inorganic (Mg silicate + Fe oxide) filamentous dubiofossils occurring in calcite veins from the pervasively oxidized serpentinites of NW Italy and speculated that they might represent coated and recrystallized mineral fibres, among other possible explanations. A misleading association with organic matter can also complicate the interpretation of mineral grains. Horodyski (1981) noted that apatite grains in a Mesoproterozoic shale had acquired a coating of organic matter that created a superficial resemblance to fossil microorganisms. Similarly, Wacey *et al.* (2016*b*) showed that carbonaceous microstructures in the 3.5-Gyr-old Apex Chert, previously interpreted as fossil filamentous bacteria, are, in fact, altered particles of potassium mica, which were expanded into worm-like structures (the mineral vermiculite) by hydrous alteration and then coated at a late stage by carbon 'moving around the system'. Hematite aggregates in the same chert unit are also filament-like and have been described as 'pseudomicrofossils' (Marshall *et al.* 2011). Even genuine microfossils can be secondarily enriched in carbon from such external sources (Rasmussen *et al.* 2021).

Organic biomorphs

According to biogenicity determination protocols, life-like morphologies with organic composition score more highly than inorganic life-like morphologies (e.g. McLoughlin and Grosch 2015; Neveu *et al.* 2018). Nevertheless, organic materials are no less capable than mineral particles of forming a wide variety of biomorphs; indeed, structural self-organization in the organic milieu necessarily preceded the origin of life on Earth (and perhaps Mars). Known organic biomorphs can be divided into the recently discovered carbon–sulfur biomorphs and the morphologically simpler spheroids that result from hydrophobic interactions with water. We are aware that chemical gardens can also be produced from organic salts and solutions, but (so far) the known examples are of limited geological relevance (e.g. Bernini *et al.* 2021).

Carbon–sulfur biomorphs

Carbon–sulfur biomorphs are microscopic spherical and tubular objects composed of elemental sulfur encapsulated within an organic envelope (Fig. 3). Their sizes range from a few tens of

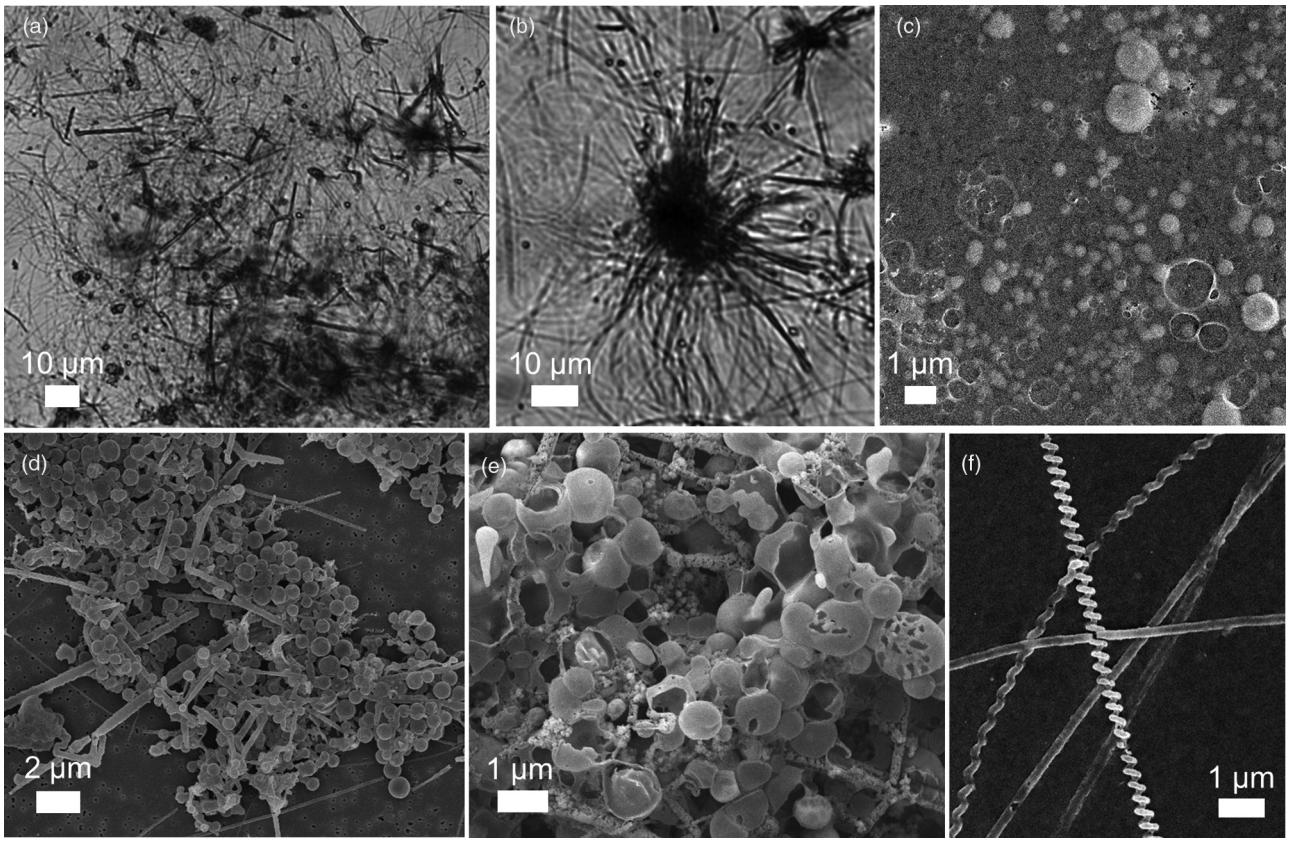

Fig. 3. Carbon–sulfur biomorphs. (**a**) Complex network formed by filaments and spheres. (**b**) Rosette. (**c**) Empty organic vesicles during early stages of carbon–sulfur biomorph formation. Small organic vesicles later coalesce into *c.* 1 µm spheres. (**d**) Aggregate of spheres and filaments. (**e**) Spheres with visible organic envelopes. (**f**) Straight and helical filaments. Images adapted from Nims *et al.* (2021) (parts a and b) or JC (parts c and f) and courtesy of C. Nims (University of Michigan) (parts d and e).

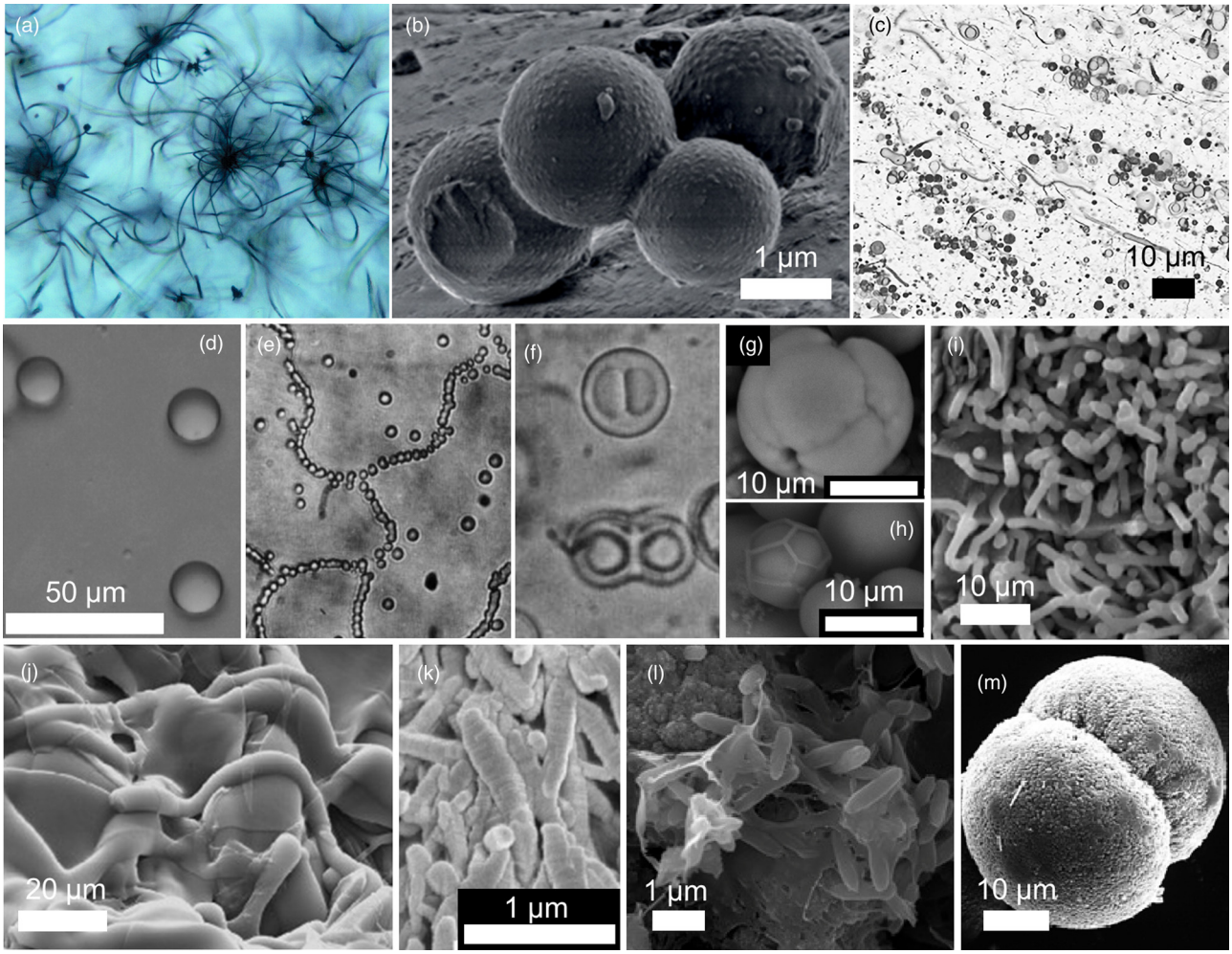

Fig. 4. Other types of organic and inorganic biomorphs. (**a**) Asteroidal trichites radiating from central magnetite grains in a natural volcanic glass (Cougar Mountain, Oregon). (**b**) Organic microspheres obtained from RNA and quartz mixtures under diagenetic conditions (Criouet *et al.* 2021). (**c**) Amphiphilic spherical and tube-like vesicles formed by mixed fatty acids and 1-alkanols (C_{10}–C_{15}) in 10 mM $CaCl_2$. Courtesy of S.F. Jordan. (**d**) Coacervate microdroplets prepared in water by mixing PDDA with ATP (M. Li *et al.* 2014). (**e**, **f**) Chain-forming and twinning proteinoid microspheres obtained by heating mixtures of amino acids (Fox and Yuyama 1963). (**g**, **h**) Apatite particles formed by double diffusion in gelatin mimicking dividing cells and raised polygonal features in embryos (Crosby and Bailey 2017). (**i**) Rod-shaped silica particles formed on the walls of basalt fractures injected with supercritical CO_2 (Schaef *et al.* 2011). (**j**) Cryogenic opal filaments and sheets formed in rapidly freezing silica-rich fluids (Channing and Butler 2007). (**k**) Cryogenic carbonate segmented filaments obtained by freezing of silica-rich alkaline brines (Fox-Powell and Cousins 2021). (**l**) Rod-shaped apatite particles forming within organic films in sediments (Mänd *et al.* 2018). (**m**) Fluoroapatite particle precipitated in the presence of citrate, mimicking dividing coccoid cells (Wu *et al.* 2010). Images reproduced with permissions (parts a, d–h, j–m) or under creative commons licenses (part b, creativecommons.org/licenses/by-nc-nd/4.0/; part i, creativecommons.org/licenses/by-nc-nd/3.0/).

nanometres to a few micrometres in diameter. Carbon–sulfur biomorphs form spontaneously in aqueous solutions in which hydrogen sulfide is oxidized in the presence of dissolved organic molecules (including simple prebiotic organic molecules such as glycine) (Cosmidis and Templeton 2016; Cosmidis *et al.* 2019). The elemental sulfur core of the biomorphs is the product of chemical sulfide oxidation, while their organic envelope is thought to form through the self-assembly of amphiphiles produced by the reaction of organic molecules with sulfides and polysulfides in solution (Cosmidis *et al.* 2019). Observations of the early stages of carbon–sulfur biomorph formation reveal numerous empty vesicles, suggesting that the organic envelope may form prior to the sulfur core (Fig. 3c).

As a result of their spherical and tubular morphologies, carbon–sulfur biomorphs are reminiscent of microbial spherical and filamentous cells. These structures display more complex morphologies than the spheroids and aggregates produced by other known biomorph systems (see previous section). The tubular biomorphs may branch at 90° and 45° angles (Cosmidis and Templeton 2016), similar to some filamentous bacteria (e.g. *Streptomyces*), and they can be helicoidal (Fig. 3f), similar to helical bacteria (e.g. cyanobacteria of the genus *Oscillatoria*, spirochaetes). Tubular carbon–sulfur biomorphs can also form rosettes (Fig. 3b), mimicking those formed by filamentous microbes such as *Thiothrix*.

Although carbon–sulfur biomorphs are originally composed of organic carbon and elemental sulfur, experiments have shown that their sulfur core rapidly diffuses away during early diagenesis in silica-rich environments, leaving behind empty organic envelopes (Nims *et al.* 2021). The morphologies of the biomorphs are finely preserved through this diagenetic process as a result of the rapid precipitation of nanocolloidal silica at the surfaces of the organic spheres and tubes (Nims *et al.* 2021). The resulting silicified organic microstructures are strikingly similar to coccoidal and filamentous organic microfossils preserved in Precambrian cherts by the rapid precipitation of silica at the seafloor, as found, for instance, in the 1.9-Gyr-old Gunflint Formation in Canada (Wacey *et al.* 2013) or the *c.* 2.4-Gyr-old Turee Creek Group in Western Australia (Schopf *et al.* 2015; Barlow and Kranendonk 2018).

Mars has long been considered a 'sulfur-rich planet' (King and McLennan 2010), but, as a result of the oxidizing conditions at the surface, the vast majority of this sulfur is currently present as sulfate minerals (Franz *et al.* 2019). However, *in situ* sulfur isotope analyses acquired by NASA's Curiosity rover in Gale Crater suggest the existence of an active and fully developed sulfur redox cycle on early Mars (Franz *et al.* 2017). Evolved gas analyses performed by Curiosity's SAM instrument showed that reduced sulfur phases are present within ancient fluviolacustrine sediments at Gale Crater (McAdam *et al.* 2014; Wong *et al.* 2020). SAM also detected evidence for sulfurized organic matter in the 3.5-billion-year-old Murray Formation, indicating interactions between organic molecules and reduced sulfur (Eigenbrode *et al.* 2018; Heinz and Schulze-Makuch 2020).

Although the full space of physicochemical parameters permitting the formation of carbon–sulfur biomorphs remains to be explored, they have been synthetized in the laboratory at temperatures ranging from 4°C to room temperature, pH values ranging from acidic (*c.* pH 4) to slightly basic (*c.* pH 8) and salinities ranging from *c.* 0% (deionized water) to 3.5% (seawater), encompassing plausible conditions for wet environments on early Mars (Fukushi *et al.* 2019). As stated earlier, carbon–sulfur biomorphs can be finely preserved through silicification in silica-rich depositional settings, mimicking fossilization in cherts, a major preserving medium for many Archean and Proterozoic putative microfossils on Earth (Schopf 2006; Javaux and Lepot 2018). On Mars, rapidly forming silica deposits may have formed in different types of ancient sedimentary environments (reviewed by McMahon *et al.* 2018), allowing the preservation of carbon–sulfur biomorphs if they were ever present on that planet.

Other organic biomorphs

Most organic compounds are hydrophobic and tend to aggregate into spheres in the presence of water, commonly with dimensions similar to microorganisms. Thus, spherical organic particles were probably fairly abundant in any prebiotic milieu on early Mars (and Earth). Some of them would have had non-negligible potential to be preserved in the rock record. For example, research in applied chemistry has found that complex organic matter subjected to 'hydrothermal carbonization' (devolatilization in water at *c.* 200°C) assembles into stable, solid spheres similar in size to bacteria, with hydrophobic aromatic cores and hydrophilic shells ('hydrochar'; Sevilla and Fuertes 2009).

Criouet *et al.* (2021) found that similar spheres were formed when a mixture of RNA, quartz and water was held at 200°C under Ar for 20 days. These objects were *c.* 0.5–5 µm in diameter, variously textured and commonly connected together like dividing cells (Fig. 4b). Their composition, as probed, for example, by carbon X-ray absorption near-edge structure (C-XANES), resembles fossil bacteria more closely than it resembles the original RNA. Criouet *et al.* (2021) infer from previous experimental work on hydrochar that further diagenetic alteration of these structures could render them hollow and thus even more similar to fossil bacteria. The viability of an RNA world on early Mars has been explored – and broadly supported – in light of geochemical considerations (Mojarro *et al.* 2021), but, in any case, similar spheroids can very probably result from many other organic precursors. Indeed, similarly robust hollow hydrocarbon spheroids <1–50 µm in diameter were recovered from deep groundwater in the Witwatersrand Basin of South Africa, where they appear to have formed through the abiotic reorganization of thermally altered (ultimately biogenic) organic matter (Wanger *et al.* 2012). Sub-micron hollow organic 'globules' have also been identified in carbonaceous meteorites (Nakamura-Messenger *et al.* 2006).

Fatty acids produced by abiotic Fischer–Tropsch type reactions under hydrothermal conditions, like other amphiphilic compounds, readily self-assemble in water to form membranous vesicles from nanometres to hundreds of micrometres in size. Such vesicles may have played a part in the origin of life by encapsulating protocells (e.g. Deamer 2017). The stability of these vesicles under different conditions depends on the mixture of amphiphiles present. Experiments have shown that relatively long-chain (C_{10}–C_{15}) fatty acids and 1-alkanols generate vesicles in the warm, saline, alkaline waters characteristic of serpentinization-driven marine hydrothermal systems on the early Earth and Mars (Fig. 4c) (Jordan *et al.* 2019). Vesicle formation by fatty acids is also favoured over a wide pH range in non-marine hot spring settings (Deamer 2021). Lipid vesicles are typically spheroidal, but can extend into tubules and thread-like filaments (e.g. Zhu and Szostak 2009; Deamer 2021). The potential for any of these rather delicate structures to be preserved as morphological fossils is unclear, but has sometimes been mooted (e.g. Javaux *et al.* 2013).

Other structures discussed in prebiotic chemistry also have relevance as potential pseudofossils. Coacervates – microdroplets of viscous fluid that separate out from a colloidal solution (Fig. 4d) – can incorporate a variety of inclusion structures and were first suggested as possible protocells nearly a century ago (Oparin 1924). Coacervates have been produced from mononucleotides and peptides of surprisingly low molecular weight (Koga *et al.* 2011). Other coacervates based on similarly small molecules have been silicified in the laboratory to form solid spheroids with multiple sub-compartments, albeit through a rather non-naturalistic chemical process (Fothergill *et al.* 2014).

'Proteinoid microspheres' represent another spheroidal biomorph system once thought to be a plausible model for prebiotic protocells. These were discovered by Sidney Fox and co-workers, who showed that spheroids 1–2 µm in diameter self-assemble from thermally polymerized mixtures of dry amino acids (e.g. at >130°C for 3 h) after the addition of water (e.g. Fox and Yuyama 1963; Brooke and Fox 1977). These objects show a range of biomimetic features, including internal spheroids, sharply defined single or concentric double boundaries, 'twinned' growth strongly reminiscent of cells dividing, and aggregation into chains and networks (Fig. 4e, f). These pseudo-cells could presumably have arisen spontaneously on the early Earth or Mars if amino acids (e.g. from meteorites, atmospheric chemistry and hydrothermal reactions) became highly concentrated and subject to dry heat. It has been shown that some of these proteinoid microspheres are readily silicified to form pseudofossils with good preservation potential that can resemble eukaryotes as well as prokaryotes (Francis *et al.* 1978). Thus, as noted earlier, the availability of silica in both groundwaters and surface waters on early Mars could have assisted the preservation of both pseudofossils and fossils.

Other biomorphs

Very few natural or experimental systems have yet been studied in relation to their capacity to produce biomorphs in geochemically plausible settings, yet there are some tantalizing hints scattered across the scientific literature. For example, Oaki and Imai (2003) demonstrated the formation of smoothly curving filamentous dendritic aggregates from the precipitation of potassium dichromate in gelatin cooled from 100°C, a finding that may be relevant to the origin of similar structures found in some agates (which precipitate from silica gel). More generally, minerals grown in gels can sometimes adopt rounded and complex shapes (e.g. Dominguez Bella and García-Ruiz 1987; Crosby and Bailey 2017) (Fig. 4g, h).

Silica deposits formed on the walls of basalt fractures injected with wet, supercritical CO_2 at sterilizing temperatures resemble rod-shaped and filamentous bacteria (Schaef *et al.* 2011) (Fig. 4i).

Biomorphic particles of opal (Channing and Butler 2007) and carbonates (Fox-Powell and Cousins 2021) resembling microbial filaments precipitate from rapidly freezing mineral-laden waters (Fig. 4j, k), a process which may be particularly relevant for ancient hydrothermal systems on Mars. Abiotic silica spheroids found in hot spring ponds of the Dallol geothermal field, Ethiopia form botryoidal clusters that resemble coccoidal bacterial colonies (Belilla *et al.* 2019). All these systems require further investigation to elucidate new classes of geologically relevant biomorphs on Mars.

In addition to these processes, mineral structures can often adopt rounded, curved or complex life-like shapes when formed in the presence of organic molecules (which can be abiotic in origin), as already illustrated for carbon–sulfur biomorphs. More generally, 'organominerals' (i.e. minerals in which formation is mediated by organic molecules) (Défarge 2011) can present unusual, non-crystallographic morphologies as a result of the templating effect of the organic matrices on which they nucleate, or under the influence of organic molecules in solution during mineral growth. Soluble organic molecules can influence mineral shapes by poisoning some crystal faces after preferential adsorption, preventing further growth, or by stabilizing amorphous precursors and favouring their assembly into complex structures (Gower 2008). Organic molecules can promote the fractal growth of crystals, leading to the formation of rod-shaped particles (Fig. 4l), dumbbells, spherules, divided spheroids mimicking cell division (Fig. 4g, h, m) and 'cauliflower-like' structures (Busch *et al.* 1999; Wu *et al.* 2010; Sand *et al.* 2012; Crosby and Bailey 2017; Mänd *et al.* 2018).

A particularly relevant example for astrobiology is the observation of calcium carbonate particles precipitated in the presence of organic matter extracted from the Murchison CM2 meteorite. The minerals present rounded morphologies reminiscent of coccoid and rod-shaped bacteria (Reitner 2004) and similar to the calcareous structures previously interpreted as fossil microorganisms in the martian meteorite ALH84001 (McKay *et al.* 1996). More exotic mineral shapes – such as trumpets, helices, twisted ribbons and stars – can also be obtained through precipitation in the presence of large organic molecules, particularly polymers (Mukkamala and Powell 2004; Yu and Cölfen 2004).

Pseudobioalteration textures

Microorganisms can dissolve, etch and bore into solid substrates (Cockell and Herrera 2008). Bioalteration textures apparently resulting from these processes have been reported in various geological materials, most commonly basaltic glass, which is probably fairly widespread on Mars. Experiments have confirmed that bacteria etch cell-sized pits in volcanic glass in the laboratory (Thorseth *et al.* 1995). Alteration features in natural samples divide into two types: granular textures and tubular textures (extensively illustrated by Staudigel *et al.* 2006; Fisk and McLoughlin 2013). The granular type consists of closely packed, micrometre-scale spheroidal cavities, giving a spongy overall appearance. The tubular type consists of elongated cavities *c.* 1–6 μm wide, which extend up to hundreds of micrometres from altered glass surfaces and fractures (McLoughlin *et al.* 2019). Complex, biogenic organic material has been found in close association with both types (e.g. Fisk *et al.* 1998; Preston *et al.* 2011; Wacey *et al.* 2014), although some examples are less convincing on close inspection than they first appeared (McLoughlin and Grosch 2015; Wacey *et al.* 2017).

Experimental work has partially succeeded in mimicking the granular form abiotically by reacting basaltic glass with seawater at 150°C (a sterilizing temperature) for 48 days (McCollom and Donaldson 2019). Tubular textures, however, have never been reproduced in experiments, either with or without microbes. Some examples are more compellingly life-like than others, showing a variety of curving, twisting, branching, coiling and other elaborate morphologies suggestive of microbial growth. High-resolution microanalysis has shown that some of the simpler tubules are probably abiotic pseudofossils of uncertain origin (e.g. Pedersen *et al.* 2015). Titanite-filled 'microborings' in Archean basalts from South Africa and Western Australia have also now been convincingly reinterpreted as abiotic mineral growths, probably resulting from thermal metamorphism and seafloor hydrothermal recrystallization, respectively (Grosch and McLoughlin 2014, 2015; McLoughlin *et al.* 2020). These same processes could probably have generated analogous pseudofossils in basalts on Mars.

Relatedly, White *et al.* (2014) found linear microtextures and organic carbon associated with fracture-filling alteration minerals in the basaltic martian meteorite Yamato 000593 and interpreted them as possible evidence of microbial bioalteration. This view was rejected by McLoughlin *et al.* (2019), who showed that the textures were not tubular, but fracture-like, and that the carbon was most likely of hydrothermal origin. McLoughlin and Grosch (2015) present biogenicity criteria for alteration textures in (meta)volcanic rocks. Significantly, they argue that 'no terrestrial example yet described' achieves the maximum score of 'Category 5' necessary to demonstrate a biogenic origin.

Some features resembling 'microborings' are, in fact, ambient inclusion trails (AITs): snaking, tunnel-like cavities (which may be mineral-filled) formed by the propulsion of mineral grains through solid substrates, including quartz/chalcedony (Fig. 5a), phosphate minerals, chlorite and (rarely) altered volcanic glass (Wacey *et al.* 2008; Lepot *et al.* 2009, 2011; McLoughlin and Grosch 2015). AITs have also been found in clastic sedimentary rocks of Precambrian age (Fig. 5b). The cross-sectional shape and diameter of AITs are determined by the formative grain, most commonly a euhedral pyrite or magnetite crystal *c.* 0.5–10 μm across. Longitudinal marks seen in the trail walls are striations made by the grain vertices. The grain is sometimes still present at the end of the AIT. AITs are sometimes found in starburst patterns, indicating that the grains moved outward from a common centre (e.g. Knoll and Barghoorn 1974; Lepot *et al.* 2009). Examples in Paleoproterozoic chert were misdiagnosed as fossil algae by Gruner (1924) and re-classified as pseudofossils by Barghoorn and Tyler (1963).

AITs typically contain some organic matter and Wacey *et al.* (2016*a*) suggested that grain propulsion can be driven by microbially mediated decomposition of this material, which would make some AITs indirect biosignatures after all (Wacey *et al.* 2016*b*). However, there is evidence to suggest that the thermal decomposition of organic matter (which can be abiogenic) and metamorphic reactions involving chlorite might have formed some AITs abiotically – for example, in volcanic rocks free of biological influence (Lepot *et al.* 2009, 2011; Wacey *et al.* 2016*a*; Fig. 5a). Thus, these structures cannot be regarded as unambiguous biosignatures despite their life-like morphology and partly organic composition.

Mineralogical signatures: pseudobiominerals

Several previous reviews have focused on the use of minerals as biosignatures (Benzerara and Menguy 2009; Benzerara *et al.* 2019), including in the context of the search for life on Mars (Banfield *et al.* 2001). Biominerals – that is, minerals whose formation is controlled by living organisms or, at a minimum, induced or influenced by them (see Lowenstam 1981; Dupraz *et al.* 2009 for definitions of these terms) – can possess specific morphological, structural, textural or chemical characteristics that may allow their discrimination from abiotically produced minerals.

The most obvious feature common to many biominerals is their unusual morphology. Unlike inorganically precipitated minerals,

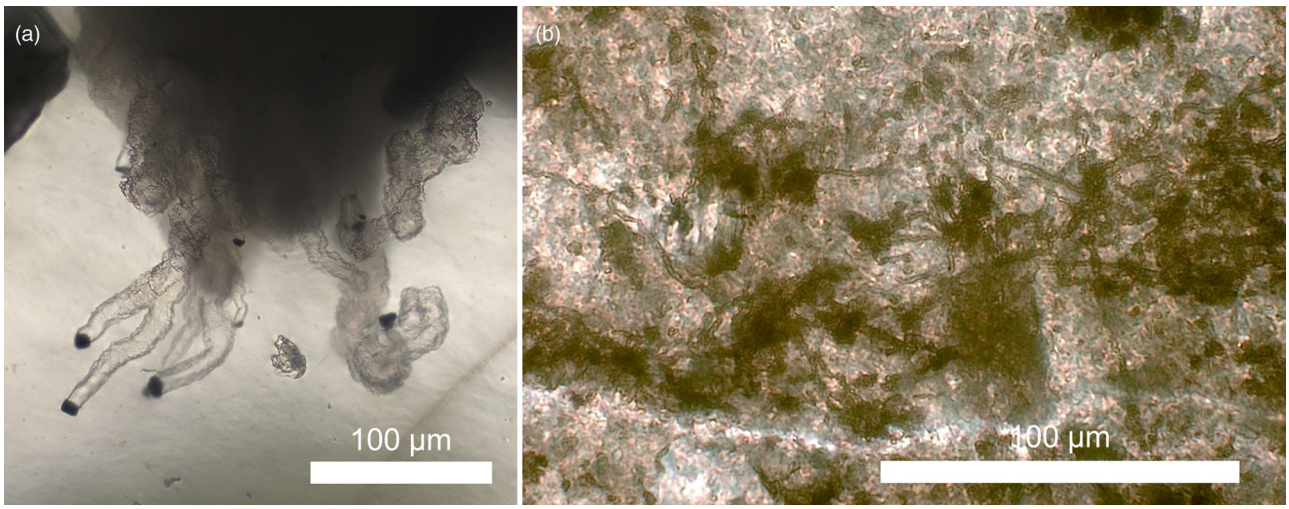

Fig. 5. Ambient inclusion trails (AITs). (**a**) AITS resembling microborings in agate (basalt-hosted chalcedony) from the Pentland Hills Volcanic Formation, Edinburgh, Lower Devonian. Note opaque terminal grains. Image: SM. (**b**) Titanite-filled AITs occurring in fine-grained sedimentary rock from the Late Ediacaran Gibbet Hill Formation of Newfoundland. Some trails terminate in pyrite crystals (not visible in this field of view). Image courtesy of J.J. Matthews (Oxford University Museum of Natural History).

which typically adopt crystal-like prismatic shapes, with sharp angles and straight faces, biominerals often have rounded or curved surfaces and overall morphologies that can be extremely complex. Although this is especially true of eukaryotic biominerals (e.g. the delicate architecture of the silica frustule of a diatom), bacterial biominerals can also display elaborate, non-crystallographic shapes, such as, for instance, the twisted iron-rich stalks and tubular sheaths produced by some microaerophilic Fe-oxidizing bacteria (Chan *et al.* 2009, 2011) or the sinuous elemental sulfur filaments produced by the sulfur-oxidizing bacterium *Candidatus* Arcobacter sulfidicus (Taylor and Wirsen 1997; Sievert *et al.* 2007). Experimental diagenesis (Picard *et al.* 2015), as well as studies of the geological record (Slack *et al.* 2007; Hofmann *et al.* 2008), show that these morphological characteristics can be preserved in rocks. However, as demonstrated in the section on biomorphs, a wide range of abiotic processes can produce mineral, organic and organic–mineral structures with similar life-like shapes, making morphology an ambiguous indicator of biogenicity (García-Ruiz *et al.* 2002).

Organic–mineral associations

Biominerals are commonly intimately associated with organic molecules and biominerals can often be described as inorganic–organic composite materials. This is especially true of Metazoan biominerals, which tend to be formed within matrices or vesicles composed of organic macromolecules controlling mineral nucleation, crystallization and growth (Weiner 2008; Addadi and Weiner 2014). In microbial systems, biominerals may be enclosed within intracellular organelles, which can be lipidic – as in the case of the magnetosome, an invagination of the cytoplasmic membrane encapsulating magnetic Fe minerals in magnetotactic bacteria (Uebe and Schüler 2016) – or proteinic – as in the case of the envelope surrounding elemental sulfur minerals in some sulfur-oxidizing bacteria (Dahl 2020). Microbial biominerals may also form within the microbial cell wall (Benzerara *et al.* 2004; Cosmidis *et al.* 2015), on the cell surface (e.g. on S-layers; Schultze-Lam *et al.* 1992; Phoenix *et al.* 2005), on extracellular polymeric substances (Dupraz *et al.* 2009; Couasnon *et al.* 2020) and polysaccharidic stalks and sheaths (Chan *et al.* 2009) or within extracellular organic vesicles (Cron *et al.* 2019; Marnocha *et al.* 2019).

Diagenesis experiments have shown that some of the resulting biomineral–organic assemblages may withstand burial at high temperatures and pressures (J. Li *et al.* 2013, 2014) and observations from the geological record confirm that minerals precipitating on or within microbial cells can lead to well-preserved organic–mineral associations in rocks (e.g. Cosmidis *et al.* 2013).

The instruments onboard the most recent and future martian rovers have the capability to detect and characterize intimate mineral–organic associations at high spatial resolution, such as SHERLOC on the Perseverance rover and MicrOmega on the Rosalind Franklin rover (using deep UV Raman and near-infrared/visible light spectromicroscopy, respectively; Table 1) (Beegle *et al.* 2015; Bibring *et al.* 2017). However, such close associations are expected to be found in non-biological contexts whenever minerals form in the presence of organic molecules (which again may be abiotic in origin).

Organic molecules can be passively adsorbed onto minerals through different types of binding interactions (e.g. Lagaly *et al.* 2013). Under certain conditions, mineral surfaces can even participate in the polymerization of these adsorbed molecules into larger, life-like macromolecules (as, for instance, in the surface-aided polymerization of amino acids on silicates, oxides and sulfides; Lambert 2008). As shown with the example of carbon–sulfur biomorphs, mineral precipitation in the presence of organic molecules may lead to self-assembled organic–mineral structures mimicking biomineral encapsulation within organic vesicles (e.g. Cron *et al.* 2019; Marnocha *et al.* 2019). Different processes on Mars may have led to the preservation of organic molecules at the surface of, or within, mineral particles (reviewed in Fornaro *et al.* (2018), but for the reasons cited here it is unlikely that the resulting mineral–organic assemblages, even if combined with biological morphologies, may serve as convincing biosignatures.

Mineral structures

Biominerals may present crystal structures that differ from those of their abiotically precipitated counterparts and whose formation is thermodynamically unfavourable under normal temperature and pressure conditions. For example, unstable phases of elemental sulfur, the monoclinic allotropes β-S_8 and ɣ-S_8, can be formed as biominerals by sulfur-oxidizing bacteria (Cron *et al.* 2019) and have been proposed as potential biosignatures in astrobiological investigations (Gleeson *et al.* 2012).

The presence of metastable crystal phases in biominerals likely results from mineral formation on or within organic matrices acting

like templates for nucleation (Falini *et al.* 1996), the stabilization of unstable mineral intermediates by organic molecules (e.g. amorphous calcium carbonate; Addadi *et al.* 2003) or modifications of the local chemical environment (for instance, increased supersaturation) within internal vesicles (Sviben *et al.* 2016; Uebe and Schüler 2016) or in the extracellular medium as a result of metabolic activity (Rodriguez-Navarro *et al.* 2007). Some aspects of the crystal structures of minerals present in martian rock and soil samples can be determined using different techniques such as Raman spectroscopy (SHERLOC and the Raman laser spectrometer onboard the Perseverance and Rosalind Franklin rovers, respectively; Table 1) (Beegle *et al.* 2015; Rull *et al.* 2017), although full crystallographic characterization will require sample return.

However, mineral precipitation in the presence of (non-biological) organic molecules can also induce the formation of metastable polymorphs, as demonstrated many times in laboratory experiments. For instance, a range of organic substances, such as alcohols (Sand *et al.* 2012), citrates (Tobler *et al.* 2015), amino acids (Hood *et al.* 2014; Tobler *et al.* 2014) and polymers (Xu *et al.* 2008; Sonobe *et al.* 2015) can impact calcium carbonate polymorphism and induce the formation of unstable carbonate phases such as aragonite and vaterite. The high-temperature sulfur allotropes β-S_8 and ɣ-S_8 can form abiotically at room temperature when sulfide is oxidized in the presence of different organic molecules, including non-biogenic organic molecules such as glycine (Cosmidis *et al.* 2019).

Precipitation under inorganic conditions can also produce thermodynamically unstable polymorphs. In the calcium carbonate system, a number of geochemical factors – such as rapid CO_2 degassing, high supersaturation or the presence of Mg and other divalent cations – can induce the formation of aragonite instead of calcite in natural springs (Jones 2017). Although rare on Earth, vaterite was found in an extremely cold and dry environment that may be a good analogue for carbonate deposits on other planetary bodies, but its formation and persistence was thought to be abiogenic and favoured by the extreme cold and high-pH waters (Grasby 2003).

These examples illustrate the fact that in order to interpret the presence of unstable polymorphs or other information on crystal structure as biosignatures, the geochemical context of mineral formation (including the fluid chemistry and presence and nature of organic molecules) must be fully known. This may be extremely difficult when investigating ancient sediments on early Mars. Other processes that may alter mineral structure after their formation (e.g. recrystallization) must also be taken into account – for instance, ageing, desiccation and exposure to high-temperature conditions (due to impact and volcanism, even in the absence of a strong geothermal influence during burial).

Beyond general crystal structure, some crystallographic features of biominerals have been proposed as potential biosignatures – for instance, crystal purity and the absence of defects in biogenic magnetites (Fischer *et al.* 2011; Li *et al.* 2015). The crystallographic properties of bacterial Mn oxides, such as an abundance of lattice vacancies, have been proposed as mineralogical biosignatures that could be detected on Mars using electron paramagnetic resonance spectroscopy (Kim *et al.* 2011). More work is needed on a wider range of biominerals and abiotic systems to validate these approaches.

Primary mineral textures

The texture of biominerals, defined here as crystallite size and organization, often differs strongly from that of abiotically precipitated minerals. This is partly due to their crystallization mode: although classical crystal growth proceeds by ion-by-ion addition, biomineralization often proceeds through the addition of pre-formed mineral nanoparticles and, as a result, many biominerals are actually polycrystalline materials (De Yoreo *et al.* 2015). When the nanoscale building blocks share a common crystallographic orientation, the resulting mineral is described as a mesocrystal (Sturm and Cölfen 2016). Examples are found in coral skeletons, the nacre layer of shells, sea urchin spines and bones (Oaki *et al.* 2006; Olszta *et al.* 2007; Seto *et al.* 2012). Mesocrystals have also been described in calcium carbonates forming in microbial mats, stromatolites and laboratory cultures (Benzerara *et al.* 2010; Peng and Jones 2013; Han *et al.* 2017).

Intracellular magnetic iron biominerals in magnetotactic bacteria are usually elongated along specific crystallographic directions and aligned into a chain within the microbial cell (Amor *et al.* 2020) and hence may be described as 1D mesocrystals (Bergström *et al.* 2015). These specific textural characteristics are encountered in a fraction of the magnetite nanocrystals present in the martian meteorite ALH84001 and they have thus been described as 'magnetofossils' (Friedmann *et al.* 2001; Thomas-Keprta *et al.* 2002), although others have argued that their crystallographic and textural signatures could be mimicked abiotically (Golden *et al.* 2001, 2004; Bell 2007; Martel *et al.* 2012). Studies of ancient eukaryotic biominerals show that nanocrystalline textures can be preserved in the geological record (Gilbert *et al.* 2019) and the mesocrystal texture of calcite particles has been used as evidence of microbial influence in the formation of Paleogene micrite deposits (Bralower *et al.* 2020).

However, polycrystalline mineral textures mimicking biominerals, including mesocrystals, can be reproduced in the laboratory, notably through precipitation with organic additives. Organic molecules appear to play an important part in crystal growth by oriented particle attachment, by stabilizing the nano-building blocks, and guiding and orienting their assembly (Cuif and Dauphin 2005; Oaki *et al.* 2006; Nouet *et al.* 2012). Hydrophilic organic polymers are particularly effective in this process and induce the formation of mesocrystals of carbonates, phosphates and metal oxides in laboratory precipitation experiments (Mukkamala and Powell 2004; Yu and Cölfen 2004; Yu *et al.* 2005; Meldrum and Cölfen 2008) (Fig. 6a), but simple inorganic additives such as Mg^{2+} can also lead to mesocrystal-like polycrystalline structures (Liu *et al.* 2020) (Fig. 6c). Magnetite mesocrystals were also obtained through the hydrolysis of organically bound ferric iron (Cai *et al.* 2014).

Organization of nanocrystallites at the mesoscale can also emerge from inorganic self-assembly. Carbonate–silica biomorphs are, for instance, composed of carbonate nanorods, uniform in shape and size, that are almost parallel to each other and aligned with respect to their *c*-axis (the slight misalignment between the nanorods occurs at fixed angles and allows for the radial growth of the sheaths composing the biomorphs) (Kellermeier *et al.* 2012*c*) (Fig. 6b). Mesocrystals can also be obtained inorganically by crystallization within silica gels (Dominguez Bella and García-Ruiz 1987) or through hydrothermal processes or solvent evaporation (Agthe *et al.* 2014; Sturm and Cölfen 2016; Sun *et al.* 2019) (Fig. 6d).

It has also been suggested that the very small sizes of microbial biominerals forming from highly supersaturated solutions as a result of microbial activity could be used as a biosignature (Banfield *et al.* 2001). Different microbial biomineralization processes can indeed result in the formation of intra- and extracellular iron, sulfur or carbonate mineral nanoparticles (i.e. with at least one dimension <100 nm) (Mansor and Xu 2020). Crystallites in the nanoparticulate range can also form through nucleation and growth within an organic matrix, as observed in carbonate microbialites (Benzerara and Menguy 2009). However, because mineral nanoparticles can precipitate chemically from highly supersaturated fluids, or as a result of multiple nucleation events on organic or inorganic seeding materials, they do not appear to be robust biosignatures.

Similar to the non-equilibrium mineral structures described in the previous section, signatures based on mineral textures will likely be

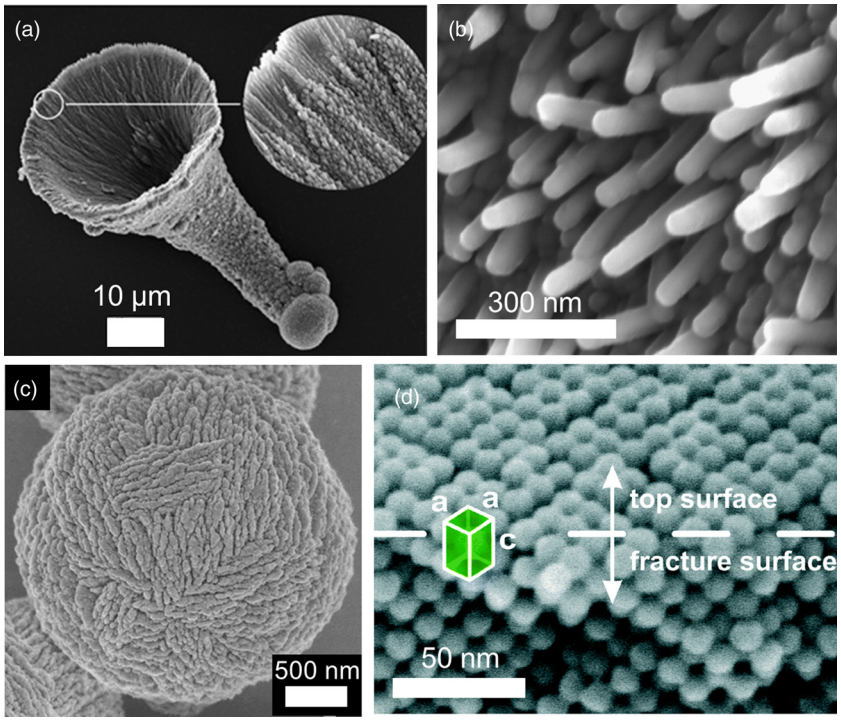

Fig. 6. Biomorphic nanocrystalline structures and mesocrystals. (**a**) Nanocrystalline calcite 'microtrumpet' formed in the presence of a carboxylic-rich organic molecule (Mukkamala and Powell 2004). (**b**) Co-oriented carbonate nanorods at the surface of a carbonate–silica biomorph (Kellermeier *et al.* 2012*a*). (**c**) Nanocrystalline calcite sphere precipitated in the presence of Mg^{2+} (Liu *et al.* 2020). (**d**) Fe oxide mesocrystal formed by droplet evaporation (Agthe *et al.* 2014). Images reproduced with permission (parts a–c) or under creative commons license (creativecommons.org/licenses/by/3.0/) (part d).

difficult to interpret, especially in deposits where organics are abundant and/or in the absence of information on their original geochemical formation environment. However, Mars is more suitable than Earth for the long-term preservation of nanocrystalline mineral textures (e.g. the survival of opaline silica over multi-billion-year timescales at many localities on Mars) as a result of its low surface temperature and geothermal gradient and less prevalent fluid circulation. The possibility that such textures will be discovered is thus considerable and more effort is needed to better constrain their biogenic and abiogenic formation mechanisms in Mars-like contexts.

Chemical signatures in minerals

Aside from their structure, the chemical composition of biominerals may be different from that expected to form at equilibrium with the surrounding fluid geochemistry. Organisms can preferentially accumulate or exclude certain elements from their intracellular medium or internal compartments. As a result, intracellular biominerals may display enrichments of specific elements compared with the chemistry of the extracellular environment (e.g. Cam *et al.* 2016) or high levels of chemical purity (Amor *et al.* 2015). The PIXL instrument onboard the Perseverance rover can map the distribution and abundance variations of major and trace chemical elements at the sub-millimetre scale in rock and soil samples (Allwood *et al.* 2020). This technique may enable the detection of fine chemical biosignatures on Mars, such as enrichments of certain trace metals associated with organic matter (Hickman-Lewis *et al.* 2020).

However, a thorough understanding of the geochemical context for mineral formation, as well as diagenetic history, are necessary to interpret mineral chemistry in terms of biosignatures. For instance, the Mg–Ca carbonate dolomite forms in an environment associated with microbial mats (e.g. DiLoreto *et al.* 2019), although, unlike calcium carbonates, this mineral is very difficult to precipitate in the laboratory at low temperatures. The presence of dolomite in microbial mats is explained by organic templating effects and the interaction of Mg^{2+} with the carboxylic groups of extracellular polymeric substances (Krause *et al.* 2012; Roberts *et al.* 2013; Petrash *et al.* 2017). Dolomite can also form abiotically at high temperatures by precipitation from hydrothermal fluids or by the replacement of other primary carbonates during diagenesis or metamorphism (Bontognali 2019), or at low temperatures under certain geochemical conditions (e.g. in evaporative saline alkaline lakes; Wanas and Sallam 2016), preventing its use as a robust biosignature. More work is required from experiments under simulated martian conditions or from studies of analogue environments on Earth (e.g. Hays *et al.* 2017) to identify relevant and unambiguous mineralogical biosignatures that might be detected on Mars.

Isotopic pseudobiosignatures

Neither the Rosalind Franklin nor Perseverance rover is equipped to measure the isotopic compositions of martian samples *in situ*, but samples returned to Earth will undoubtedly be analysed with isotope mass spectrometry in due course. Unidirectional, enzyme-catalysed metabolic reactions tend to select the lighter isotopes of carbon, sulfur, nitrogen, iron and many other elements because of their lower bond energies. This kinetic effect generates isotopically light products while leaving the substrates depleted in the light isotopes (i.e. relatively enriched in heavier isotopes. In some heavy elements this pattern is actually reversed for reasons to do with nuclear size and shape (e.g. uranium; Brown *et al.* 2018).

The interpretation of isotopic anomalies as biosignatures in geological materials (including fluids, minerals and organic matter) is a well-established practice on Earth, but relies critically on a thorough understanding of the history and context of the sample as well as the (bio)geochemical cycle of the relevant element – that is, the isotopic composition of the major reservoirs and the fractionations associated with the main fluxes between them (which, in the case of biotic processes, depend on the particular enzymes involved) – and changes in these values across geological time. As others have noted, such an understanding is not available for Mars, which limits (but does not completely eliminate) the potential for discovering definitive isotopic biosignatures on that planet (Summons *et al.* 2011; Vago *et al.* 2017).

More generally, false positive isotopic biosignatures can occur where the interpreter does not take sufficient account of the abiotic pathways of isotope fractionation involving either kinetic or

equilibrium processes (van Zuilen *et al.* 2003; Anbar 2004; Thomazo *et al.* 2009; Brown *et al.* 2018). This broad caveat applies to both bulk measurements and to more sophisticated analyses of the isotopic structure of molecules (e.g. clumped or site-specific isotope compositions), although the latter hold great promise for astrobiological applications (Eiler *et al.* 2018). We briefly discuss how false isotopic biosignatures may arise in the carbon, sulfur, nitrogen and iron systems.

Carbon isotopes

Biological uptake of carbon causes a kinetic isotope fractionation such that biologically fixed carbon exhibits a relatively negative $\delta^{13}C$ value (the $^{13}C/^{12}C$ ratio of a sample expressed as a per mil deviation relative to a standard). On Earth, organic matter in the marine sedimentary rock record is characterized by $\delta^{13}C$ values 20–30‰ lower than carbonates of the same age. The persistence and ubiquity of this offset over *c.* 3.5 Gyr of global geological history is considered strong evidence for the antiquity of life (Schidlowski 2001).

However, attributing individual samples of ancient carbonaceous matter to biotic or abiotic carbon fixation on the basis of $\delta^{13}C$ values alone can be problematic even on Earth. On the one hand, the biological fractionation effect can be small in some circumstances (e.g. Takai *et al.* 2008; Reeves and Fiebig 2020). On the other hand, kinetic isotope effects associated with several abiotic pathways yield CH_4 and/or other organic compounds with highly negative $\delta^{13}C$ values (Horita 2005). For example, hydrocarbons produced by experimental Fischer–Tropsch type synthesis (at 250°C and 325–350 bar using formic acid as a carbon source) are reportedly depleted in ^{13}C by as much as 36‰ (McCollom and Seewald 2006; McCollom *et al.* 2010).

Some researchers have noted that 'abiotic photosynthesis' (CO_2 reduction photo-catalysed on mineral surfaces, with water as an electron donor) may also have produced isotopically light organic matter on early Mars (Franz *et al.* 2020), although experimental work is needed to test this hypothesis and to explore the isotopic effects of abiotic organic synthesis more generally. Van Zuilen (2008) has pointed out two further challenges for the identification of carbon isotopic biosignatures on Mars. First, martian sedimentary rocks may preserve debris from carbonaceous chondrites, which contain reduced carbon phases (some of them macromolecular) with $\delta^{13}C$ values of about −15 to −20‰, similar to biomass on Earth. This material may be difficult to discriminate from biological organic matter. Second, the carbon isotopic composition of CO_2 in the martian atmosphere probably changed significantly with the decline of volcanic outgassing and the drawdown and loss of CO_2 early in martian history. To establish the isotopic fractionation associated with the formation of any endogenous organic carbon in recovered samples, it will therefore be necessary to identify carbonate minerals representative of contemporaneous atmospheric CO_2, which may be challenging.

More generally, the isotopic composition of martian carbon is poorly understood. Martian meteorites contain reduced magmatic carbon characterized by $\delta^{13}C$ values of about −20‰ (i.e. about 15‰ lighter than magmatic carbon in basalts on Earth, for unclear reasons), as well as carbonates with widely varying positive $\delta^{13}C_{PDB}$ values, up to about +60‰ (Grady *et al.* 2004; Steele *et al.* 2016). Pyrolysis of aeolian fines by the SAM instrument suite onboard the Curiosity rover yielded CO_2 with $\delta^{13}C$ values between *c.* −6 and +20‰ (Leshin *et al.* 2013). Subsequently, Noachian–Hesperian siliciclastic sedimentary rocks analysed by the same instrument yielded CO_2 with $\delta^{13}C$ values ranging from -25 ± 20 to $+56 \pm 11$‰ (Franz *et al.* 2020). Both datasets suggest the presence of multiple carbon-bearing phases, including carbonates and reduced carbon, but little is known about their age and identity.

Sulfur isotopes

Variations in sulfur isotope ratios have been investigated as potential biosignatures in martian meteorites (Farquhar *et al.* 2000*b*) and sedimentary rocks (Franz *et al.* 2017) based on the fact that some microbial metabolisms produce mass-dependent fractionations of the sulfur isotopes (Ono 2008). In particular, microbial sulfate reduction can produce sulfide significantly depleted in the heavier ^{34}S (i.e. relatively enriched in ^{32}S) compared with the substrate (sulfate), resulting in isotopic fractionations of several tens of $\delta^{34}S$ units (‰) (Kaplan and Rittenberg 1964; Canfield and Teske 1996). High-temperature abiotic sulfate reduction also fractionates sulfur isotopes (up to 20‰ at 100°C; Thomazo *et al.* 2009), but can probably be ruled out for many samples obtainable from the martian near-surface, which have not been exposed to high temperatures.

Microbial sulfur disproportionation and sulfide oxidation also fractionate sulfur isotopes and it can be difficult to disentangle the effects of these different metabolisms in sediments (Canfield *et al.* 1998; Philippot *et al.* 2007; Sim *et al.* 2011; Pellerin *et al.* 2019), particularly after further sulfur-cycling by post-depositional and diagenetic processes (Fike *et al.* 2015). Isotopically light sulfide has been interpreted as evidence of microbial sulfur-cycling microorganisms in Archean rocks on Earth, often in combination with other biosignatures such as microfossils or stromatolites (e.g, Wacey *et al.* 2011; Bontognali *et al.* 2012; Marin-Carbonne *et al.* 2018). However, this interpretation requires ruling out contributions from abiogenic processes that can also fractionate sulfur isotopes. For instance, isotopic exchange with sulfate in hydrothermal contexts can endow sulfide with $\delta^{34}S$ values similar to microbially reduced sulfide (Ohmoto and Lasaga 1982).

Atmospheric processes such as SO_2 photolysis can lead to mass-independent fractionation of sulfur isotopes (Farquhar *et al.* 2001). Signatures of mass-independent fractionation are commonly recorded in Archean rocks (Farquhar *et al.* 2000*a*), but are rarely observed today on Earth because the creation and preservation of mass-independent fractionation signals is unlikely in an oxygen-rich atmosphere (Pavlov and Kasting 2002; Halevy 2013).

Sulfur in martian meteorites records clear isotopic evidence of atmospheric photochemical mass-independent fractionation effects (Farquhar *et al.* 2000*b*; Franz *et al.* 2014). The Curiosity rover's SAM instrument suite measured $\delta^{34}S$ values ranging from −47 to +28‰ in samples collected in Gale Crater, some of which are 'broadly consistent with' the effects of microbial sulfur-cycling (Franz *et al.* 2017). However, these isotopic compositions could also be explained by the effects of equilibrium fractionation in the impact-driven hydrothermal system of the crater, combined with atmospheric chemical and photochemical processes (Franz *et al.* 2017).

High-precision measurements of the abundances of all four sulfur isotopes (^{32}S, ^{33}S, ^{34}S and ^{36}S) introduce new $\Delta^{33}S$ and $\Delta^{36}S$ isotopic ratios, which, in combination with geological contextual analysis, may help to discriminate the effects of biological, hydrothermal and photochemical fractionation processes (Philippot *et al.* 2007; Ono 2008; Kamyshny *et al.* 2014; Aoyaa and Ueno 2018). Such techniques will no doubt be applied to returned samples. The study of sulfur-rich Mars-analogue environments suggest that combining $\delta^{34}S$, $\Delta^{33}S$ and $\Delta^{36}S$ measurements with steady-state models of sulfur-cycling may be a possible diagnostic tool for biosignature detection (Moreras-Marti *et al.* 2021). However, this method requires an in-depth understanding of the martian geological, geochemical and atmospheric context, which, despite significant recent advances (Franz *et al.* 2019), may still be out of reach in the near future.

Nitrogen isotopes

Nitrogen undergoes a highly complex biogeochemical cycle on Earth, in which several important metabolic pathways impart isotopic fractionations of different amplitudes and directions (reported as $\delta^{15}N$, with Earth's atmospheric N_2 providing the usual standard). The $\delta^{15}N$ signature of marine biomass (about +5‰ today) can be preserved in fossil organic matter and as mineral-bound NH_4^+ derived from organic decay, with minimal diagenetic modification (Boyd and Philippot 1998; Thomazo *et al.* 2009). Organic matter in Archean metasediments records a systematic variation in $\delta^{15}N$ over geological time, probably reflecting changes in the preponderance of different microbial metabolisms under increasingly oxidizing conditions (Ader *et al.* 2016); there are some interpretative difficulties relating to metamorphic overprint, but these will not be an issue on Mars.

The martian atmosphere is *c.* 3% nitrogen today and nitrogen-bearing organic molecules of uncertain origin have already been found in martian meteorites (Koike *et al.* 2020); they may soon be encountered in returned samples. It will be challenging to interpret $\delta^{15}N$ in this material without a broader understanding of Noachian–Hesperian nitrogen cycling, particularly in relation to the isotopic effects of atmospheric escape and declining volcanism over geological time; NH_4^+ in clay minerals may provide a contemporaneous standard (van Zuilen 2008).

The risk of isotopic false positives arising in this context is not yet well understood, but large $\delta^{15}N$ fractionations are already known to result from several relevant abiotic processes. Nitrate fixed by lightning may be isotopically light (Stüeken 2016). Organic nitrogen produced experimentally from NH_3 in Miller–Urey reactions with CH_4 and H_2 is reportedly enriched in ^{15}N by 10–12‰, while plasma discharge in mixtures of N_2, CH_4, CO and H_2 causes fractionation of up to 25‰ in the opposite direction (Kung *et al.* 1979; Thomazo *et al.* 2009; Kuga *et al.* 2014). Nitrogen isotope fractionation may also occur during Fischer–Tropsch type organic synthesis (Kung *et al.* 1979; Thomazo *et al.* 2009). Chondritic meteoritic debris may also be present in returned samples and can contain organic nitrogen with $\delta^{15}N$ values ranging from +25 to +150‰ (Sephton *et al.* 2003).

Iron isotopes

Fe isotopes have been investigated as potential signatures of microbial Fe cycling (Johnson *et al.* 2008; Poitrasson 2015), including in the context of Mars (Anand *et al.* 2006; van Zuilen 2008), although candidates for Fe isotopic biosignatures have not yet been detected in martian materials.

It has been reported that magnetite biomineralized by the magnetotactic bacterium *Magnetospirillum magneticum* AMB-1 is strongly depleted in heavy Fe isotopes (Amor *et al.* 2016). Moreover, mass-independent fractionation in ^{57}Fe was observed during magnetite biomineralization, but not in the even Fe isotopes (^{54}Fe, ^{56}Fe and ^{58}Fe), implying a magnetic isotope effect. This signature is apparently not produced abiotically or by other Fe-metabolizing bacteria (Amor *et al.* 2016), but it remains to be seen whether it can be detected in the rock record.

The oxidation of aqueous Fe(II) precipitates solid Fe(III) phases that are typically slightly enriched in the heavy Fe isotopes regardless of whether Fe(II) oxidation was biologically mediated or not (e.g. Bullen *et al.* 2001; Balci *et al.* 2006), so it is generally admitted that microbial Fe oxidation does not leave any robust isotopic biosignature (e.g. van Zuilen 2008; Thomazo *et al.* 2009). However, microbial dissimilatory Fe reduction, which couples the reduction of Fe(III) to the oxidation of organic matter, leads to an enrichment of the Fe(II) product in the light Fe isotopes (e.g. Percak-Dennett *et al.* 2011). Under certain conditions (in particular, low pH), the Fe isotope fractionation induced by microbial dissimilatory Fe reduction may exceed in amplitude the fractionation associated with the abiotic reductive dissolution of Fe(III) (e.g. Johnson *et al.* 2008; Thomazo *et al.* 2009; Chanda *et al.* 2021).

On Earth, isotopic signals related to microbial dissimilatory Fe reduction are, for instance, thought to be recorded in some banded iron formations (Johnson *et al.* 2008). However, a number of processes may overprint or even erase biologically driven Fe isotopic signals, such as the preferential binding of heavy Fe isotopes by organic ligands in solution (e.g. Lotfi-Kalahroodi *et al.* 2021) or isotopic exchange between Fe minerals during diagenesis or metamorphism (Whitehouse and Fedo 2007; Hyslop *et al.* 2008). Here again, the use of Fe isotopes to search for traces of biological activity necessarily requires an in-depth understanding of the mineralogical and geochemical context during primary sediment deposition and subsequent history, and their interpretation should be conducted in conjunction with other mineralogical, chemical and isotopic indicators (Poitrasson 2015).

Discussion

In writing this review, we have been struck by the following five points. First, abiotic processes can mimic not only morphological biosignatures, but also chemical/molecular, mineralogical, isotopic and textural biosignatures; a critical attitude is required in all cases and morphological data are not necessarily less reliable than other possible lines of evidence for life (cf. García-Ruiz *et al.* 2002). Indeed, independent categories of false biosignature may often coincide in the same sample and thus 'multiple lines of evidence' suggestive of biology can be found in some non-biological systems.

Second, many abiotic materials that resemble life are produced by the dissipation of energy in systems characterized by strong thermodynamic and/or chemical gradients and the presence of liquid water (e.g. the hydrothermal synthesis of complex organic matter, the hydrothermal fractionation of carbon isotopes; chemical gardens, carbon–sulfur biomorphs and carbonate–silica biomorphs). Although in many ways unsurprising, this has paradoxical implications. Environments conducive to the origin and maintenance of life may also, by their very nature, be conducive to the formation of false biosignatures. Therefore a cell-like, organic, ambiguously biogenic structure found in a tenuously habitable, energy-poor environment (e.g. a cold desert) may be more credible as a biosignature than a similar structure found in the midst of a reducing hydrothermal system because the former is more difficult to explain abiotically than the latter. It follows that the search for evidence of life should not focus only on environments where life is most likely to have arisen (cf. Longo and Damer 2020) because it is here that the evidence will be most ambiguous.

Third, silica precipitation plays a key part in the formation of a wide variety of false biosignatures (e.g. carbonate–silicate biomorphs, chemical gardens, cryogenic opal biomorphs and, potentially, the formation of pseudomicrobialites in splash zones). Siliceous materials might be favoured targets for analysis and sample return because silica can help to preserve organic matter and morphological fossils as a cement and entombing medium (e.g. McMahon *et al.* 2018). It will be especially important to consider how self-organization might have influenced the textural and morphological features of these samples.

Fourth, interactions between water and basaltic lava, although probably contributing to habitability on early Mars in various important ways, is also associated with a number of pseudobiosignatures (e.g. quench crystallites, alteration textures, the production of chemical garden 'seed' minerals and the production of alkaline, silica-rich fluids that can generate biomorphs). Neither the potential occurrence of biosignatures nor the potential occurrence of

pseudobiosignatures should be overlooked in the sampling and analysis of aqueously altered volcanic materials (Ivarsson *et al.* 2020, 2021).

Fifth, the study of false biosignatures requires input from colleagues and methods across several disciplines. Physical chemists, condensed matter physicists and materials scientists have long been interested in symmetry-breaking, self-assembly and the emergence of complex structures and materials under far from equilibrium conditions. There is a vast literature – only a tiny sample of which has been cited in this review – on the numerical and experimental interrogation of these processes and the analytical characterization of their products. This expertise now needs to be translated into a geological and astrobiological context by focusing on the minerals, fluids and pressure–temperature conditions present on Mars today and in the geological past (e.g. Sainz-Díaz *et al.* 2021). Some important theoretical foundations have been laid (e.g. Ortoleva 1994; García-Ruiz *et al.* 2020), but there is more work to be done, both to identify relevant sources of false biosignatures and to characterize them in detail. Ideally, multiple high-resolution analytical techniques should be used to facilitate in-depth comparisons with candidate biosignatures. Recent studies of probable Precambrian fossils have presented rich, multi-scale, multi-proxy datasets combining morphological, textural and compositional (chemical, mineralogical and isotopic) information (e.g. Alleon *et al.* 2018; Lepot *et al.* 2019; Hickman-Lewis *et al.* 2020; Marin-Carbonne *et al.* 2020). Studies of false biosignatures should be similarly comprehensive.

What about biogenicity criteria?

A number of protocols and strategies have been devised to assess the credibility of candidate biosignatures (e.g. Buick 1990; Brasier and Wacey 2012; McLoughlin and Grosch 2015; Vago *et al.* 2017; Neveu *et al.* 2018; Rouillard *et al.* 2021). Most of these schemes use multiple, nested criteria to assess biogenicity: did the object (or population of objects) form in a demonstrably habitable (palaeo) environment, with appropriate evidence of endogeneity and syngenicity? If so, is its morphology consistent with a biotic origin and inconsistent with an abiotic origin? If so, is its chemical composition distinctively life-like? And so on. The more definitely and completely the object (including its geological context) meets the criteria, the higher the biogenicity score.

Biogenicity determination protocols meet an important need, but most real fossils (whether on Earth or Mars) are likely to fall short of ideal standards and achieve only middling scores, along with pseudofossils. Thus a failure to meet some of the relevant biogenicity criteria is expected and can often be explained away by researchers claiming to have discovered biosignatures. A deeper worry is that biogenicity criteria are unable to discriminate sensitively and reliably between biosignatures and pseudobiosignatures unless they are grounded in extensive knowledge and understanding of both classes of phenomena. Even protocols that do not explicitly rely on binary criteria must necessarily appeal to reference data from relevant abiotic systems (e.g. Rouillard *et al.* 2021). However, most known varieties of pseudobiosignature have not been characterized or understood in sufficient detail for this to be possible. Moreover, given the haphazard and unsystematic way in which varieties of false biosignature have so far been identified, we can only assume that many others remain undiscovered. Here, the expertise and methods of mineralogists, chemists, physicists and materials scientists are as valuable to biosignature science as those of microbiologists and palaeontologists.

Although the discovery of new forms of pseudobiosignature will tend to undermine existing biogenicity protocols (e.g. McMahon 2019; Nims *et al.* 2021), in the long run this will lead to better protocols (e.g. McLoughlin *et al.* 2007; Johannessen *et al.* 2020).

Conclusions

If we are lucky, plain and unequivocal biosignatures will be discovered on Mars in the coming decades. But in light of the many cautionary tales in the history of palaeontology and astrobiology, it seems prudent to anticipate more ambiguous results. In interpreting these, it will be important to understand how misleadingly life-like objects and substances might have formed abiotically on Mars. We have summarized some of the examples that have already been discovered in the laboratory, in terrestrial rocks and in meteorites. We have argued that many other examples probably await discovery because abiotic self-organization processes relevant to the geology of Mars have not been explored systematically. Because life itself is presumed to be the product of self-organization in abiotic geochemical reactions, the complexity of abiotic natural products should not be underestimated. Nevertheless, we are optimistic that the problem of false biosignatures is not intractable. The better these phenomena are understood, the more sensitively we will be able to discriminate between true evidence of life and these impostors.

Relevant false biosignatures should therefore now be sought systematically in Mars-analogue field and experimental systems and characterized in detail with multiple analytical instruments and at multiple scales to provide datasets that are as rich as those available for biosignatures. Further work on the physics and chemistry of far-from-equilibrium systems will ultimately reveal the limits of abiotic self-organization and may even lead to new discoveries on the organizing principles at the origin of life on Earth. Such efforts have an important part to play in the interpretation of Earth's rock record as well as the search for life on Mars and elsewhere in the solar system.

Acknowledgements The perspectives in this article were shaped in part by SM's participation in the EU Cost Action CA17120 Chemobrionics. We thank an anonymous reviewer and Mark van Zuilen for helpful comments that improved this paper.

Author contributions **SM**: conceptualization (lead), investigation (equal), writing – original draft (lead), writing – review & editing (equal); **JC**: conceptualization (supporting), investigation (equal), writing – original draft (supporting), writing – review & editing (equal).

Funding This research received no specific grant from any funding agency in the public, commercial, or not-for-profit sectors.

Data availability Data sharing is not applicable to this article as no datasets were generated or analysed during the current study.

Scientific editing by Peter Grindrod

References

Addadi, L. and Weiner, S. 2014. Biomineralization: mineral formation by organisms. *Physica Scripta*, **89**, 098003, https://doi.org/10.1088/0031-8949/89/9/098003

Addadi, L., Raz, S. and Weiner, S. 2003. Taking advantage of disorder: amorphous calcium carbonate and its roles in biomineralization. *Advanced Materials*, **15**, 959–970, https://doi.org/10.1002/adma.200300381

Adelman, J. 2007. Eozoön: debunking the dawn animal. *Endeavour*, **31**, 94–98, https://doi.org/10.1016/j.endeavour.2007.07.002

Ader, M., Thomazo, C. *et al.* 2016. Interpretation of the nitrogen isotopic composition of Precambrian sedimentary rocks: assumptions and perspectives. *Chemical Geology*, **429**, 93–110, https://doi.org/10.1016/j.chemgeo.2016.02.010

Agthe, M., Wetterskog, E., Mouzon, J., Salazar-Alvarez, G. and Bergström, L. 2014. Dynamic growth modes of ordered arrays and mesocrystals during drop-casting of iron oxide nanocubes. *CrystEngComm*, **16**, 1443–1450, https://doi.org/10.1039/C3CE41871E

Alleon, J. and Summons, R.E. 2019. Organic geochemical approaches to understanding early life. *Free Radical Biology and Medicine*, **140**, 103–112, https://doi.org/10.1016/j.freeradbiomed.2019.03.005

Alleon, J., Bernard, S., Le Guillou, C., Beyssac, O., Sugitani, K. and Robert, F. 2018. Chemical nature of the 3.4 Ga Strelley Pool microfossils. *Geochemical Perspectives Letters*, **7**, 37–42, https://doi.org/10.7185/geochemlet.1817

Alleon, J., Flannery, D.T., Ferralis, N., Williford, K.S.H., Zhang, Y., Schuessler, J.A. and Summons, R.E. 2019. Organo-mineral associations in chert of the 3.5 Ga Mount Ada Basalt raise questions about the origin of organic matter in Paleoarchean hydrothermally influenced sediments. *Scientific Reports*, **9**, 16712, https://doi.org/10.1038/s41598-019-53272-5

Allwood, A.C., Rosing, M.T., Flannery, D.T., Hurowitz, J.A. and Heirwegh, C.M. 2018. Reassessing evidence of life in 3700-million-year-old rocks of Greenland. *Nature*, **563**, 241–244, https://doi.org/10.1038/s41586-018-0610-4

Allwood, A.C., Wade, L.A. *et al.* 2020. PIXL: Planetary instrument for X-ray lithochemistry. *Space Science Reviews*, **216**, 134, https://doi.org/10.1007/s11214-020-00767-7

Amor, M., Busigny, V. *et al.* 2015. Chemical signature of magnetotactic bacteria. *Proceedings of the National Academy of Sciences of the United States of America*, **112**, 1699–1703, https://doi.org/10.1073/pnas.1414112112

Amor, M., Busigny, V. *et al.* 2016. Mass-dependent and -independent signature of Fe isotopes in magnetotactic bacteria. *Science*, **352**, 705–708, https://doi.org/10.1126/science.aad7632

Amor, M., Mathon, F.P., Monteil, C.L., Busigny, V. and Lefevre, C.T. 2020. Iron-biomineralizing organelle in magnetotactic bacteria: function, synthesis and preservation in ancient rock samples. *Environmental Microbiology*, **22**, 3611–3632, https://doi.org/10.1111/1462-2920.15098

Anand, M., Russell, S.S., Blackhurst, R.L. and Grady, M.M. 2006. Searching for signatures of life on Mars: an Fe-isotope perspective. *Philosophical Transactions of the Royal Society B: Biological Sciences*, **361**, 1715–1720, https://doi.org/10.1098/rstb.2006.1899

Anbar, A.D. 2004. Iron stable isotopes: beyond biosignatures. *Earth and Planetary Science Letters*, **217**, 223–236, https://doi.org/10.1016/S0012-821X(03)00572-7

Antcliffe, J. and McLoughlin, N. 2008. Deciphering fossil evidence for the origin of life and the origin of animals. Cellular Origin, Life in Extreme Habitats and Astrobiology, **12**, 211–229, https://doi.org/10.1007/978-1-4020-8837-7_10

Aoyaa, S. and Ueno, Y. 2018. Multiple sulfur isotope constraints on microbial sulfate reduction below an Archean seafloor hydrothermal system. *Geobiology*, **16**, 107–120, https://doi.org/10.1111/gbi.12268

Balci, N., Bullen, T.D., Witte-Lien, K., Shanks, W.C., Motelica, M. and Mandernack, K.W. 2006. Iron isotope fractionation during microbially stimulated Fe(II) oxidation and Fe(III) precipitation. *Geochimica et Cosmochimica Acta*, **70**, 622–639, https://doi.org/10.1016/j.gca.2005.09.025

Banfield, J.F., Moreau, J.W., Chan, C.S., Welch, S.A. and Little, B. 2001. Mineralogical biosignatures and the search for life on Mars. *Astrobiology*, **1**, 447–465, https://doi.org/10.1089/153110701753593856

Barge, L.M., Cardoso, S.S.S. *et al.* 2015. From chemical gardens to chemobrionics. *Chemical Reviews*, **115**, 8652–8703, https://doi.org/10.1021/acs.chemrev.5b00014

Barghoorn, E.S. and Tyler, S.A. 1963. Fossil organisms from Precambrian sediments. *Annals of the New York Academy of Sciences*, **108**, 451–452, https://doi.org/10.1111/j.1749-6632.1963.tb13399.x

Barghoorn, E.S. and Tyler, S.A. 1965. Microorganisms from the Gunflint Chert: these structurally preserved Precambrian fossils from Ontario are the most ancient organisms known. *Science*, **147**, 563–575, https://doi.org/10.1126/science.147.3658.563

Barlow, E.V. and Kranendonk, M.J.V. 2018. Snapshot of an early Paleoproterozoic ecosystem: two diverse microfossil communities from the Turee Creek Group, Western Australia. *Geobiology*, **16**, 449–475, https://doi.org/10.1111/gbi.12304

Batchelor, M.T., Burne, R.V., Henry, B.I. and Jackson, M.J. 2004. A case for biotic morphogenesis of coniform stromatolites. *Physica A: Statistical Mechanics and its Applications*, **337**, 319–326, https://doi.org/10.1016/j.physa.2004.01.065

Baumgartner, R.J., Kranendonk, M.J.V. *et al.* 2019. Nano-porous pyrite and organic matter in 3.5-billion-year-old stromatolites record primordial life. *Geology*, **47**, 1039–1043, https://doi.org/10.1130/G46365.1

Beegle, L., Bhartia, R. *et al.* 2015. SHERLOC: scanning habitable environments with Raman and luminescence for organics and chemicals. Paper presented at the 2015 IEEE Aerospace Conference, Big Sky, MT, USA, 1–11, https://doi.org/10.1109/AERO.2015.7119105

Belilla, J., Moreira, D. *et al.* 2019. Hyperdiverse Archaea near life limits at the polyextreme geothermal Dallol area. *Nature Ecology & Evolution*, **3**, 1552–1561, https://doi.org/10.1038/s41559-019-1005-0

Bell, J.F., Maki, J.N. *et al.* 2021. The Mars 2020 Perseverance rover mast camera zoom (Mastcam-Z) multispectral, stereoscopic imaging investigation. *Space Science Reviews*, **217**, 24, https://doi.org/10.1007/s11214-020-00755-x

Bell, M.S. 2007. Experimental shock decomposition of siderite and the origin of magnetite in Martian meteorite ALH 84001. *Meteoritics & Planetary Science*, **42**, 935–949, https://doi.org/10.1111/j.1945-5100.2007.tb01142.x

Benzerara, K. and Menguy, N. 2009. Looking for traces of life in minerals. *Comptes Rendus Palevol*, **8**, 617–628, https://doi.org/10.1016/j.crpv.2009.03.006

Benzerara, K., Menguy, N., Guyot, F., Skouri, F., de Luca, G., Barakat, M. and Heulin, T. 2004. Biologically controlled precipitation of calcium phosphate by *Ramlibacter tataouinensis*. *Earth and Planetary Science Letters*, **228**, 439–449, https://doi.org/10.1016/j.epsl.2004.09.030

Benzerara, K., Meibom, A., Gautier, Q., Kazmierczak, J., Stolarski, J., Menguy, N. and Brown, G.E. 2010. Nanotextures of aragonite in stromatolites from the quasi-marine Satonda crater lake, Indonesia. *Geological Society, London, Special Publications*, **336**, 211–224, https://doi.org/10.1144/SP336.10

Benzerara, K., Bernard, S. and Miot, J. 2019. Mineralogical identification of traces of life. *Advances in Astrobiology and Biogeophysics*, 123–144, https://doi.org/10.1007/978-3-319-96175-0_6

Bergström, L., Sturm née Rosseeva, E.V., Salazar-Alvarez, G. and Cölfen, H. 2015. Mesocrystals in biominerals and colloidal arrays. *Accounts of Chemical Research*, **48**, 1391–1402, https://doi.org/10.1021/ar500440b

Bernini, F., Castellini, E. *et al.* 2021. Self-assembled structures from solid cadmium(II) acetate in thiol/ethanol solutions: a novel type of organic chemical garden. *ChemSystemsChem*, **3**, e2000048, https://doi.org/10.1002/syst.202000048

Bibring, J.-P., Hamm, V., Pilorget, C., Vago, J.L. and the MicrOmega Team 2017. The MicrOmega investigation onboard ExoMars. *Astrobiology*, **17**, 621–626, https://doi.org/10.1089/ast.2016.1642

Bishop, J.L., Dobrea, E.Z.N. *et al.* 2008. Phyllosilicate diversity and past aqueous activity revealed at Mawrth Vallis, Mars. *Science*, **321**, 830–833, https://doi.org/10.1126/science.1159699

Bishop, J.L., Parente, M. *et al.* 2009. Mineralogy of Juventae Chasma: sulfates in the light-toned mounds, mafic minerals in the bedrock, and hydrated silica and hydroxylated ferric sulfate on the plateau. *Journal of Geophysical Research: Planets*, **114**, https://doi.org/10.1029/2009JE003352.

Bonev, I.K., García-Ruiz, J.M., Atanassova, R., Otalora, F. and Petrussenko, S. 2005. Genesis of filamentary pyrite associated with calcite crystals. *European Journal of Mineralogy*, **17**, 905–913, https://doi.org/10.1127/0935-1221/2005/0017-0905

Bontognali, T.R.R. 2019. Anoxygenic phototrophs and the forgotten art of making dolomite. *Geology*, **47**, 591–592, https://doi.org/10.1130/focus062019.1

Bontognali, T.R.R., Sessions, A.L., Allwood, A.C., Fischer, W.W., Grotzinger, J.P., Summons, R.E. and Eiler, J.M. 2012. Sulfur isotopes of organic matter preserved in 3.45-billion-year-old stromatolites reveal microbial metabolism. *Proceedings of the National Academy of Sciences of the United States of America*, **109**, 15146–15151, https://doi.org/10.1073/pnas.1207491109

Botta, O. and Bada, J.L. 2002. Extraterrestrial organic compounds in meteorites. *Surveys in Geophysics*, **23**, 411–467, https://doi.org/10.1023/A:1020139302770

Bowerbank, J.S. 1842. IV.—On the spongeous origin of moss agates and other siliceous bodies. *Annals and Magazine of Natural History*, **10**, 9–18, https://doi.org/10.1080/03745484209445187

Boyd, S.R. and Philippot, P. 1998. Precambrian ammonium biogeochemistry: a study of the Moine metasediments, Scotland. *Chemical Geology*, **144**, 257–268, https://doi.org/10.1016/S0009-2541(97)00135-6

Brack, A. 2007. From interstellar amino acids to prebiotic catalytic peptides: a review. *Chemistry & Biodiversity*, **4**, 665–679, https://doi.org/10.1002/cbdv.200790057

Bralower, T.J., Cosmidis, J. *et al.* 2020. Origin of a global carbonate layer deposited in the aftermath of the Cretaceous–Paleogene boundary impact. *Earth and Planetary Science Letters*, **548**, 116476, https://doi.org/10.1016/j.epsl.2020.116476

Brasier, A.T., Culwick, T., Battison, L., Callow, R.H.T. and Brasier, M.D. 2017. Evaluating evidence from the Torridonian Supergroup (Scotland, UK) for eukaryotic life on land in the Proterozoic. *Geological Society, London, Special Publications*, **448**, 121–144, https://doi.org/10.1144/SP448.13

Brasier, A.T., Dennis, P.F. *et al.* 2019. Detecting ancient life: investigating the nature and origin of possible stromatolites and associated calcite from a one billion year old lake. *Precambrian Research*, **328**, 309–320, https://doi.org/10.1016/j.precamres.2019.04.025

Brasier, M.D. and Wacey, D. 2012. Fossils and astrobiology: new protocols for cell evolution in deep time. *International Journal of Astrobiology*, **11**, 217–228, https://doi.org/10.1017/S1473550412000298

Brasier, M.D., Green, O.R. *et al.* 2002. Questioning the evidence for Earth's oldest fossils. *Nature*, **416**, 76–81, https://doi.org/10.1038/416076a

Brasier, M.D., Green, O., Lindsay, J., McLoughlin, N., Steele, A. and Stoakes, C. 2005. Critical testing of Earth's oldest putative fossil assemblage from the *c.* 3.5 Ga Apex chert, Chinaman Creek, Western Australia. *Precambrian Research*, **140**, 55–102, https://doi.org/10.1016/j.precamres.2005.06.008

Bristow, T.F. and Milliken, R.E. 2011. Terrestrial perspective on authigenic clay mineral production in ancient Martian lakes. *Clays and Clay Minerals*, **59**, 339–358, https://doi.org/10.1346/CCMN.2011.0590401

Brooke, S. and Fox, S.W. 1977. Compartmentalization in proteinoid microspheres. *Biosystems*, **9**, 1–22, https://doi.org/10.1016/0303-2647(77)90028-4

Brown, A.J., Viviano, C.E. and Goudge, T.A. 2020. Olivine–carbonate mineralogy of the Jezero Crater region. *Journal of Geophysical Research: Planets*, **125**, e2019JE006011, https://doi.org/10.1029/2019JE006011

Brown, R.W. 1957. Plantlike features in thunder-eggs and geodes. *Annual Report of the Board of Regents of the Smithsonian Institution for 1956*, 329–339.

Brown, S.T., Basu, A., Ding, X., Christensen, J.N. and DePaolo, D.J. 2018. Uranium isotope fractionation by abiotic reductive precipitation. *Proceedings of the National Academy of Sciences of the United States of America*, **115**, 8688–8693, https://doi.org/10.1073/pnas.1805234115

Buick, R. 1990. Microfossil recognition in Archean rocks: an appraisal of spheroids and filaments from a 3500 m.y. old chert–barite unit at North Pole, Western Australia. *PALAIOS*, **5**, 441–459, https://doi.org/10.2307/3514837

Bullen, T.D., White, A.F., Childs, C.W., Vivit, D.V. and Schulz, M.S. 2001. Demonstration of significant abiotic iron isotope fractionation in nature. *Geology*, **29**, 699–702, https://doi.org/10.1130/0091-7613(2001)029<0699:DOSAII>2.0.CO;2

Busch, S., Dolhaine, H. *et al.* 1999. Biomimetic morphogenesis of fluorapatite–gelatin composites: fractal growth, the question of intrinsic electric fields, core/shell assemblies, hollow spheres and reorganization of denatured collagen. *European Journal of Inorganic Chemistry*, **1999**, 1643–1653, https://doi.org/10.1002/(SICI)1099-0682(199910)1999:10<1643::AID-EJIC1643>3.0.CO;2-J

Burne, R.V. and Moore, L.S. 1987. Microbialites; organosedimentary deposits of benthic microbial communities. *PALAIOS*, **2**, 241–254, https://doi.org/10.2307/3514674

Cady, S.L., Farmer, J.D., Grotzinger, J.P., Schopf, J.W. and Steele, A. 2003. Morphological biosignatures and the search for life on Mars. *Astrobiology*, **3**, 351–368, https://doi.org/10.1089/153110703769016442

Cai, J., Chen, S., Ji, M., Hu, J., Ma, Y. and Qi, L. 2014. Organic additive-free synthesis of mesocrystalline hematite nanoplates via two-dimensional oriented attachment. *CrystEngComm*, **16**, 1553–1559, https://doi.org/10.1039/C3CE41716F

Cam, N., Benzerara, K. *et al.* 2016. Selective uptake of alkaline earth metals by cyanobacteria forming intracellular carbonates. *Environmental Science & Technology*, **50**, 11654–11662, https://doi.org/10.1021/acs.est.6b02872

Canfield, D.E. and Teske, A. 1996. Late Proterozoic rise in atmospheric oxygen concentration inferred from phylogenetic and sulphur-isotope studies. *Nature*, **382**, 127–132, https://doi.org/10.1038/382127a0

Canfield, D.E., Thamdrup, B. and Fleischer, S. 1998. Isotope fractionation and sulfur metabolism by pure and enrichment cultures of elemental sulfur-disproportionating bacteria. *Limnology and Oceanography*, **43**, 253–264, https://doi.org/10.4319/lo.1998.43.2.0253

Chan, C.S., Fakra, S.C., Edwards, D.C., Emerson, D. and Banfield, J.F. 2009. Iron oxyhydroxide mineralization on microbial extracellular polysaccharides. *Geochimica et Cosmochimica Acta*, **73**, 3807–3818, https://doi.org/10.1016/j.gca.2009.02.036

Chan, C.S., Fakra, S.C., Emerson, D., Fleming, E.J. and Edwards, K.J. 2011. Lithotrophic iron-oxidizing bacteria produce organic stalks to control mineral growth: implications for biosignature formation. *The ISME Journal*, **5**, 717–727, https://doi.org/10.1038/ismej.2010.173

Chan, C.S., McAllister, S.M., Leavitt, A.H., Glazer, B.T., Krepski, S.T. and Emerson, D. 2016. The architecture of iron microbial mats reflects the adaptation of chemolithotrophic iron oxidation in freshwater and marine environments. *Frontiers in Microbiology*, **7**, https://doi.org/10.3389/fmicb.2016.00796

Chan, M.A., Hinman, N.W. *et al.* 2019. Deciphering biosignatures in planetary contexts. *Astrobiology*, **19**, 1075–1102, https://doi.org/10.1089/ast.2018.1903

Chanda, P., Amenabar, M.J., Boyd, E.S., Beard, B.L. and Johnson, C.M. 2021. Stable Fe isotope fractionation during dissimilatory Fe(III) reduction by a thermoacidophile in acidic hydrothermal environments. *Geochimica et Cosmochimica Acta*, **292**, 427–451, https://doi.org/10.1016/j.gca.2020.09.025

Channing, A. and Butler, I.B. 2007. Cryogenic opal-A deposition from Yellowstone hot springs. *Earth and Planetary Science Letters*, **257**, 121–131, https://doi.org/10.1016/j.epsl.2007.02.026

Chyba, C. and Sagan, C. 1992. Endogenous production, exogenous delivery and impact-shock synthesis of organic molecules: an inventory for the origins of life. *Nature*, **355**, 125–132, https://doi.org/10.1038/355125a0

Cloud, P. 1973. Pseudofossils: a plea for caution. *Geology*, **1**, 123–127, https://doi.org/10.1130/0091-7613(1973)1 < 123:PAPFC>2.0.CO;2

Cloud, P. 1976. Beginnings of Biospheric Evolution and Their Biogeochemical Consequences. *Paleobiology*, **2**, 351–387.

Coates, A.J., Jaumann, R. *et al.* 2017. The PanCam instrument for the ExoMars rover. *Astrobiology*, **17**, 511–541, https://doi.org/10.1089/ast.2016.1548

Cockell, C.S. and Herrera, A. 2008. Why are some microorganisms boring? *Trends in Microbiology*, **16**, 101–106, https://doi.org/10.1016/j.tim.2007.12.007

Cosmidis, J. and Templeton, A.S. 2016. Self-assembly of biomorphic carbon/sulfur microstructures in sulfidic environments. *Nature Communications*, **7**, 12812, https://doi.org/10.1038/NCOMMS12812

Cosmidis, J., Benzerara, K., Gheerbrant, E., Estève, I., Bouya, B. and Amaghzaz, M. 2013. Nanometer-scale characterization of exceptionally preserved bacterial fossils in Paleocene phosphorites from Ouled Abdoun (Morocco). *Geobiology*, **11**, 139–153, https://doi.org/10.1111/gbi.12022

Cosmidis, J., Benzerara, K. *et al.* 2015. Calcium-phosphate biomineralization induced by alkaline phosphatase activity in *Escherichia coli*: localization, kinetics, and potential signatures in the fossil record. *Frontiers in Earth Science*, **3**, https://doi.org/10.3389/feart.2015.00084

Cosmidis, J., Nims, C.W., Diercks, D. and Templeton, A.S. 2019. Formation and stabilization of elemental sulfur through organomineralization. *Geochimica et Cosmochimica Acta*, **247**, 59–82, https://doi.org/10.1016/j.gca.2018.12.025

Couasnon, T., Alloyeau, D., Ménez, B., Guyot, F., Ghigo, J.-M. and Gélabert, A. 2020. In situ monitoring of exopolymer-dependent Mn mineralization on bacterial surfaces. *Science Advances*, **6**, eaaz3125, https://doi.org/10.1126/sciadv.aaz3125

Criouet, I., Viennet, J.-C., Jacquemot, P., Jaber, M. and Bernard, S. 2021. Abiotic formation of organic biomorphs under diagenetic conditions. *Geochemical Perspectives Letters*, **16**, 40–46, https://doi.org/10.7185/geochemlet.2102

Cron, B., Henri, P., Chan, C.S., Macalady, J.L. and Cosmidis, J. 2019. Elemental sulfur formation by *Sulfuricurvum kujiense* is mediated by extracellular organic compounds. *Frontiers in Microbiology*, **10**, 2710, https://doi.org/10.3389/fmicb.2019.02710

Crosby, C.H. and Bailey, J.V. 2017. Experimental precipitation of apatite pseudofossils resembling fossil embryos. *Geobiology*, **16**, 80–87,https://doi.org/10.1111/gbi.12264

Cuif, J.-P. and Dauphin, Y. 2005. The two-step mode of growth in the scleractinian coral skeletons from the micrometre to the overall scale. *Journal of Structural Biology*, **150**, 319–331, https://doi.org/10.1016/j.jsb.2005.03.004

Dahl, C. 2020. Bacterial intracellular sulphur globules. *Microbiology Monographs*, **34**, 19–51, https://doi.org/10.1007/978-3-030-60173-7_2

Dalai, P., Kaddour, H. and Sahai, N. 2016. Incubating life: prebiotic sources of organics for the origin of life. *Elements*, **12**, 401–406, https://doi.org/10.2113/gselements.12.6.401

Daubenton, L.J.M. 1782. Sur les causes qui produisent trois sortes d'herborisations dans les pierres. *Mémoires de l'Académie Royale des Sciences*, 667–673.

Davies, N.S., Liu, A.G., Gibling, M.R. and Miller, R.F. 2016. Resolving MISS conceptions and misconceptions: a geological approach to sedimentary surface textures generated by microbial and abiotic processes. *Earth-Science Reviews*, **154**, 210–246, https://doi.org/10.1016/j.earscirev.2016.01.005

De Sanctis, M.C., Altieri, F. *et al.* 2017. Ma_MISS on ExoMars: mineralogical characterization of the martian subsurface. *Astrobiology*, **17**, 612–620, https://doi.org/10.1089/ast.2016.1541

De Yoreo, J.J., Gilbert, P.U.P.A. *et al.* 2015. Crystallization by particle attachment in synthetic, biogenic, and geologic environments. *Science*, **349**, aaa6760, https://doi.org/10.1126/science.aaa6760

Deamer, D. 2017. The role of lipid membranes in life's origin. *Life*, **7**, 5, https://doi.org/10.3390/life7010005

Deamer, D. 2021. Where did life begin? Testing ideas in prebiotic analogue conditions. *Life*, **11**, 134, https://doi.org/10.3390/life11020134

Défarge, C. 2011. Organomineralization. *In*: Reitner, J. and Thiel, V. (eds) *Encyclopedia of Geobiology*. Springer, 697–701, https://doi.org/10.1007/978-1-4020-9212-1_159

Dehouck, E., Chevrier, V., Gaudin, A., Mangold, N., Mathé, P.-E. and Rochette, P. 2012. Evaluating the role of sulfide-weathering in the formation of sulfates or carbonates on Mars. *Geochimica et Cosmochimica Acta*, **90**, 47–63, https://doi.org/10.1016/j.gca.2012.04.057

Des Marais, D.J., Nuth, J.A. *et al.* 2008. The NASA astrobiology roadmap. *Astrobiology*, **8**, 715–730, https://doi.org/10.1089/ast.2008.0819

DiLoreto, Z.A., Bontognali, T.R.R. *et al.* 2019. Microbial community composition and dolomite formation in the hypersaline microbial mats of the Khor Al-Adaid sabkhas, Qatar. *Extremophiles*, **23**, 201–218, https://doi.org/10.1007/s00792-018-01074-4

Dodd, M.S., Papineau, D. *et al.* 2017. Evidence for early life in Earth's oldest hydrothermal vent precipitates. *Nature*, **543**, 60–64, https://doi.org/10.1038/nature21377

Dominguez Bella, S. and García-Ruiz, J.M. 1987. Banding structures in induced morphology crystal aggregates of $CaCO_3$. *Journal of Materials Science*, **22**, 3095–3102, https://doi.org/10.1007/BF01161169

Duarte-Neto, P., Stošić, T., Stošić, B., Lessa, R. and Milošević, M.V. 2014. Interplay of model ingredients affecting aggregate shape plasticity in diffusion-limited aggregation. *Physical Review E*, **90**, 012312, https://doi.org/10.1103/PhysRevE.90.012312

Duda, J.-P., Thiel, V., *et al.* 2018. Ideas and perspectives: hydrothermally driven redistribution and sequestration of early Archaean biomass – the "hydrothermal pump hypothesis". *Biogeosciences*, **15**, 1535–1548, https://doi.org/10.5194/bg-15-1535-2018

Dupraz, C., Reid, R.P., Braissant, O., Decho, A.W., Norman, R.S. and Visscher, P.T. 2009. Processes of carbonate precipitation in modern microbial mats. *Earth-Science Reviews*, **96**, 141–162, https://doi.org/10.1016/j.earscirev.2008.10.005

Ehlmann, B.L., Mustard, J.F. and Murchie, S.L. 2010. Geologic setting of serpentine deposits on Mars. *Geophysical Research Letters*, **37**, https://doi.org/10.1029/2010GL042596

Eigenbrode, J.L., Summons, R.E. *et al.* 2018. Organic matter preserved in 3-billion-year-old mudstones at Gale crater, Mars. *Science*, **360**, 1096–1101, https://doi.org/10.1126/science.aas9185

Eiler, J.M., Clog, M., Lawson, M., Lloyd, M., Piasecki, A., Ponton, C. and Xie, H. 2018. The isotopic structures of geological organic compounds. *Geological Society, London, Special Publications*, **468**, 53–81, https://doi.org/10.1144/SP468.4

Emerson, D. and Moyer, C.L. 2002. Neutrophilic Fe-oxidizing bacteria are abundant at the Loihi Seamount hydrothermal vents and play a major role in Fe oxide deposition. *Applied and Environmental Microbiology*, **68**, 3085–3093, https://doi.org/10.1128/AEM.68.6.3085-3093.2002

Engelhardt, W.V., Arndt, J., Fecker, B. and Pankau, H.G. 1995. Suevite breccia from the Ries crater, Germany: origin, cooling history and devitrification of

impact glasses. *Meteoritics*, **30**, 279–293, https://doi.org/10.1111/j.1945-5100.1995.tb01126.x

Erastova, V., Degiacomi, M.T.G., Fraser, D. and Greenwell, H.C. 2017. Mineral surface chemistry control for origin of prebiotic peptides. *Nature Communications*, **8**, 2033, https://doi.org/10.1038/s41467-017-02248-y

Falini, G., Albeck, S., Weiner, S. and Addadi, L. 1996. Control of aragonite or calcite polymorphism by mollusk shell macromolecules. *Science*, **271**, 67–69, https://doi.org/10.1126/science.271.5245.67

Farley, K.A., Malespin, C. *et al.* 2014. In situ radiometric and exposure age dating of the martian surface. *Science*, **343**, https://doi.org/10.1126/science.1247166

Farquhar, J., Bao, H. and Thiemens, M.H. 2000*a*. Atmospheric influence of Earth's earliest sulfur cycle. *Science*, **289**, 756–759, https://doi.org/10.1126/science.289.5480.756

Farquhar, J., Savarino, J., Jackson, T.L. and Thiemens, M.H. 2000*b*. Evidence of atmospheric sulphur in the martian regolith from sulphur isotopes in meteorites. *Nature*, **404**, 50–52, https://doi.org/10.1038/35003517

Farquhar, J., Savarino, J., Airieau, S. and Thiemens, M.H. 2001. Observation of wavelength-sensitive mass-independent sulfur isotope effects during SO_2 photolysis: implications for the early atmosphere. *Journal of Geophysical Research: Planets*, **106**, 32829–32839, https://doi.org/10.1029/2000JE001437

Fike, D.A., Bradley, A.S. and Rose, C.V. 2015. Rethinking the ancient sulfur cycle. *Annual Review of Earth and Planetary Sciences*, **43**, 593–622, https://doi.org/10.1146/annurev-earth-060313-054802

Fischer, A., Schmitz, M., Aichmayer, B., Fratzl, P. and Faivre, D. 2011. Structural purity of magnetite nanoparticles in magnetotactic bacteria. *Journal of the Royal Society Interface*, **8**, 1011–1018, https://doi.org/10.1098/rsif.2010.0576

Fisk, M. and McLoughlin, N. 2013. Atlas of alteration textures in volcanic glass from the ocean basins. *Geosphere*, **9**, 317–341, https://doi.org/10.1130/GES00827.1https://doi.org/10.1130/GES00827.1

Fisk, M.R., Giovannoni, S.J. and Thorseth, I.H. 1998. Alteration of oceanic volcanic glass: textural evidence of microbial activity. *Science*, **281**, 978–980, https://doi.org/10.1126/science.281.5379.978

Fornaro, T., Steele, A. and Brucato, J.R. 2018. Catalytic/protective properties of martian minerals and implications for possible origin of life on Mars. *Life*, **8**, https://doi.org/10.3390/life8040056

Fothergill, J., Li, M., Davis, S.A., Cunningham, J.A. and Mann, S. 2014. Nanoparticle-based membrane assembly and silicification in coacervate microdroplets as a route to complex colloidosomes. *Langmuir*, **30**, 14591–14596, https://doi.org/10.1021/la503746u

Fox, S.W. and Yuyama, S. 1963. Abiotic production of primitive protein and formed microparticles. *Annals of the New York Academy of Sciences*, **108**, 487–494, https://doi.org/10.1111/j.1749-6632.1963.tb13404.x

Fox-Powell, M.G. and Cousins, C.R. 2021. Partitioning of crystalline and amorphous phases during freezing of simulated Enceladus ocean fluids. *Journal of Geophysical Research: Planets*, **126**, e2020JE006628, https://doi.org/10.1029/2020JE006628

Francis, S., Margulis, L. and Barghoorn, E.S. 1978. On the experimental silicification of microorganisms II. On the time of appearance of eukaryotic organisms in the fossil record. *Precambrian Research*, **6**, 65–100, https://doi.org/10.1016/0301-9268(78)90055-4

Franz, H.B., Kim, S.-T. *et al.* 2014. Isotopic links between atmospheric chemistry and the deep sulphur cycle on Mars. *Nature*, **508**, 364–368, https://doi.org/10.1038/nature13175

Franz, H.B., McAdam, A.C. *et al.* 2017. Large sulfur isotope fractionations in Martian sediments at Gale crater. *Nature Geoscience*, **10**, 658–662, https://doi.org/10.1038/ngeo3002

Franz, H.B., King, P.L. and Gaillard, F. 2019. Sulfur on Mars from the atmosphere to the core. *In*: Filiberto, J. and Schwenzer, S.P. (eds) *Volatiles in the Martian Crust*. Elsevier, 119–183, https://doi.org/10.1016/B978-0-12-804191-8.00006-4

Franz, H.B., Mahaffy, P.R. *et al.* 2020. Indigenous and exogenous organics and surface–atmosphere cycling inferred from carbon and oxygen isotopes at Gale crater. *Nature Astronomy*, **4**, 526–532, https://doi.org/10.1038/s41550-019-0990-x

Freissinet, C., Glavin, D.P. *et al.* 2015. Organic molecules in the Sheepbed Mudstone, Gale Crater, Mars. *Journal of Geophysical Research: Planets*, **120**, 495–514, https://doi.org/10.1002/2014JE004737

Friedmann, E.I., Wierzchos, J., Ascaso, C. and Winklhofer, M. 2001. Chains of magnetite crystals in the meteorite ALH84001: evidence of biological origin. *Proceedings of the National Academy of Sciences of the United States of America*, **98**, 2176–2181, https://doi.org/10.1073/pnas.051514698

Fukushi, K., Sekine, Y., Sakuma, H., Morida, K. and Wordsworth, R. 2019. Semiarid climate and hyposaline lake on early Mars inferred from reconstructed water chemistry at Gale. *Nature Communications*, **10**, 4896, https://doi.org/10.1038/s41467-019-12871-6

Furukawa, Y., Chikaraishi, Y. *et al.* 2019. Extraterrestrial ribose and other sugars in primitive meteorites. *Proceedings of the National Academy of Sciences of the United States of America*, **116**, 24440–24445, https://doi.org/10.1073/pnas.1907169116

Gan, T., Luo, T. *et al.* 2021. Cryptic terrestrial fungus-like fossils of the early Ediacaran Period. *Nature Communications*, **12**, 641, https://doi.org/10.1038/s41467-021-20975-1

García-Ruiz, J. 1994. Inorganic self-organization in Precambrian charts. *Origins of Life and Evolution of the Biosphere*, **24**, 451–467, https://doi.org/10.1007/BF01582030

García-Ruiz, J.M. 2000. Geochemical scenarios for the precipitation of biomimetic inorganic carbonates. *SEPM, Special Publications*, **67**, 75–89.

García-Ruiz, J.M. and Amorós, J.L. 1981*a*. Morphological aspects of some symmetrical crystal aggregates grown by silica gel technique. *Journal of Crystal Growth*, **55**, 379–383, https://doi.org/10.1016/0022-0248(81)90038-5

García-Ruiz, J.M. and Amorós, J.L. 1981*b*. Crystal aggregates with induced morphologies grown by silica gel technique. *Bulletin de Minéralogie*, **104**, 107–113, https://doi.org/10.3406/bulmi.1981.7442

García-Ruiz, J.M., Carnerup, A., Christy, A.G., Welham, N.J. and Hyde, S.T. 2002. Morphology: an ambiguous indicator of biogenicity. *Astrobiology*, **2**, 353–369, https://doi.org/10.1089/153110702762027925

García-Ruiz, J.M., Melero-Garcia, E. and Hyde, S.T. 2009. Morphogenesis of self-assembled nanocrystalline materials of barium carbonate and silica. *Science*, **323**, 362–365, https://doi.org/10.1126/science.1165349

García-Ruiz, J.M., Nakouzi, E., Kotopoulou, E., Tamborrino, L. and Steinbock, O. 2017. Biomimetic mineral self-organization from silica-rich spring waters. *Science Advances*, **3**, e1602285, https://doi.org/10.1126/sciadv.1602285

García-Ruiz, J.M., van Zuilen, M.A. and Bach, W. 2020. Mineral self-organization on a lifeless planet. *Physics of Life Reviews*, **34**–35, 62–82, https://doi.org/10.1016/j.plrev.2020.01.001

Garwood, R.J., Oliver, H. and Spencer, A.R.T. 2020. An introduction to the Rhynie chert. *Geological Magazine*, **157**, 47–64, https://doi.org/10.1017/S0016756819000670

Georgieva, M.N., Little, C.T.S., Maslennikov, V.V., Glover, A.G., Ayupova, N.R. and Herrington, R.J. 2021. The history of life at hydrothermal vents. *Earth-Science Reviews*, **217**, 103602, https://doi.org/10.1016/j.earscirev.2021.103602

Gilbert, P.U.P.A., Porter, S.M., Sun, C.-Y., Xiao, S., Gibson, B.M., Shenkar, N. and Knoll, A.H. 2019. Biomineralization by particle attachment in early animals. *Proceedings of the National Academy of Sciences of the United States of America*, **116**, 17659–17665, https://doi.org/10.1073/pnas.1902273116

Glauber, J.R. 1646. LXXXV. Wie man in diesem Liquore von allen Metallen in wenig Stunden Bäume mit Farben soll wachsen machen. *In*: *Furni Novi Philosophici*, T. Williams (London), 186–189.

Glavin, D.P., Freissinet, C. *et al.* 2013. Evidence for perchlorates and the origin of chlorinated hydrocarbons detected by SAM at the Rocknest aeolian deposit in Gale Crater. *Journal of Geophysical Research: Planets*, **118**, 1955–1973, https://doi.org/10.1002/jgre.20144

Gleeson, D.F., Pappalardo, R.T., Anderson, M.S., Grasby, S.E., Mielke, R.E., Wright, K.E. and Templeton, A.S. 2012. Biosignature detection at an Arctic analog to Europa. *Astrobiology*, **12**, 135–150, https://doi.org/10.1089/ast.2010.0579

Goesmann, F., Brinckerhoff, W.B. *et al.* 2017. The Mars organic molecule analyzer (MOMA) instrument: characterization of organic material in martian sediments. *Astrobiology*, **17**, 655–685, https://doi.org/10.1089/ast.2016.1551

Golden, D.C., Ming, D.W. *et al.* 2001. A simple inorganic process for formation of carbonates, magnetite, and sulfides in Martian meteorite ALH84001. *American Mineralogist*, **86**, 370–375, https://doi.org/10.2138/am-2001-2-321

Golden, D.C., Ming, D.W. *et al.* 2004. Evidence for exclusively inorganic formation of magnetite in Martian meteorite ALH84001. *American Mineralogist*, **89**, 681–695, https://doi.org/10.2138/am-2004-5-602

Göppert, J.H.R. 1848. Über pflanzenähnliche Einschlüsse in den Chalcedonen. *Flora*, **16**, 257–266.

Götze, J., Hofmann, B. *et al.* 2020. Biosignatures in subsurface filamentous fabrics (SFF) from the Deccan Volcanic Province, India. *Minerals*, **10**, 540, https://doi.org/10.3390/min10060540

Gower, L.B. 2008. Biomimetic model systems for investigating the amorphous precursor pathway and its role in biomineralization. *Chemical Reviews*, **108**, 4551–4627, https://doi.org/10.1021/cr800443h

Grady, M.M., Verchovsky, A.B. and Wright, I.P. 2004. Magmatic carbon in Martian meteorites: attempts to constrain the carbon cycle on Mars. *International Journal of Astrobiology*, **3**, 117–124, https://doi.org/10.1017/S1473550404002071

Grasby, S.E. 2003. Naturally precipitating vaterite (μ-$CaCO_3$) spheres: unusual carbonates formed in an extreme environment. *Geochimica et Cosmochimica Acta*, **67**, 1659–1666, https://doi.org/10.1016/S0016-7037(02)01304-2

Grosch, E.G. and McLoughlin, N. 2014. Reassessing the biogenicity of Earth's oldest trace fossil with implications for biosignatures in the search for early life. *Proceedings of the National Academy of Sciences of the United States of America*, **111**, 8380–8385, https://doi.org/10.1073/pnas.1402565111

Grosch, E.G. and McLoughlin, N. 2015. Questioning the biogenicity of titanite mineral trace fossils in Archean pillow lavas. *Proceedings of the National Academy of Sciences of the United States of America*, **112**, E3090–E3091, https://doi.org/10.1073/pnas.1506995112

Grotzinger, J.P. and Rothman, D.H. 1996. An abiotic model for stromatolite morphogenesis. *Nature*, **383**, 423–425, https://doi.org/10.1038/383423a0

Gruner, J.W. 1924. Contributions to the geology of the Mesabi range: with special reference to the magnetites of the iron-bearing formation west of Mesaba. *Minnesota Geological Survey Bulletin*, **19**, 1–71.

Halevy, I. 2013. Production, preservation, and biological processing of mass-independent sulfur isotope fractionation in the Archean surface environment.

Proceedings of the National Academy of Sciences of the United States of America, **110**, 17644–17649, https://doi.org/10.1073/pnas.1213148110

Han, Z., Meng, R. *et al.* 2017. Calcium carbonate precipitation by *Synechocystis* sp. PCC6803 at different Mg/Ca molar ratios under the laboratory condition. *Carbonates and Evaporites*, **32**, 561–575, https://doi.org/10.1007/s13146-016-0322-5

Hawley, J.E. 1926. An evaluation of the evidence of life in the Archean. *The Journal of Geology*, **34**, 441–461, https://doi.org/10.1086/623331

Hays, L.E., Graham, H.V. *et al.* 2017. Biosignature preservation and detection in Mars analog environments. *Astrobiology*, **17**, 363–400, https://doi.org/10.1089/ast.2016.1627

Heinz, J. and Schulze-Makuch, D. 2020. Thiophenes on Mars: biotic or abiotic origin? *Astrobiology*, **20**, 552–561, https://doi.org/10.1089/ast.2019.2139

Hickman-Lewis, K., Cavalazzi, B. *et al.* 2020. Metallomics in deep time and the influence of ocean chemistry on the metabolic landscapes of Earth's earliest ecosystems. *Scientific Reports*, **10**, 4965, https://doi.org/10.1038/s41598-020-61774-w

Hofmann, B.A. and Farmer, J.D. 2000. Filamentous fabrics in low-temperature mineral assemblages: are they fossil biomarkers? Implications for the search for a subsurface fossil record on the early Earth and Mars. *Planetary and Space Science*, **48**, 1077–1086, https://doi.org/10.1016/S0032-0633(00)00081-7

Hofmann, B.A., Farmer, J.D., von Blanckenburg, F. and Fallick, A.E. 2008. Subsurface filamentous fabrics: an evaluation of origins based on morphological and geochemical criteria, with implications for exopaleontology. *Astrobiology*, **8**, 87–117, https://doi.org/10.1089/ast.2007.0130

Hood, M.A., Landfester, K. and Muñoz-Espí, R. 2014. The role of residue acidity on the stabilization of vaterite by amino acids and oligopeptides. *Crystal Growth & Design*, **14**, 1077–1085, https://doi.org/10.1021/cg401580y

Hopkinson, L., Roberts, S., Herrington, R. and Wilkinson, J. 1998. Self-organization of submarine hydrothermal siliceous deposits: evidence from the TAG hydrothermal mound, 26°N Mid-Atlantic Ridge. *Geology*, **26**, 347–350, https://doi.org/10.1130/0091-7613(1998)026<0347:SOOSHS>2.3.CO;2

Horgan, B. and Bell, J.F. 2012. Widespread weathered glass on the surface of Mars. *Geology*, **40**, 391–394, https://doi.org/10.1130/G32755.1

Horgan, B.H.N., Anderson, R.B., Dromart, G., Amador, E.S. and Rice, M.S. 2020. The mineral diversity of Jezero crater: evidence for possible lacustrine carbonates on Mars. *Icarus*, **339**, 113526, https://doi.org/10.1016/j.icarus.2019.113526

Horita, J. 2005. Some perspectives on isotope biosignatures for early life. *Chemical Geology*, **218**, 171–186, https://doi.org/10.1016/j.chemgeo.2005.01.017

Horodyski, R.J. 1981. Pseudomicrofossils and altered microfossils from a middle Proterozoic shale belt supergroup, Montana. *Precambrian Research*, **16**, 143–154, https://doi.org/10.1016/0301-9268(81)90009-7

Hyslop, E.V., Valley, J.W., Johnson, C.M. and Beard, B.L. 2008. The effects of metamorphism on O and Fe isotope compositions in the Biwabik Iron Formation, northern Minnesota. *Contributions to Mineralogy and Petrology*, **155**, 313–328, https://doi.org/10.1007/s00410-007-0244-2

Ivarsson, M., Drake, H., Neubeck, A., Sallstedt, T., Bengtson, S., Roberts, N.M.W. and Rasmussen, B. 2020. The fossil record of igneous rock. *Earth-Science Reviews*, **210**, 103342, https://doi.org/10.1016/j.earscirev.2020.103342

Ivarsson, M., Drake, H., Neubeck, A., Snoeyenbos-West, O., Belivanova, V. and Bengtson, S. 2021. Introducing palaeolithobiology. *GFF*, https://doi.org/10.1080/11035897.2021.1895302

Javaux, E.J. and Lepot, K. 2018. The Paleoproterozoic fossil record: implications for the evolution of the biosphere during Earth's middle-age. *Earth-Science Reviews*, **176**, 68–86, https://doi.org/10.1016/j.earscirev.2017.10.001

Javaux, E.J., Marshall, C.P. and Bekker, A. 2010. Organic-walled microfossils in 3.2-billion-year-old shallow-marine siliciclastic deposits. *Nature*, **463**, 934–938, https://doi.org/10.1038/nature08793

Javaux, E.J., Asael, D. *et al.* 2013. Identifying early Earth microfossils in unsilicified sediments. Abstract presented at the EGU General Assembly Conference, EGU2013-7748, Vienna, Austria.

Johannessen, K.C., McLoughlin, N., Vullum, P.E. and Thorseth, I.H. 2020. On the biogenicity of Fe-oxyhydroxide filaments in silicified low-temperature hydrothermal deposits: implications for the identification of Fe-oxidizing bacteria in the rock record. *Geobiology*, **18**, 31–53, https://doi.org/10.1111/gbi.12363

Johnson, C.M., Beard, B.L. and Roden, E.E. 2008. The iron isotope fingerprints of redox and biogeochemical cycling in modern and ancient Earth. *Annual Review of Earth and Planetary Sciences*, **36**, 457–493, https://doi.org/10.1146/annurev.earth.36.031207.124139

Johnson, J.R., Bell, J.F. *et al.* 2007. Mineralogic constraints on sulfur-rich soils from Pancam spectra at Gusev crater, Mars. *Geophysical Research Letters*, **34**, https://doi.org/10.1029/2007GL029894

Jones, B. 2017. Review of calcium carbonate polymorph precipitation in spring systems. *Sedimentary Geology*, **353**, 64–75, https://doi.org/10.1016/j.sedgeo.2017.03.006

Jordan, D. 2008. *Aspects of Landscape Evolution, Lineaments and Fault Zone Mineralisation in Southeast Ireland*. PhD thesis, Trinity College Dublin.

Jordan, S.F., Rammu, H., Zheludev, I.N., Hartley, A.M., Maréchal, A. and Lane, N. 2019. Promotion of protocell self-assembly from mixed amphiphiles at the origin of life. *Nature Ecology & Evolution*, **3**, 1705–1714, https://doi.org/10.1038/s41559-019-1015-y

Josset, J.-L., Westall, F. *et al.* 2017. The close-up imager onboard the ESA ExoMars rover: objectives, description, operations, and science validation activities. *Astrobiology*, **17**, 595–611, https://doi.org/10.1089/ast.2016.1546

Kamyshny, A., Druschel, G., Mansaray, Z.F. and Farquhar, J. 2014. Multiple sulfur isotopes fractionations associated with abiotic sulfur transformations in Yellowstone National Park geothermal springs. *Geochemical Transactions*, **15**, 7, https://doi.org/10.1186/1467-4866-15-7

Kaplan, I.R. and Rittenberg, S.C. 1964. Microbiological fractionation of sulphur isotopes. *Journal of General Microbiology*, **34**, 195–212, https://doi.org/10.1099/00221287-34-2-195

Kellermeier, M., Eiblmeier, J., Melero-García, E., Pretzl, M., Fery, A. and Kunz, W. 2012*a*. Evolution and control of complex curved form in simple inorganic precipitation systems. *Crystal Growth & Design*, **12**, 3647–3655, https://doi.org/10.1021/cg3004646

Kellermeier, M., Melero-García, E., Kunz, W. and García-Ruiz, J.M. 2012*b*. Local autocatalytic co-precipitation phenomena in self-assembled silica–carbonate materials. *Journal of Colloid and Interface Science*, **380**, 1–7, https://doi.org/10.1016/j.jcis.2012.05.009

Kellermeier, M., Cölfen, H. and García-Ruiz, J.M. 2012*c*. Silica biomorphs: complex biomimetic hybrid materials from 'sand and chalk'. *European Journal of Inorganic Chemistry*, **2012**, 5123–5144, https://doi.org/10.1002/ejic.201201029

Kim, S.S., Bargar, J.R. *et al.* 2011. Searching for biosignatures using electron paramagnetic resonance (EPR) analysis of manganese oxides. *Astrobiology*, **11**, 775–786, https://doi.org/10.1089/ast.2011.0619

King, P.L. and McLennan, S.M. 2010. Sulfur on Mars. *Elements*, **6**, 107–112, https://doi.org/10.2113/gselements.6.2.107

Knoll, A.H. and Barghoorn, E.S. 1974. Ambient pyrite in Precambrian chert: new evidence and a theory. *Proceedings of the National Academy of Sciences of the United States of America*, **71**, 2329–2331, https://doi.org/10.1073/pnas.71.6.2329

Koga, S., Williams, D.S., Perriman, A.W. and Mann, S. 2011. Peptide–nucleotide microdroplets as a step towards a membrane-free protocell model. *Nature Chemistry*, **3**, 720–724, https://doi.org/10.1038/nchem.1110

Koike, M., Nakada, R., Kajitani, I., Usui, T., Tamenori, Y., Sugahara, H. and Kobayashi, A. 2020. In-situ preservation of nitrogen-bearing organics in Noachian Martian carbonates. *Nature Communications*, **11**, 1988, https://doi.org/10.1038/s41467-020-15931-4

Korablev, O.I., Dobrolensky, Y. *et al.* 2017. Infrared spectrometer for ExoMars: a mast-mounted instrument for the rover. *Astrobiology*, **17**, 542–564, https://doi.org/10.1089/ast.2016.1543

Kotopoulou, E., Lopez-Haro, M., Gamez, J.J.C. and García-Ruiz, J.M. 2021. Nanoscale anatomy of iron–silica self-organized membranes: implications for prebiotic chemistry. *Angewandte Chemie*, **133**, 1416–1422, https://doi.org/10.1002/ange.202012059

Krause, S., Liebetrau, V., Gorb, S., Sánchez-Román, M., McKenzie, J.A. and Treude, T. 2012. Microbial nucleation of Mg-rich dolomite in exopolymeric substances under anoxic modern seawater salinity: new insight into an old enigma. *Geology*, **40**, 587–590, https://doi.org/10.1130/G32923.1

Kuga, M., Carrasco, N. *et al.* 2014. Nitrogen isotopic fractionation during abiotic synthesis of organic solid particles. *Earth and Planetary Science Letters*, **393**, 2–13, https://doi.org/10.1016/j.epsl.2014.02.037

Kung, C.-C., Hayatsu, R., Studier, M.H. and Clayton, R.N. 1979. Nitrogen isotope fractionations in the Fischer–Tropsch synthesis and in the Miller–Urey reaction. *Earth and Planetary Science Letters*, **46**, 141–146, https://doi.org/10.1016/0012-821X(79)90072-4

Lagaly, G., Ogawa, M. and Dékány, I. 2013. Clay mineral–organic interactions. *Developments in Clay Science*, **5**, 435–505, https://doi.org/10.1016/B978-0-08-098258-8.00015-8

Lai, J.C.-Y., Pearce, B.K.D., Pudritz, R.E. and Lee, D. 2019. Meteoritic abundances of fatty acids and potential reaction pathways in planetesimals. *Icarus*, **319**, 685–700, https://doi.org/10.1016/j.icarus.2018.09.028

Lambert, J.-F. 2008. Adsorption and polymerization of amino acids on mineral surfaces: a review. *Origins of Life and Evolution of Biospheres*, **38**, 211–242, https://doi.org/10.1007/s11084-008-9128-3

Leduc, S. 1911. *The Mechanism of Life*, Rebman (London).

Lepot, K., Philippot, P., Benzerara, K. and Wang, G.-Y. 2009. Garnet-filled trails associated with carbonaceous matter mimicking microbial filaments in Archean basalt. *Geobiology*, **7**, 393–402, https://doi.org/10.1111/j.1472-4669.2009.00208.x

Lepot, K., Benzerara, K. and Philippot, P. 2011. Biogenic versus metamorphic origins of diverse microtubes in 2.7 Gyr old volcanic ashes: multi-scale investigations. *Earth and Planetary Science Letters*, **312**, 37–47, https://doi.org/10.1016/j.epsl.2011.10.016

Lepot, K., Williford, K.H. *et al.* 2019. Extreme ^{13}C-depletions and organic sulfur content argue for S-fueled anaerobic methane oxidation in 2.72 Ga old stromatolites. *Geochimica et Cosmochimica Acta*, **244**, 522–547, https://doi.org/10.1016/j.gca.2018.10.014

Leshin, L.A., Mahaffy, P.R. *et al.* 2013. Volatile, isotope, and organic analysis of martian fines with the Mars Curiosity rover. *Science*, **341**, 1238937, https://doi.org/10.1126/science.1238937

Li, J., Benzerara, K., Bernard, S. and Beyssac, O. 2013. The link between biomineralization and fossilization of bacteria: insights from field and

experimental studies. *Chemical Geology*, **359**, 49–69, https://doi.org/10.1016/j.chemgeo.2013.09.013

Li, J., Bernard, S., Benzerara, K., Beyssac, O., Allard, T., Cosmidis, J. and Moussou, J. 2014. Impact of biomineralization on the preservation of microorganisms during fossilization: an experimental perspective. *Earth and Planetary Science Letters*, **400**, 113–122, https://doi.org/10.1016/j.epsl.2014.05.031

Li, J., Menguy, N. *et al.* 2015. Crystal growth of bullet-shaped magnetite in magnetotactic bacteria of the Nitrospirae phylum. *Journal of the Royal Society Interface*, **12**, 20141288, https://doi.org/10.1098/rsif.2014.1288

Li, M., Huang, X., Tang, T.-Y.D. and Mann, S. 2014. Synthetic cellularity based on non-lipid micro-compartments and protocell models. *Current Opinion in Chemical Biology*, **22**, 1–11, https://doi.org/10.1016/j.cbpa.2014.05.018

Liesegang, R.E. 1914. Die achate. *In*: d' Achiardi, G., Amberg, R. *et al.* (eds) *Silicate: Band II Erste Hälfte*, Springer. 186–190, https://doi.org/10.1007/978-3-642-49866-4_8

Lindsay, J.F., Brasier, M.D., McLoughlin, N., Green, O.R., Fogel, M., Steele, A. and Mertzman, S.A. 2005. The problem of deep carbon—an Archean paradox. *Precambrian Research*, **143**, 1–22, https://doi.org/10.1016/j.precamres.2005.09.003

Liu, Z., Zhang, Z. *et al.* 2020. Shape-preserving amorphous-to-crystalline transformation of $CaCO_3$ revealed by in situ TEM. *Proceedings of the National Academy of Sciences of the United States of America*, **117**, 3397–3404, https://doi.org/10.1073/pnas.1914813117

Lotfi-Kalahroodi, E., Pierson-Wickmann, A.-C., Rouxel, O., Marsac, R., Bouhnik-Le Coz, M., Hanna, K. and Davranche, M. 2021. More than redox, biological organic ligands control iron isotope fractionation in the riparian wetland. *Scientific Reports*, **11**, 1933, https://doi.org/10.1038/s41598-021-81494-z

Longo, A. and Damer, B. 2020. Factoring origin of life hypotheses into the search for life in the solar system and beyond. *Life*, **10**, 52, https://doi.org/10.3390/life10050052

Lowenstam, H. 1981. Minerals formed by organisms. *Science*, **211**, 1126–1131, https://doi.org/10.1126/science.7008198

MacCulloch, J. 1814. XXIII. On vegetable remains preserved in chalcedony. *Transactions of the Geological Society of London*, **S1-2**, 510–527, https://doi.org/10.1144/transgsla.2.510

Mänd, K., Kirsimäe, K. *et al.* 2018. Authigenesis of biomorphic apatite particles from Benguela upwelling zone sediments off Namibia: the role of organic matter in sedimentary apatite nucleation and growth. *Geobiology*, **16**, 640–658, https://doi.org/10.1111/gbi.12309

Mansor, M. and Xu, J. 2020. Benefits at the nanoscale: a review of nanoparticle-enabled processes favouring microbial growth and functionality. *Environmental Microbiology*, **22**, 3633–3649, https://doi.org/10.1111/1462-2920.15174

Marin-Carbonne, J., Remusat, L., Sforna, M.C., Thomazo, C., Cartigny, P. and Philippot, P. 2018. Sulfur isotope's signal of nanopyrites enclosed in 2.7 Ga stromatolitic organic remains reveal microbial sulfate reduction. *Geobiology*, **16**, 121–138, https://doi.org/10.1111/gbi.12275

Marin-Carbonne, J., Busigny, V. *et al.* 2020. In situ Fe and S isotope analyses in pyrite from the 3.2 Ga Mendon Formation (Barberton Greenstone Belt, South Africa): evidence for early microbial iron reduction. *Geobiology*, **18**, 306–325, https://doi.org/10.1111/gbi.12385

Marnocha, C.L., Sabanayagam, C.R. *et al.* 2019. Insights into the mineralogy and surface chemistry of extracellular biogenic S^0 globules produced by *Chlorobaculum tepidum*. *Frontiers in Microbiology*, **10**, 271, https://doi.org/10.3389/fmicb.2019.00271

Marshall, C.P., Emry, J.R. and Olcott Marshall, A. 2011. Haematite pseudomicrofossils present in the 3.5-billion-year-old Apex Chert. *Nature Geoscience*, **4**, 240–243, https://doi.org/10.1038/ngeo1084

Marshall, S.M., Murray, A.R.G. and Cronin, L. 2017. A probabilistic framework for identifying biosignatures using Pathway Complexity. *Philosophical Transactions of the Royal Society A: Mathematical, Physical and Engineering Sciences*, **375**, 20160342, https://doi.org/10.1098/rsta.2016.0342

Martel, J., Young, D., Peng, H.-H., Wu, C.-Y. and Young, J.D. 2012. Biomimetic properties of minerals and the search for life in the Martian meteorite ALH84001. *Annual Review of Earth and Planetary Sciences*, **40**, 167–193, https://doi.org/10.1146/annurev-earth-042711-105401

Maurice, S., Wiens, R.C. *et al.* 2021. The SuperCam instrument suite on the Mars 2020 rover: science objectives and mast-unit description. *Space Science Reviews*, **217**, 47, https://doi.org/10.1007/s11214-021-00807-w

McAdam, A.C., Franz, H.B. *et al.* 2014. Sulfur-bearing phases detected by evolved gas analysis of the Rocknest aeolian deposit, Gale Crater, Mars. *Journal of Geophysical Research: Planets*, **119**, 373–393, https://doi.org/10.1002/2013JE004518

McCollom, T.M. 2013. Laboratory simulations of abiotic hydrocarbon formation in Earth's deep subsurface. *Reviews in Mineralogy and Geochemistry*, **75**, 467–494, https://doi.org/10.2138/rmg.2013.75.15

McCollom, T.M. and Donaldson, C. 2019. Experimental constraints on abiotic formation of tubules and other proposed biological structures in subsurface volcanic glass. *Astrobiology*, **19**, 53–63, https://doi.org/10.1089/ast.2017.1811

McCollom, T.M. and Seewald, J.S. 2006. Carbon isotope composition of organic compounds produced by abiotic synthesis under hydrothermal conditions. *Earth and Planetary Science Letters*, **243**, 74–84, https://doi.org/10.1016/j.epsl.2006.01.027

McCollom, T.M., Lollar, B.S., Lacrampe-Couloume, G. and Seewald, J.S. 2010. The influence of carbon source on abiotic organic synthesis and carbon isotope fractionation under hydrothermal conditions. *Geochimica et Cosmochimica Acta*, **74**, 2717–2740, https://doi.org/10.1016/j.gca.2010.02.008

McKay, D.S., Gibson, E.K. *et al.* 1996. Search for past life on Mars: possible relic biogenic activity in martian meteorite ALH84001. *Science*, **273**, 924–930, https://doi.org/10.1126/science.273.5277.924

McLennan, S.M., Bell, J.F. *et al.* 2005. Provenance and diagenesis of the evaporite-bearing Burns Formation, Meridiani Planum, Mars. *Earth and Planetary Science Letters*, **240**, 95–121, https://doi.org/10.1016/j.epsl.2005.09.041

McLoughlin, N. and Grosch, E.G. 2015. A hierarchical system for evaluating the biogenicity of metavolcanic- and ultramafic-hosted microalteration textures in the search for extraterrestrial life. *Astrobiology*, **15**, 901–921, https://doi.org/10.1089/ast.2014.1259

McLoughlin, N., Brasier, M.D., Wacey, D., Green, O.R. and Perry, R.S. 2007. On biogenicity criteria for endolithic microborings on early Earth and beyond. *Astrobiology*, **7**, 10–26, https://doi.org/10.1089/ast.2006.0122

McLoughlin, N., Wilson, L.A. and Brasier, M.D. 2008. Growth of synthetic stromatolites and wrinkle structures in the absence of microbes – implications for the early fossil record. *Geobiology*, **6**, 95–105, https://doi.org/10.1111/j.1472-4669.2007.00141.x

McLoughlin, N., Grosch, E.G., Vullum, P.E., Guagliardo, P., Saunders, M. and Wacey, D. 2019. Critically testing olivine-hosted putative martian biosignatures in the Yamato 000593 meteorite—geobiological implications. *Geobiology*, **17**, 691–707, https://doi.org/10.1111/gbi.12361

McLoughlin, N., Wacey, D., Phunguphungu, S., Saunders, M. and Grosch, E.G. 2020. Deconstructing Earth's oldest ichnofossil record from the Pilbara Craton, West Australia: implications for seeking life in the Archean subseafloor. *Geobiology*, **18**, 525–543, https://doi.org/10.1111/gbi.12399

McMahon, S. 2019. Earth's earliest and deepest purported fossils may be iron-mineralized chemical gardens. *Proceedings of the Royal Society B: Biological Sciences*, **286**, https://doi.org/10.1098/rspb.2019.2410

McMahon, S. and Ivarsson, M. 2019. A new frontier for palaeobiology: Earth's vast deep biosphere. *BioEssays*, **41**, 1900052, https://doi.org/10.1002/bies.201900052

McMahon, S., van Smeerdijk Hood, A. and McIlroy, D. 2017. The origin and occurrence of subaqueous sedimentary cracks. *Geological Society, London, Special Publications*, **448**, 285–309, https://doi.org/10.1144/SP448.15

McMahon, S., Bosak, T. *et al.* 2018. A field guide to finding fossils on Mars. *Journal of Geophysical Research: Planets*, **123**, 1012–1040, https://doi.org/10.1029/2017JE005478

McMahon, S., Ivarsson, M. *et al.* 2021. Dubiofossils from a Mars-analogue subsurface palaeoenvironment: the limits of biogenicity criteria. *Geobiology*, **19**, 473–488, https://doi.org/10.1111/gbi.12445

Meldrum, F.C. and Cölfen, H. 2008. Controlling mineral morphologies and structures in biological and synthetic systems. *Chemical Reviews*, **108**, 4332–4432, https://doi.org/10.1021/cr8002856

Michalski, J.R., Onstott, T.C., Mojzsis, S.J., Mustard, J., Chan, Q.H.S., Niles, P.B. and Johnson, S.S. 2018. The Martian subsurface as a potential window into the origin of life. *Nature Geoscience*, **11**, 21–26, https://doi.org/10.1038/s41561-017-0015-2

Milesi, V., Guyot, F. *et al.* 2015. Formation of CO_2, H_2 and condensed carbon from siderite dissolution in the 200–300°C range and at 50 MPa. *Geochimica et Cosmochimica Acta*, **154**, 201–211, https://doi.org/10.1016/j.gca.2015.01.015

Ming, D.W., Archer, P.D. *et al.* 2014. Volatile and organic compositions of sedimentary rocks in Yellowknife Bay, Gale Crater, Mars. *Science*, **343**, 1245267, https://doi.org/10.1126/science.1245267

Mojarro, A., Jin, L., Szostak, J.W., Head, J.W. and Zuber, M.T. 2021. In search of the RNA world on Mars. *Geobiology*, **19**, 307–321, https://doi.org/10.1111/gbi.12433

Moreras-Marti, A., Fox-Powell, M. *et al.* 2021. Quadruple sulfur isotope biosignatures from terrestrial Mars analogue systems. *Geochimica et Cosmochimica Acta*, **308**, 157–172, https://doi.org/10.1016/j.gca.2021.06.007

Muirhead, B.K., Nicholas, A.K., Umland, J., Sutherland, O. and Vijendran, S. 2020. Mars sample return campaign concept status. *Acta Astronautica*, **176**, 131–138, https://doi.org/10.1016/j.actaastro.2020.06.026

Mukkamala, S.B. and Powell, A.K. 2004. Biomimetic assembly of calcite microtrumpets: crystal tectonics in action. *Chemical Communications*, 918–919, https://doi.org/10.1039/B401754D

Muscente, A.D., Czaja, A.D., Tuggle, J., Winkler, C. and Xiao, S. 2018. Manganese oxides resembling microbial fabrics and their implications for recognizing inorganically preserved microfossils. *Astrobiology*, **18**, 249–258, https://doi.org/10.1089/ast.2017.1699

Myrgorodska, I., Meinert, C., Martins, Z., d'Hendecourt, L.L.S. and Meierhenrich, U.J. 2015. Molecular chirality in meteorites and interstellar ices, and the chirality experiment on board the ESA cometary Rosetta mission. *Angewandte Chemie International Edition*, **54**, 1402–1412, https://doi.org/10.1002/anie.201409354

Nakamura-Messenger, K., Messenger, S., Keller, L.P., Clemett, S.J. and Zolensky, M.E. 2006. Organic globules in the Tagish Lake meteorite: remnants of the protosolar disk. *Science*, **314**, 1439–1442, https://doi.org/10.1126/science.1132175

Neveu, M., Hays, L.E., Voytek, M.A., New, M.H. and Schulte, M.D. 2018. The ladder of life detection. *Astrobiology*, **18**, 1375–1402, https://doi.org/10.1089/ast.2017.1773

Niles, P.B., Michalski, J., Ming, D.W. and Golden, D.C. 2017. Elevated olivine weathering rates and sulfate formation at cryogenic temperatures on Mars. *Nature Communications*, **8**, 998, https://doi.org/10.1038/s41467-017-01227-7

Nilson, F.P.R. 2002. Possible impact of a primordial oil slick on atmospheric and chemical evolution. *Origins of Life and Evolution of the Biosphere*, **32**, 247–253, https://doi.org/10.1023/A:1016577923630

Nims, C., Lafond, J., Alleon, J., Templeton, A.S. and Cosmidis, J. 2021. Organic biomorphs may be better preserved than microorganisms in early Earth sediments. *Geology*, **49**, 629–634, https://doi.org/10.1130/G48152.1

Noffke, N. 2015. Ancient sedimentary structures in the <3.7 Ga Gillespie Lake Member, Mars, that resemble macroscopic morphology, spatial associations, and temporal succession in terrestrial microbialites. *Astrobiology*, **15**, 169–192, https://doi.org/10.1089/ast.2014.1218

Noffke, N. 2018. Comment on the paper by Davies *et al.*. 'Resolving MISS conceptions and misconceptions: a geological approach to sedimentary surface textures generated by microbial and abiotic processes' (Earth Science Reviews, 154 (2016), 210–246). *Earth-Science Reviews*, **176**, 373–383, https://doi.org/10.1016/j.earscirev.2017.11.021

Noffke, N., Gerdes, G., Klenke, T. and Krumbein, W.E. 2001. Microbially induced sedimentary structures: a new category within the classification of primary sedimentary structures. *Journal of Sedimentary Research*, **71**, 649–656, https://doi.org/10.1306/2DC4095D-0E47-11D7-8643000102C1865D

Noffke, N., Eriksson, K.A., Hazen, R.M. and Simpson, E.L. 2006. A new window into Early Archean life: microbial mats in Earth's oldest siliciclastic tidal deposits (3.2 Ga Moodies Group, South Africa). *Geology*, **34**, 253–256, https://doi.org/10.1130/G22246.1

Nouet, J., Baronnet, A. and Howard, L. 2012. Crystallization in organo-mineral micro-domains in the crossed-lamellar layer of *Nerita undata* (Gastropoda, Neritopsina). *Micron*, **43**, 456–462, https://doi.org/10.1016/j.micron.2011.10.027

Nutman, A.P., Bennett, V.C., Friend, C.R.L., Van Kranendonk, M.J. and Chivas, A.R. 2016. Rapid emergence of life shown by discovery of 3700-million-year-old microbial structures. *Nature*, **537**, 535–538, https://doi.org/10.1038/nature19355

Nutman, A.P., Bennett, V.C., Friend, C.R.L. and Van Kranendonk, M.J. 2021. In support of rare relict c. 3700 Ma stromatolites from Isua (Greenland). *Earth and Planetary Science Letters*, **562**, 116850, https://doi.org/10.1016/j.epsl.2021.116850

Oaki, Y. and Imai, H. 2003. Experimental demonstration for the morphological evolution of crystals grown in gel media. *Crystal Growth & Design*, **3**, 711–716, https://doi.org/10.1021/cg034053e

Oaki, Y., Kotachi, A., Miura, T. and Imai, H. 2006. Bridged nanocrystals in biominerals and their biomimetics: classical yet modern crystal growth on the nanoscale. *Advanced Functional Materials*, **16**, 1633–1639, https://doi.org/10.1002/adfm.200600262

Ohmoto, H. and Lasaga, A.C. 1982. Kinetics of reactions between aqueous sulfates and sulfides in hydrothermal systems. *Geochimica et Cosmochimica Acta*, **46**, 1727–1745, https://doi.org/10.1016/0016-7037(82)90113-2

Ojha, L., Wilhelm, M.B. *et al.* 2015. Spectral evidence for hydrated salts in recurring slope lineae on Mars. *Nature Geoscience*, **8**, 829–832, https://doi.org/10.1038/ngeo2546

Olszta, M.J., Cheng, X. *et al.* 2007. Bone structure and formation: a new perspective. *Materials Science and Engineering R: Reports*, **58**, 77–116, https://doi.org/10.1016/j.mser.2007.05.001

Ono, S. 2008. Multiple-sulphur isotope biosignatures. *Space Sciences Series of ISSI*, **25**, 203–220, https://doi.org/10.1007/978-0-387-77516-6_14

Oparin, A.I. 1924. *Proiskhozhdenie Zhizny (The Origin of Life)*, Moskovski Rabochii (Moscow).

Opel, J., Wimmer, F.P., Kellermeier, M. and Cölfen, H. 2016. Functionalisation of silica–carbonate biomorphs. *Nanoscale Horizons*, **1**, 144–149, https://doi.org/10.1039/C5NH00094G

Opel, J., Kellermeier, M., Sickinger, A., Morales, J., Cölfen, H. and García-Ruiz, J.-M. 2018. Structural transition of inorganic silica–carbonate composites towards curved lifelike morphologies. *Minerals*, **8**, 75, https://doi.org/10.3390/min8020075

Orgel, L.E. 2004. Prebiotic chemistry and the origin of the RNA world. *Critical Reviews in Biochemistry and Molecular Biology*, **39**, 99–123, https://doi.org/10.1080/10409230490460765

Ortoleva, P. 1994. *Geochemical Self-Organization*. *Oxford Monographs on Geology and Geophysics. Oxford University Press*.

Pan, L., Carter, J. *et al.* 2021. Voluminous silica precipitated from martian waters during late-stage aqueous alteration. *The Planetary Science Journal*, **2**, 65, https://doi.org/10.3847/PSJ/abe541

Pavlov, A.A. and Kasting, J.F. 2002. Mass-independent fractionation of sulfur isotopes in Archean sediments: strong evidence for an anoxic Archean atmosphere. *Astrobiology*, **2**, 27–41, https://doi.org/10.1089/153110702753621321

Pedersen, L.-E.R., McLoughlin, N., Vullum, P.E. and Thorseth, I.H. 2015. Abiotic and candidate biotic micro-alteration textures in subseafloor basaltic glass: a high-resolution in-situ textural and geochemical investigation. *Chemical Geology*, **410**, 124–137, https://doi.org/10.1016/j.chemgeo.2015.06.005

Pellerin, A., Antler, G. *et al.* 2019. Large sulfur isotope fractionation by bacterial sulfide oxidation. *Science Advances*, **5**, eaaw1480, https://doi.org/10.1126/sciadv.aaw1480

Peng, X. and Jones, B. 2013. Patterns of biomediated $CaCO_3$ crystal bushes in hot spring deposits. *Sedimentary Geology*, **294**, 105–117, https://doi.org/10.1016/j.sedgeo.2013.05.009

Percak-Dennett, E.M., Beard, B.L., Xu, H., Konishi, H., Johnson, C.M. and Roden, E.E. 2011. Iron isotope fractionation during microbial dissimilatory iron oxide reduction in simulated Archaean seawater. *Geobiology*, **9**, 205–220, https://doi.org/10.1111/j.1472-4669.2011.00277.x

Petrash, D.A., Bialik, O.M., Bontognali, T.R.R., Vasconcelos, C., Roberts, J.A., McKenzie, J.A. and Konhauser, K.O. 2017. Microbially catalyzed dolomite formation: from near-surface to burial. *Earth-Science Reviews*, **171**, 558–582, https://doi.org/10.1016/j.earscirev.2017.06.015

Petroff, A.P., Sim, M.S., Maslov, A., Krupenin, M., Rothman, D.H. and Bosak, T. 2010. Biophysical basis for the geometry of conical stromatolites. *Proceedings of the National Academy of Sciences of the United States of America*, **107**, 9956–9961, https://doi.org/10.1073/pnas.1001973107

Philippot, P., Zuilen, M.V., Lepot, K., Thomazo, C., Farquhar, J. and Kranendonk, M.J.V. 2007. Early Archaean microorganisms preferred elemental sulfur, not sulfate. *Science*, **317**, 1534–1537, https://doi.org/10.1126/science.1145861

Phoenix, V.R., Renaut, R.W., Jones, B. and Ferris, F.G. 2005. Bacterial S-layer preservation and rare arsenic–antimony–sulphide bioimmobilization in siliceous sediments from Champagne Pool hot spring, Waiotapu, New Zealand. *Journal of the Geological Society, London*, **162**, 323–331, https://doi.org/10.1144/0016-764903-058

Picard, A., Kappler, A., Schmid, G., Quaroni, L. and Obst, M. 2015. Experimental diagenesis of organo-mineral structures formed by microaerophilic Fe(II)-oxidizing bacteria. *Nature Communications*, **6**, 6277, https://doi.org/10.1038/ncomms7277

Pickersgill, A.E., Sapers, H.M., Lee, M.R., Wildman, M., Lindgren, P. and Hallis, L. 2021. Microtubules, trichites, and bioalteration in impact glasses. Paper presented at the Lunar and Planetary Science Conference (virtual conference), 2035.

Poitrasson, F. 2015. Iron isotopes. *In*: Gargaud, M., Irvine, W.M. *et al.* (eds) *Encyclopedia of Astrobiology*. Springer, 1264–1268, https://doi.org/10.1007/978-3-662-44185-5_811

Preston, L.J., Izawa, M.R.M. and Banerjee, N.R. 2011. Infrared spectroscopic characterization of organic matter associated with microbial bioalteration textures in basaltic glass. *Astrobiology*, **11**, 585–599, https://doi.org/10.1089/ast.2010.0604

Quantin-Nataf, C., Carter, J. *et al.* 2021. Oxia planum: the landing site for the ExoMars 'Rosalind Franklin' rover mission: geological context and prelanding interpretation. *Astrobiology*, **21**, 345–366, https://doi.org/10.1089/ast.2019.2191

Rasmussen, B., Muhling, J.R. and Fischer, W.W. 2021. Ancient oil as a source of carbonaceous matter in 1.88-billion-year-old Gunflint stromatolites and microfossils. *Astrobiology*, **21**, 655–672, https://doi.org/10.1089/ast.2020.2376

Reeves, E.P. and Fiebig, J. 2020. Abiotic synthesis of methane and organic compounds in Earth's lithosphere. *Elements*, **16**, 25–31, https://doi.org/10.2138/gselements.16.1.25

Reitner, J. 2004. Organomineralization: a clue to the understanding of meteorite-related 'bacteria-shaped' carbonate particles. *Cellular Origin, Life in Extreme Habitats and Astrobiology*, **6**, 195–212, https://doi.org/10.1007/1-4020-2522-X_13

Roberts, J.A., Kenward, P.A., Fowle, D.A., Goldstein, R.H., González, L.A. and Moore, D.S. 2013. Surface chemistry allows for abiotic precipitation of dolomite at low temperature. *Proceedings of the National Academy of Sciences of the United States of America*, **110**, 14540–14545, https://doi.org/10.1073/pnas.1305403110

Rodriguez-Navarro, C., Jimenez-Lopez, C., Rodriguez-Navarro, A., Gonzalez-Muñoz, M.T. and Rodriguez-Gallego, M. 2007. Bacterially mediated mineralization of vaterite. *Geochimica et Cosmochimica Acta*, **71**, 1197–1213, https://doi.org/10.1016/j.gca.2006.11.031

Ross, C.S. 1962. Microlites in glassy volcanic rocks. *American Mineralogist*, **47**, 723–740.

Rouillard, J., García-Ruiz, J.-M., Gong, J. and van Zuilen, M.A. 2018. A morphogram for silica–witherite biomorphs and its application to microfossil identification in the early Earth rock record. *Geobiology*, **16**, 279–296, https://doi.org/10.1111/gbi.12278

Rouillard, J., van Zuilen, M., Pisapia, C. and Garcia-Ruiz, J.-M. 2021. An alternative approach for assessing biogenicity. *Astrobiology*, **21**, 151–164, https://doi.org/10.1089/ast.2020.2282

Ruff, S.W. and Farmer, J.D. 2016. Silica deposits on Mars with features resembling hot spring biosignatures at El Tatio in Chile. *Nature Communications*, **7**, 13554, https://doi.org/10.1038/ncomms13554

Ruff, S.W., Campbell, K.A., Van Kranendonk, M.J., Rice, M.S. and Farmer, J.D. 2020. The case for ancient hot springs in Gusev Crater, Mars. *Astrobiology*, **20**, 475–499, https://doi.org/10.1089/ast.2019.2044

Rull, F., Maurice, S. *et al.* 2017. The Raman laser spectrometer for the ExoMars rover mission to Mars. *Astrobiology*, **17**, 627–654, https://doi.org/10.1089/ast.2016.1567

Sainz-Díaz, C.I., Escribano, B., Sánchez-Almazo, I. and Cartwright, J.H.E. 2021. Chemical gardens under Mars conditions: imaging chemical garden growth in situ in an environmental scanning electron microscope. *Geophysical Research Letters*, **48**, e2021GL092883, https://doi.org/10.1029/2021GL092883

Sand, K.K., Rodriguez-Blanco, J.D., Makovicky, E., Benning, L.G. and Stipp, S.L.S. 2012. Crystallization of $CaCO_3$ in water–alcohol mixtures: spherulitic growth, polymorph stabilization, and morphology change. *Crystal Growth & Design*, **12**, 842–853, https://doi.org/10.1021/cg2012342

Sapers, H.M., Osinski, G.R., Banerjee, N.R. and Preston, L.J. 2014. Enigmatic tubular features in impact glass. *Geology*, **42**, 471–474, https://doi.org/10.1130/G35293.1

Sasselov, D.D., Grotzinger, J.P. and Sutherland, J.D. 2020. The origin of life as a planetary phenomenon. *Science Advances*, **6**, eaax3419, https://doi.org/10.1126/sciadv.aax3419

Schaef, H.T., McGrail, B.P. and Owen, A.T. 2011. Basalt reactivity variability with reservoir depth in supercritical CO_2 and aqueous phases. *Energy Procedia*, **4**, 4977–4984, https://doi.org/10.1016/j.egypro.2011.02.468

Schidlowski, M. 2001. Carbon isotopes as biogeochemical recorders of life over 3.8 Ga of Earth history: evolution of a concept. *Precambrian Research*, **106**, 117–134, https://doi.org/10.1016/S0301-9268(00)00128-5

Schmidt, B., Sánchez, L.A., Fretschner, T., Kreps, G., Ferrero, M.A., Siñeriz, F. and Szewzyk, U. 2014. Isolation of *Sphaerotilus–Leptothrix* strains from iron bacteria communities in Tierra del Fuego wetlands. *FEMS Microbiology Ecology*, **90**, 454–466, https://doi.org/10.1111/1574-6941.12406

Schopf, J.W. 1968. Microflora of the Bitter Springs Formation, Late Precambrian, central Australia. *Journal of Paleontology*, **42**, 651–688.

Schopf, J.W. 1993. Microfossils of the Early Archean Apex Chert: new evidence of the antiquity of life. *Science*, **260**, 640–646, https://doi.org/10.1126/science.260.5108.640

Schopf, J.W. 2006. Fossil evidence of Archaean life. *Philosophical Transactions of the Royal Society B: Biological Sciences*, **361**, 869–885, https://doi.org/10.1098/rstb.2006.1834

Schopf, J.W., Kudryavtsev, A.B. *et al.* 2015. Sulfur-cycling fossil bacteria from the 1.8-Ga Duck Creek Formation provide promising evidence of evolution's null hypothesis. *Proceedings of the National Academy of Sciences of the United States of America*, **112**, 2087–2092, https://doi.org/10.1073/pnas.1419241112

Schopf, J.W., Kitajima, K., Spicuzza, M.J., Kudryavtsev, A.B. and Valley, J.W. 2018. SIMS analyses of the oldest known assemblage of microfossils document their taxon-correlated carbon isotope compositions. *Proceedings of the National Academy of Sciences of the United States of America*, **115**, 53–58, https://doi.org/10.1073/pnas.1718063115

Schultze-Lam, S., Harauz, G. and Beveridge, T.J. 1992. Participation of a cyanobacterial S layer in fine-grain mineral formation. *Journal of Bacteriology*, **174**, 7971–7981, https://doi.org/10.1128/jb.174.24.7971-7981.1992

Sephton, M.A., Verchovsky, A.B., Bland, P.A., Gilmour, I., Grady, M.M. and Wright, I.P. 2003. Investigating the variations in carbon and nitrogen isotopes in carbonaceous chondrites. *Geochimica et Cosmochimica Acta*, **67**, 2093–2108, https://doi.org/10.1016/S0016-7037(02)01320-0

Seto, J., Ma, Y. *et al.* 2012. Structure–property relationships of a biological mesocrystal in the adult sea urchin spine. *Proceedings of the National Academy of Sciences of the United States of America*, **109**, 3699–3704, https://doi.org/10.1073/pnas.1109243109

Sevilla, M. and Fuertes, A.B. 2009. Chemical and structural properties of carbonaceous products obtained by hydrothermal carbonization of saccharides. *Chemistry*, **15**, 4195–4203, https://doi.org/10.1002/chem.200802097

Siebach, K.L., Grotzinger, J.P., Kah, L.C., Stack, K.M., Malin, M., Léveillé, R. and Sumner, D.Y. 2014. Subaqueous shrinkage cracks in the Sheepbed mudstone: implications for early fluid diagenesis, Gale crater, Mars. *Journal of Geophysical Research: Planets*, **119**, 1597–1613, https://doi.org/10.1002/2014JE004623

Sievert, S.M., Wieringa, E.B.A., Wirsen, C.O. and Taylor, C.D. 2007. Growth and mechanism of filamentous-sulfur formation by Candidatus Arcobacter sulfidicus in opposing oxygen-sulfide gradients. *Environmental Microbiology*, **9**, 271–276, https://doi.org/10.1111/j.1462-2920.2006.01156.x

Sim, M.S., Bosak, T. and Ono, S. 2011. Large sulfur isotope fractionation does not require disproportionation. *Science*, **333**, 74–77, https://doi.org/10.1126/science.1205103

Simoneit, B.R.T. 2004. Biomarkers (molecular fossils) as geochemical indicators of life. *Advances in Space Research*, **33**, 1255–1261, https://doi.org/10.1016/j.asr.2003.04.045

Slack, J.F., Grenne, T., Bekker, A., Rouxel, O.J. and Lindberg, P.A. 2007. Suboxic deep seawater in the late Paleoproterozoic: evidence from hematitic chert and iron formation related to seafloor-hydrothermal sulfide deposits, central Arizona, USA. *Earth and Planetary Science Letters*, **255**, 243–256, https://doi.org/10.1016/j.epsl.2006.12.018

Sonobe, Y., Watamura, H. and Hirasawa, I. 2015. Polymorphism, size and shape control of calcium carbonate crystals in the presence of a polyelectrolyte. *Chemical Engineering & Technology*, **38**, 1053–1058, https://doi.org/10.1002/ceat.201400731

Staudigel, H., Furnes, H., Banerjee, N.R., Dilek, Y. and Muehlenbachs, K. 2006. Microbes and volcanoes: a tale from the oceans, ophiolites, and greenstone belts. *GSA Today*, **16**, 4, https://doi.org/10.1130/GSAT01610A.1

Steele, A., McCubbin, F.M. *et al.* 2012. A reduced organic carbon component in martian basalts. *Science*, **337**, 212–215, https://doi.org/10.1126/science.1220715

Steele, A., McCubbin, F.M. and Fries, M.D. 2016. The provenance, formation, and implications of reduced carbon phases in Martian meteorites. *Meteoritics & Planetary Science*, **51**, 2203–2225, https://doi.org/10.1111/maps.12670

Steele, A., Benning, L.G. *et al.* 2018. Organic synthesis on Mars by electrochemical reduction of CO_2. *Science Advances*, **4**, eaat5118, https://doi.org/10.1126/sciadv.aat5118

Stüeken, E.E. 2016. Nitrogen in ancient mud: a biosignature? *Astrobiology*, **16**, 730–735, https://doi.org/10.1089/ast.2016.1478

Sturm, E.V. and Cölfen, H. 2016. Mesocrystals: structural and morphogenetic aspects. *Chemical Society Reviews*, **45**, 5821–5833, https://doi.org/10.1039/C6CS00208K

Summons, R.E., Amend, J.P. *et al.* 2011. Preservation of martian organic and environmental records: final report of the Mars biosignature working group. *Astrobiology*, **11**, 157–181, https://doi.org/10.1089/ast.2010.0506

Sun, S., Yu, X., Yang, Q., Yang, Z. and Liang, S. 2019. Mesocrystals for photocatalysis: a comprehensive review on synthesis engineering and functional modifications. *Nanoscale Advances*, **1**, 34–63, https://doi.org/10.1039/C8NA00196K

Sviben, S., Gal, A. *et al.* 2016. A vacuole-like compartment concentrates a disordered calcium phase in a key coccolithophorid alga. *Nature Communications*, **7**, 11228, https://doi.org/10.1038/ncomms11228

Szopa, C., Freissinet, C. *et al.* 2020. First detections of dichlorobenzene isomers and trichloromethylpropane from organic matter indigenous to Mars mudstone in Gale Crater, Mars: results from the Sample Analysis at Mars instrument onboard the Curiosity rover. *Astrobiology*, **20**, 292–306, https://doi.org/10.1089/ast.2018.1908

Takai, K., Nakamura, K. *et al.* 2008. Cell proliferation at 122°C and isotopically heavy CH_4 production by a hyperthermophilic methanogen under high-pressure cultivation. *Proceedings of the National Academy of Sciences of the United States of America*, **105**, 10949–10954, https://doi.org/10.1073/pnas.0712334105

Taylor, C.D. and Wirsen, C.O. 1997. Microbiology and ecology of filamentous sulfur formation. *Science*, **277**, 1483–1485, https://doi.org/10.1126/science.277.5331.1483

Teichert, J.S., Kruse, F.M. and Trapp, O. 2019. Direct prebiotic pathway to DNA nucleosides. *Angewandte Chemie International Edition*, **58**, 9944–9947, https://doi.org/10.1002/anie.201903400

Thomas-Keprta, K.L., Clemett, S.J. *et al.* 2002. Magnetofossils from ancient Mars: a robust biosignature in the martian meteorite ALH84001. *Applied and Environmental Microbiology*, **68**, 3663–3672, https://doi.org/10.1128/AEM.68.8.3663-3672.2002

Thomazo, C., Pinti, D.L., Busigny, V., Ader, M., Hashizume, K. and Philippot, P. 2009. Biological activity and the Earth's surface evolution: insights from carbon, sulfur, nitrogen and iron stable isotopes in the rock record. *Comptes Rendus Palevol*, **8**, 665–678, https://doi.org/10.1016/j.crpv.2009.02.003

Thorseth, I.H., Furnes, H. and Tumyr, O. 1995. Textural and chemical effects of bacterial activity on basaltic glass: an experimental approach. *Chemical Geology*, **119**, 139–160, https://doi.org/10.1016/0009-2541(94)00098-S

Tobler, D.J., Blanco, J.D.R., Dideriksen, K., Sand, K.K., Bovet, N., Benning, L.G. and Stipp, S.L.S. 2014. The effect of aspartic acid and glycine on amorphous calcium carbonate (ACC) structure, stability and crystallization. *Procedia Earth and Planetary Science*, **10**, 143–148, https://doi.org/10.1016/j.proeps.2014.08.047

Tobler, D.J., Rodriguez-Blanco, J.D., Dideriksen, K., Bovet, N., Sand, K.K. and Stipp, S.L.S. 2015. Citrate effects on amorphous calcium carbonate (ACC) structure, stability, and crystallization. *Advanced Functional Materials*, **25**, 3081–3090, https://doi.org/10.1002/adfm.201500400

Toramaru, A., Harada, T. and Okamura, T. 2003. Experimental pattern transitions in a Liesegang system. *Physica D: Nonlinear Phenomena*, **183**, 133–140, https://doi.org/10.1016/S0167-2789(03)00139-8

Tosca, N.J., McLennan, S.M., Lindsley, D.H. and Schoonen, M.A.A. 2004. Acid-sulfate weathering of synthetic Martian basalt: the acid fog model revisited. *Journal of Geophysical Research: Planets*, **109**, https://doi.org/10.1029/2003JE002218

Uebe, R. and Schüler, D. 2016. Magnetosome biogenesis in magnetotactic bacteria. *Nature Reviews Microbiology*, **14**, 621–637, https://doi.org/10.1038/nrmicro.2016.99

Vago, J.L., Westall, F. *et al.* 2017. Habitability on early Mars and the search for biosignatures with the ExoMars rover. *Astrobiology*, **17**, 471–510, https://doi.org/10.1089/ast.2016.1533

Vago, J.L., Westall, F. and Cavalazzi, B. 2019. Searching for signs of life on other planets: Mars a case study. *Advances in Astrobiology and Biogeophysics*, 283–300, https://doi.org/10.1007/978-3-319-96175-0_14

van Zuilen, M. 2008. Stable isotope ratios as a biomarker on mars. *Space Science Reviews*, **135**, 221–232, https://doi.org/10.1007/s11214-007-9268-1

van Zuilen, M.A., Lepland, A., Teranes, J., Finarelli, J., Wahlen, M. and Arrhenius, G. 2003. Graphite and carbonates in the 3.8 Ga old Isua

Supracrustal Belt, southern West Greenland. *Precambrian Research*, **126**, 331–348, https://doi.org/10.1016/S0301-9268(03)00103-7

Wacey, D., Kilburn, M., Stoakes, C., Aggleton, H. and Brasier, M. 2008. Ambient inclusion trails: their recognition, age range and applicability to early life on Earth. *Modern Approaches in Solid Earth Sciences*, **4**, 113–134, https://doi.org/10.1007/978-1-4020-8306-8_3

Wacey, D., Kilburn, M.R., Saunders, M., Cliff, J. and Brasier, M.D. 2011. Microfossils of sulphur-metabolizing cells in 3.4-billion-year-old rocks of Western Australia. *Nature Geoscience*, **4**, 698–702, https://doi.org/10.1038/ngeo1238

Wacey, D., McLoughlin, N. *et al.* 2013. Nanoscale analysis of pyritized microfossils reveals differential heterotrophic consumption in the *c*. 1.9–Ga Gunflint chert. *Proceedings of the National Academy of Sciences of the United States of America*, **110**, 8020–8024, https://doi.org/10.1073/pnas.1221965110

Wacey, D., McLoughlin, N., Saunders, M. and Kong, C. 2014. The nano-scale anatomy of a complex carbon-lined microtube in volcanic glass from the *c*. 92 Ma Troodos Ophiolite, Cyprus. *Chemical Geology*, **363**, 1–12, https://doi.org/10.1016/j.chemgeo.2013.10.028

Wacey, D., Saunders, M., Kong, C. and Kilburn, M.R. 2016*a*. A new occurrence of ambient inclusion trails from the *c.* 1900-million-year-old Gunflint Formation, Ontario: nanocharacterization and testing of potential formation mechanisms. *Geobiology*, **14**, 440–456, https://doi.org/10.1111/gbi.12186

Wacey, D., Saunders, M., Kong, C., Brasier, A. and Brasier, M. 2016*b*. 3.46 Ga Apex chert 'microfossils' reinterpreted as mineral artefacts produced during phyllosilicate exfoliation. *Gondwana Research*, **36**, 296–313, https://doi.org/10.1016/j.gr.2015.07.010

Wacey, D., Fisk, M., Saunders, M., Eiloart, K. and Kong, C. 2017. Critical testing of potential cellular structures within microtubes in 145 Ma volcanic glass from the Argo Abyssal Plain. *Chemical Geology*, **466**, 575–587, https://doi.org/10.1016/j.chemgeo.2017.07.006

Wacey, D., Noffke, N., Saunders, M., Guagliardo, P. and Pyle, D.M. 2018. Volcanogenic pseudo-fossils from the ~3.48 Ga Dresser Formation, Pilbara, Western Australia. *Astrobiology*, **18**, 539–555, https://doi.org/10.1089/ast.2017.1734

Wanas, H.A. and Sallam, E. 2016. Abiotically-formed, primary dolomite in the mid-Eocene lacustrine succession at Gebel El-Goza El-Hamra, NE Egypt: an approach to the role of smectitic clays. *Sedimentary Geology*, **343**, 132–140, https://doi.org/10.1016/j.sedgeo.2016.08.003

Wanger, G., Moser, D., Hay, M., Myneni, S., Onstott, T.C. and Southam, G. 2012. Mobile hydrocarbon microspheres from >2-billion-year-old carbon-bearing seams in the South African deep subsurface. *Geobiology*, **10**, 496–505, https://doi.org/10.1111/j.1472-4669.2012.00340.x

Weiner, S. 2008. Biomineralization: a structural perspective. *Journal of Structural Biology*, **163**, 229–234, https://doi.org/10.1016/j.jsb.2008.02.001

Westall, F., Foucher, F. *et al.* 2015. Biosignatures on Mars: what, where, and how? Implications for the search for martian life. *Astrobiology*, **15**, 998–1029, https://doi.org/10.1089/ast.2015.1374

Westall, F., Hickman-Lewis, K. and Cavalazzi, B. 2018. Biosignatures in deep time. *Advances in Astrobiology and Biogeophysics*, 145–164, https://doi.org/10.1007/978-3-319-96175-0_7

White, L.M., Gibson, E.K., Thomas-Keprta, K.L., Clemett, S.J. and McKay, D.S. 2014. Putative indigenous carbon-bearing alteration features in martian meteorite Yamato 000593. *Astrobiology*, **14**, 170–181, https://doi.org/10.1089/ast.2011.0733

Whitehouse, M.J. and Fedo, C.M. 2007. Microscale heterogeneity of Fe isotopes in >3.71 Ga banded iron formation from the Isua Greenstone Belt, southwest Greenland. *Geology*, **35**, 719–722, https://doi.org/10.1130/G23582A.1

Wiens, R.C., Maurice, S. *et al.* 2020. The SuperCam instrument suite on the NASA Mars 2020 rover: body unit and combined system tests. *Space Science Reviews*, **217**, 4, https://doi.org/10.1007/s11214-020-00777-5

Wilmeth, D.T., Corsetti, F.A., Beukes, N.J., Awramik, S.M., Petryshyn, V., Spear, J.R. and Celestian, A.J. 2019. Neoarchean (2.7 Ga) lacustrine stromatolite deposits in the Hartbeesfontein Basin, Ventersdorp Supergroup, South Africa: implications for oxygen oases. *Precambrian Research*, **320**, 291–302, https://doi.org/10.1016/j.precamres.2018.11.009

Wołos, A., Roszak, R. *et al.* 2020. Synthetic connectivity, emergence, and self-regeneration in the network of prebiotic chemistry. *Science*, **369**, https://doi.org/10.1126/science.aaw1955

Wong, G.M., Lewis, J.M.T. *et al.* 2020. Detection of reduced sulfur on Vera Rubin Ridge by quadratic discriminant analysis of volatiles observed during evolved gas analysis. *Journal of Geophysical Research: Planets*, **125**, e2019JE006304, https://doi.org/10.1029/2019JE006304

Wu, Y.-J., Tseng, Y.-H. and Chan, J.C.C. 2010. Morphology control of fluorapatite crystallites by citrate ions. *Crystal Growth & Design*, **10**, 4240–4242, https://doi.org/10.1021/cg100859m

Xu, A.-W., Dong, W.-F., Antonietti, M. and Cölfen, H. 2008. Polymorph switching of calcium carbonate crystals by polymer-controlled crystallization. *Advanced Functional Materials*, **18**, 1307–1313, https://doi.org/10.1002/adfm.200700895

Xu, J., Chmela, V. *et al.* 2020. Selective prebiotic formation of RNA pyrimidine and DNA purine nucleosides. *Nature*, **582**, 60–66, https://doi.org/10.1038/s41586-020-2330-9

Yu, S.-H. and Cölfen, H. 2004. Bio-inspired crystal morphogenesis by hydrophilic polymers. *Journal of Materials Chemistry*, **14**, 2124–2147, https://doi.org/10.1039/b401420k

Yu, S.-H., Cölfen, H., Tauer, K. and Antonietti, M. 2005. Tectonic arrangement of $BaCO_3$ nanocrystals into helices induced by a racemic block copolymer. *Nature Materials*, **4**, 51–55, https://doi.org/10.1038/nmat1268

Zastrow, A.M. and Glotch, T.D. 2021. Distinct carbonate lithologies in Jezero Crater, Mars. *Geophysical Research Letters*, **48**, e2020GL092365, https://doi.org/10.1029/2020GL092365

Zawaski, M.J., Kelly, N.M., Orlandini, O.F., Nichols, C.I.O., Allwood, A.C. and Mojzsis, S.J. 2020. Reappraisal of purported *c*. 3.7 Ga stromatolites from the Isua Supracrustal Belt (West Greenland) from detailed chemical and structural analysis. *Earth and Planetary Science Letters*, **545**, 116409, https://doi.org/10.1016/j.epsl.2020.116409

Zhu, T.F. and Szostak, J.W. 2009. Coupled growth and division of model protocell membranes. *Journal of the American Chemical Society*, **131**, 5705–5713, https://doi.org/10.1021/ja900919c